Acta Geologica Polonica, Vol. 48 (1998), No. 1, pp. 43-106

Facies, stratigraphy and diagenesis of Middle Devonian reef- and mud-mounds in the Mader (eastern Anti-Atlas, Morocco)[1]

BERND KAUFMANN

Institut für Geologie und Paläontologie der Universität Tübingen, Sigwartstr. 10, D-72076 Tübingen, Germany. E-mail: bernd.kaufmann@uni-tuebingen.de

ABSTRACT:

KAUFMANN, B. 1998. Facies, stratigraphy and diagenesis of Middle Devonian reef- and mud-mounds in the Mader (eastern Anti-Atlas, Morocco). *Acta Geol. Polon.*, **48** (1), 43-106. Warszawa.

During the Devonian, the eastern Anti-Atlas formed a part of the northwestern continental margin of Gondwana which was a mid-latitudinal (30-40°S), temperate-water carbonate province. In the Mader region, ten carbonate mounds (one reef-mound and nine mud-mounds), distributed over five discrete localities, are intercalated within a 200-400 m thick Middle Devonian succession. The arid climate of the northwestern margin of the Sahara has exhumed these mounds which display perfectly their original morphologies and relations to off-mound lithologies.

The carbonate mounds of the Mader area consist of massive, stromatactis-bearing boundstones (wackestones and floatstones in a purely descriptive manner) with the bulk of the mound volume consisting of fine-grained carbonate (microspar). High accumulation rates (0.2-0.8 m/1000 a), purity of mound carbonates (> 95% $CaCO_3$) and homogeneous Mg-calcite mineralogy strongly argue for *in situ* carbonate production by microbial (cyanobacterial/bacterial) communities. In addition, other indications (calcified cyanobacteria in the immediate neighbourhood of stromatactis fabrics, dark crusts surrounding stromatactis fabrics and alignment of stromatactis fabrics parallel to the accretionary mound surfaces) suggest a close relationship between stromatactis formation and carbonate production. Microbial communities probably flourished on the mound surfaces, precipitating fine-grained carbonates and consolidating the steep mound flanks by their mucilages. Once embedded, these communities decayed and were successively replaced by calcite cements, finally resulting in stromatactis fabrics.

The facies model proposed for the three most conspicuous mound occurrences (Aferdou el Mrakib, Guelb el Maharch, Jebel el Otfal) is a 40 km wide, tectonically-controlled homoclinal ramp, which developed between an area of uplift (Mader Platform) and another area of strong subsidence (depocentre of the Mader Basin). The bathymetric gradient of this ramp is reflected by a Middle Devonian facies pattern varying from shallow to deeper water environments and by different faunal associations of the carbonate mounds. The Aferdou el Mrakib reef-mound was established at moderate water depth (mid-ramp setting), because it contains abundant frame-builders (stromatoporoids, colonial rugose corals) but lacks indications for euphotic conditions, like calcareous algae and micritic envelopes. The Guelb el

[1] This paper represents the original version of the author's Ph.D. thesis which was submitted to the Faculty of Earth Sciences of the University of Tübingen (Germany) in December 1996.

Maharch and Jebel el Otfal mud-mounds contain a much more impoverished fauna, dominated by crinoids and tabulate corals (auloporids), indicating a deeper bathymetric position (outer ramp setting) on the ramp. Further, but rather unspectacular mud-mounds (SE' Zireg, Jebel Ou Driss) are situated apart from the ramp at localities in the southern and the southwestern Mader area respectively.

Mound growth was possibly initiated by hydrothermal seepage at the seafloor though no evidences for hydrothermal activity, like mineralizations or depleted $\delta^{13}C$ values, have been found to date. Slightly elevated temperatures may have stimulated the benthic fauna, especially crinoids, forming flat *in situ* lenses, which in turn served as substrates for microbial colonization.

Termination of mound growth in the Mader Basin is connected with the subsidence-caused drowning of the carbonate ramp. Poorly-fossiliferous, laminated mudstones overlie the mounds and suggest a southward-directed extension of basinal facies onlapping the ramp and its mounds and resulting in poorly oxygenated seafloor conditions.

Diagenesis of the Mader Basin carbonate mounds includes early marine, shallow marine burial and deeper burial cementation, recrystallization of the fine-grained mound carbonates, stylolitization and dolomitization. Radiaxial calcites (RC) precipitated in the marine environment and are believed to have preserved a nearly primary marine stable isotopic composition of the Mader Basin seawater with mean values of $\delta^{18}O$ = -2.6 (±0.2)‰ PDB and $\delta^{13}C$ = +2.7 (±0.5)‰ PDB. The exceptional high $\delta^{18}O$ values, compared with other Middle Devonian data derived from North American studies, are interpreted as resulting from the mid-latitudinal, temperate-water settings of the Mader Basin carbonate mounds. The diagenetic history is characterized by progressive burial conditions. Meteoric influences can be ruled out because the progressively deepening bathymetric evolution of the Mader Basin excludes subaerial exposure. All diagenetic events, especially cement zones, are probably diachronous and therefore cannot be correlated within the Mader Basin and not even within individual mounds. Fault-related dolomitization, postdating Variscan compression was the last diagenetic event which affected the carbonate mounds of the Mader area

Contents

INTRODUCTION 46

PREVIOUS WORK 47

GEOLOGICAL SETTING AND HISTORY 47

LOWER TO MIDDLE DEVONIAN STRATIGRAPHY, FACIES PATTERN AND PALAEOGEOGRAPHY 50

Lower Devonian 50
Lochkovian to Pragian 50
Emsian 54

Middle Devonian 54
Eifelian 54
Givetian 55

Early to Middle Devonian events and eustatic sea-level changes 56
End-*pesavis* Event 56
Daleje Event 56
Chotec Event 56
Kacak Event 58
Taghanic Event 58
Pumilio Events 58

MIDDLE DEVONIAN CARBONATE MOUNDS OF THE MADER AREA 58

Aferdou el Mrakib 58
Geological and stratigraphical setting, off-mound succession 58
Size and geometry 59
Lithology and sedimentary structures 61
Fauna 61

Guelb el Maharch 62
Geological and stratigraphical setting, off-mound succession 62
Size and geometry 62
Lithology and sedimentary structures 63
Fauna 64

Jebel el Otfal 64
Geological and stratigraphical setting, off-mound succession 64
Size and geometry 66
Lithology and sedimentary structures 69
Fauna 69

Jebel Ou Driss 70
Geological and stratigraphical setting, off-mound succession 70
Size and geometry 70
Lithology 70
Fauna 71

SE' Jebel Zireg 71

CONODONT FAUNA AND BIOSTRATIGRAPHY OF THE MADER CARBONATE MOUNDS 71

Aferdou el Mrakib 72

Guelb el Maharch 73

Jebel el Otfal 73

Jebel Ou Driss 74

SE' Jebel Zireg 74

FACIES MODEL (CARBONATE RAMP) 74

Facies zones 75
Shallow ramp facies (stromatoporoid--coral-cyanobacteria boundstones) 75
Mid-ramp facies (burrowed, skeletal wackestones) 77
Outer ramp facies (burrowed, argillaceous skeletal wackestones) 77
Transitional outer ramp to basinal facies (blue-grey, laminated mudstones) 77
Basinal facies (monotonous, poorly-fossiliferous shales) 77

Bathymetric positions of carbonate mounds 77

Drowning of the ramp and its mounds . . . 78

DIAGENESIS 79

Methods 79
Calcite cements 81
Radiaxial calcite 81
Scalenohedral cement 83
Bright-luminescent and banded--luminescent cements 83
Syntaxial cement 83
Blocky calcite cements 83

Interpretation 83
Marine signature of radiaxial calcites and brachiopod shells 83
Marine shallow burial origin of scalenohedral cement, bright- and banded-luminescent cement and blocky spar I 85
Deeper burial origin of ferroan calcite cements 87
Cement sequence 88

Pressure solution 88

Recrystallization of fine-grained mound carbonates 89

Dolomitization 89
Petrographic types of dolomite 89
Interpretation 91
Dolostone porosity 91

DISCUSSION 91

Origin of fine-grained mound carbonates 91

Stromatactis 93

Stability of steep mound flanks 94

Ecological succession 94

Accumulation rates and growth times 95

Initiation of mound growth 95

Modern analogues of ancient mud-mounds 96

SUMMARY 96

Acknowledgements 98

REFERENCES 99

INTRODUCTION

Mud-mounds are widespread types of carbonate buildups, which mainly consist of fine-grained carbonate. In contrast to reefs, they lack a rigid framework of skeletal organisms, like coralline sponges, corals and calcareous algae. Nevertheless, they often display a high diversity of invertebrate faunas. Generally, mud-mounds were established in deeper water environments (PRATT 1995). Their sizes vary between a few tens of metres up to 1 km in diameter, but they can also be developed as extensive complexes covering hundreds of square kilometres (*e.g.* LEES 1964). Mound geometries are mostly lens- or dome-shaped with evidences for a significant relief and often steep flanks. Stromatactis fabrics are typical features of mud-mounds.

The term 'mud-mound', as far as I know, was used at first by DUMESTRE & ILLING (1967, p. 339) in describing some steep-sided, cone-shaped bioherms in the neighbourhood to the spectacular Devonian reefs of former Spanish Sahara. WILSON (1975) applied the term more widely to all kinds of mud dominated carbonate buildups. JAMES & BOURQUE (1992) distinguished between 'biogenic mounds' (including microbial mounds and skeletal mounds) and 'mud-mounds', which were formed by inorganic accumulation of mud. In this study, I take a broader definition of a mud-mound *sensu* BOSENCE & BRIDGES (1995) as 'a carbonate buildup having depositional relief and being composed dominantly of carbonate mud, peloidal mud, or micrite'. The term reef-mound is not used *sensu* JAMES (1984), but as a mud-mound, which contains considerable amounts of potential reef-builders (stromatoporoids, colonial rugose corals) without them forming a rigid framework. The general term 'carbonate mound' is used in this study to include both reef- and mud-mounds.

Mud-mounds are most common in the Palaeozoic, but they also occur in the Mesozoic and Cenozoic (MONTY & *al*. 1995). Close recent analogues, which correspond to Palaeozoic mud-mounds concerning their dimensions, shapes, faunal compositions and bathymetric positions are not known. The actual origins of mud-mounds are still controversial. The two major unsolved problems are: 1) Why are the mounds where they are? and 2) Wherefrom does the fine-grained carbonate originate?

Recent investigations of mud-mounds have focused on the origin of the fine-grained carbonate and the mechanisms of accretion. Some modern lime mud bodies are purely hydrodynamic accumulations (*e.g.* Florida Bay mud banks, STOCKMAN & *al*. 1967), whereas others are related to the baffling of carbonate mud by sea-grasses (GINSBURG & LOWENSTAM 1958). Mound growth by sediment baffling of benthic invertebrates, like crinoids and bryozoans has been suggested by many authors (*e.g.* PRAY 1958, WILSON 1975). PRATT (1982) has proposed that cryptalgal mats may have trapped and bound the mud. However, the most recent investigators have assumed that the fine-grained carbonate in the mounds must have been produced *in situ* by microbial precipitation (*e.g.* MONTY & *al*. 1982, LEES & MILLER 1985, TSIEN 1985a, BRIDGES & CHAPMAN 1988). In particular, the peloidal textures in most ancient mud-mounds are considered to be related to microbial activity. A further main subject of recent mud-mound investigations is the origin of the common stromatactis fabrics (*e.g.* BOURQUE & BOULVAIN 1993, FLAJS & HÜSSNER 1993).

The Devonian is a period of extensive development of carbonate buildups. Many attempts have been made to summarize different types and major features of Devonian carbonate buildups (*see* reviews by HECKEL 1974, KREBS 1974, BURCHETTE 1981, MOORE 1988 and TSIEN 1988). Devonian reefs are mostly constructed by stromatoporoids and corals (*e.g.* KREBS 1974, PLAYFORD 1980, TSIEN 1988), a trend carried over from the Silurian (HECKEL 1974, LONGMAN 1981). Other less important contributors to carbonate buildup growth were calcareous algae, sponges and bryozoans. In contrast to 'true' reefs, Devonian reef- and mud-mounds lack a rigid framework, though potential reef-builders might be present and the mounds often display a high faunal diversity. Devonian mud-mounds are known from North America (HECKEL 1973, GIBSON & *al*. 1988), Australia (WALLACE 1987), Europe (TSIEN 1977, GNOLI & *al*. 1981, WELLER 1989, BOULVAIN 1993, FLAJS & HÜSSNER 1993) and from North Africa (DUMESTRE & ILLING 1967, MOUSSINE-POUCHKINE 1971, ELLOY 1972, BRACHERT & *al*. 1992, WENDT 1993, WENDT & *al*. 1993, BELKA 1994, KAUFMANN 1995). Because of the limited outcrops of Devonian mud-mounds worldwide, it is difficult to draw conclusions about their exact dimensions, morphologies and off-mound relations. In contrast to most previously examined mud-mounds, the

Devonian ones of the eastern Anti-Atlas of Morocco are exposed spectacularly. The arid weathering at the northwestern margin of the Sahara has exhumed them, displaying their depositional setting very clearly. They offer an excellent opportunity to study mound sizes, geometries and the lateral and vertical transitions to the bedded off-mound sediments.

The aim of this study is to present a detailed description of the Middle Devonian reef- and mud-mound facies of the Mader area and of their spatial and temporal distribution. In addition, the mounds are incorporated into the palaeogeographical evolution of the eastern Anti-Atlas. Data of shapes, dimensions and fauna of the mounds as well as the relations of mound and off-mound facies are used to decipher factors that controlled their development. In addition, common mud-mound models, especially concerning the origin and accumulation of the fine-grained carbonates, are discussed. A further objective of this study is to document the diagenetic processes that affected the carbonate mounds of the Mader area.

PREVIOUS WORK

The occurrence of carbonate mounds in the Devonian of the eastern Anti-Atlas, mostly referred to as 'reefs, has long been known. Previous studies dealt almost exclusively with the spectacular Lower Devonian Hamar Laghdad mud-mounds in the Tafilalt (MASSA 1965, ELLOY 1972, ALBERTI 1981a, BRACHERT & *al*. 1992). In contrast to these well documented and easily accessible mud-mounds, the more remote Middle Devonian carbonate mounds of the Mader area have received much less attention. In shape and dimension, they resemble the mounds of Hamar Laghdad and the Middle Devonian mud-mounds in the southwestern Tindouf Basin (DUMESTRE & ILLING 1967) and the Algerian Sahara (MOUSSINE-POUCHKINE 1971, WENDT & *al*. 1993, BELKA 1994). HOLLARD (1974) was the first to mention the three most conspicuous mound occurrences (Aferdou el Mrakib, Guelb el Maharch and Jebel el Otfal) of the Mader area. He recognized their reefal nature and provided some data about their shape, faunal composition and stratigraphic setting. A more detailed description concerning dimensions, geometries, facies, biostratigraphy and palaeogeographical setting was given by WENDT (1993). He emphasized the asymmetrical shapes of the smaller mounds and presented a facies model, in which the mounds of the Mader Basin were constructed on a gently sloping ramp at moderate water depth.

GEOLOGICAL SETTING AND HISTORY

The Anti-Atlas of Morocco is a NE-SW-trending, about 700 km long and up to 200 km wide Variscan anticlinorium at the northern margin of the Sahara Craton (PIQUE & MICHARD 1989) (Text-fig. 1). It is separated from the highly deformed Mesozoic rocks in the north by the South-Atlas Fault. The Precambrian crystalline core of the Anti-Atlas is exposed in its northern central part and consists of granitic plutons, which are covered by sedimentary and volcanic rocks of Late Precambrian age. Mainly towards the south, the basement is overlain by a weakly folded Palaeozoic sequence, which continues in that direction towards the rather undeformed Tindouf Basin (Text-fig. 1). An almost complete succession of Palaeozoic sediments, ranging from the Lower Cambrian to the Lower Carboniferous was deposited along the NE-SW-trending passive continental margin of northwestern Gondwana (Sahara Craton). Its thickness exceeds 10 km in the central Anti-Atlas and the northern flank of the Tindouf Basin, strongly decreasing towards the east (DESTOMBES & *al*. 1985).

In the eastern Anti-Atlas (regions of the Tafilalt and the Mader), the Palaeozoic succession generally crops out in W-E- and NW-SE-trending synclines. The easternmost outcrops of the Precambrian basement of the Anti-Atlas are located at Jebel Sarhro and Jebel Ougnate in the northwestern and northern Mader area respectively (Text-fig. 2). The folded Palaeozoic succession of the eastern Anti-Atlas is overlain by undeformed, flat-lying Upper Cretaceous deposits of the Kem-Kem towards the south and Tertiary deposits of the Hamada du Guir towards the east. Palaeozoic rocks reappear in Algeria about 100 km southeast of the Tafilalt in the NW-SE-trending Ougarta fold belt and 50 km to the east in the Carboniferous Béchar Basin (Text-fig. 1).

The oldest sedimentary rocks in the eastern Anti-Atlas are terrestrial clastic deposits (conglomerates, sandstones and shales) of latest

Precambrian age with considerable intercalations of calcalkaline volcanic rocks (JEANNETTE & TISSERANT 1977). The Lower to Middle Cambrian consists mainly of marine silt- and sandstones with a maximum thickness of about 700 m (eastern end of Jebel Sarhro), extremely diminishing towards the east (DESTOMBES & *al*. 1985). Volcanic activity as indicated by basalts, dolerites, volcanic breccias and tuffs is common in the Middle Cambrian at Jebel Ougnate (DESTOMBES & *al*. 1985). Upper Cambrian deposits have not been recognized in the eastern Anti-Atlas so far (Carte Géologique du Maroc, 1:200.000, sheets 'Tafilalt-Taouz' and 'Todrha-Ma'der'). The lower part of the Ordovician (Tremadoc to Llanvirn) consists of 300-800 m thick marine shales with graptolites, trilobites, brachiopods and echinoderms (DESTOMBES & *al*. 1985). The upper Ordovician (Llandeilo to Ashgill) consists of 300-600 m thick sandstones which, in the upper part (upper Asghillian), are supposed to be of glacial origin (DEYNOUX 1985). A post-glacial transgression with graptolite shales and siltstones marks the lower Silurian. They are followed by Ludlowian *Orthoceras* limestones, which are the first significant carbonate deposits in the Palaeozoic sequence of the eastern Anti-Atlas. Fine-grained sandstones and *Scyphocrinites* limestones represent the uppermost Silurian. Thickness of Silurian sediments in

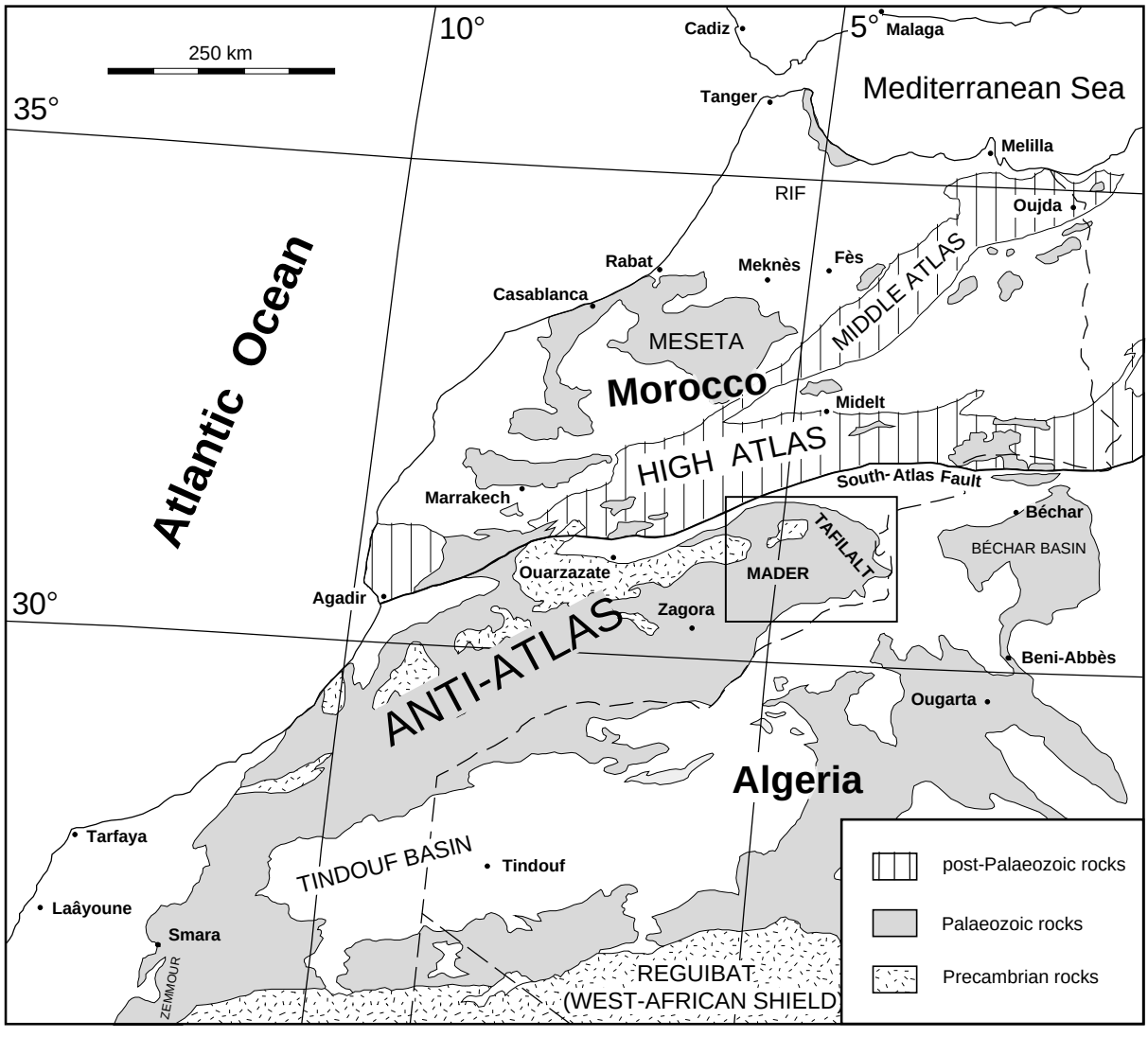

Fig. 1. Major tectonic units of Morocco (modified from PIQUE & MICHARD 1989); boxed area indicates location of the study area and fields of Text-figs 2-5

the eastern Anti-Atlas decreases from 500 m in the Mader area to 150 m in the northern Tafilalt (HOLLARD 1970).

Devonian sediments are exposed over an area of about 20000 km^2 (Text-fig. 2). They were deposited in an extensive epicontinental sea, which changed its palaeogeographical position during the Devonian northward drift of Gondwana from about 45° to 30°S (SCOTESE & MCKERROW 1990). The Lower Devonian consists predominantly of shales interbedded with cephalopod limestones. In the higher part of the Lower Devonian and in the transition to the Middle Devonian, marls and nodular cephalopod limestones become more frequent. Carbonate deposition was most widespread in Middle and Late Devonian times. At that time, a differentiated facies pattern developed in the eastern Anti-Atlas. Differential subsidence, resulting from early Variscan tensional block faulting, caused the disintegration of the formerly stable shelf into a platform and basin topography (WENDT 1985, 1988). In the Mader Basin, a 200-400 m thick neritic succession of argillaceous, fossiliferous wackestones, locally with intercalated mud-mounds and coral-stromatoporoid floatstones, was deposited during Middle Devonian times (HOLLARD 1974; WENDT 1988, 1993). In the Late Devonian, the basin was filled with up to 800 m of shales interbedded with some sandstones (WENDT 1991). In contrast, only some tens of metres of condensed cephalopod limestones were deposited on the pelagic Tafilalt Platform during the Middle and Late Devonian (WENDT 1991).

During the Early Carboniferous, the whole basin and platform topography was levelled by thick deltaic sandstones. The Lower Carboniferous (Tournaisian and Viséan) clastic succession is best developed in the southern Tafilalt where it is about 2000 m thick (BELKA 1991). Huge allochthonous mud-mound boulders (lower Viséan) occur in the southeastern Tafilalt (Jebel Bega and farther east, PAREYN 1961). The youngest preserved Palaeozoic strata of the eastern Anti-Atlas are lower Namurian shales (DELÉPINE 1941), which are exposed near the

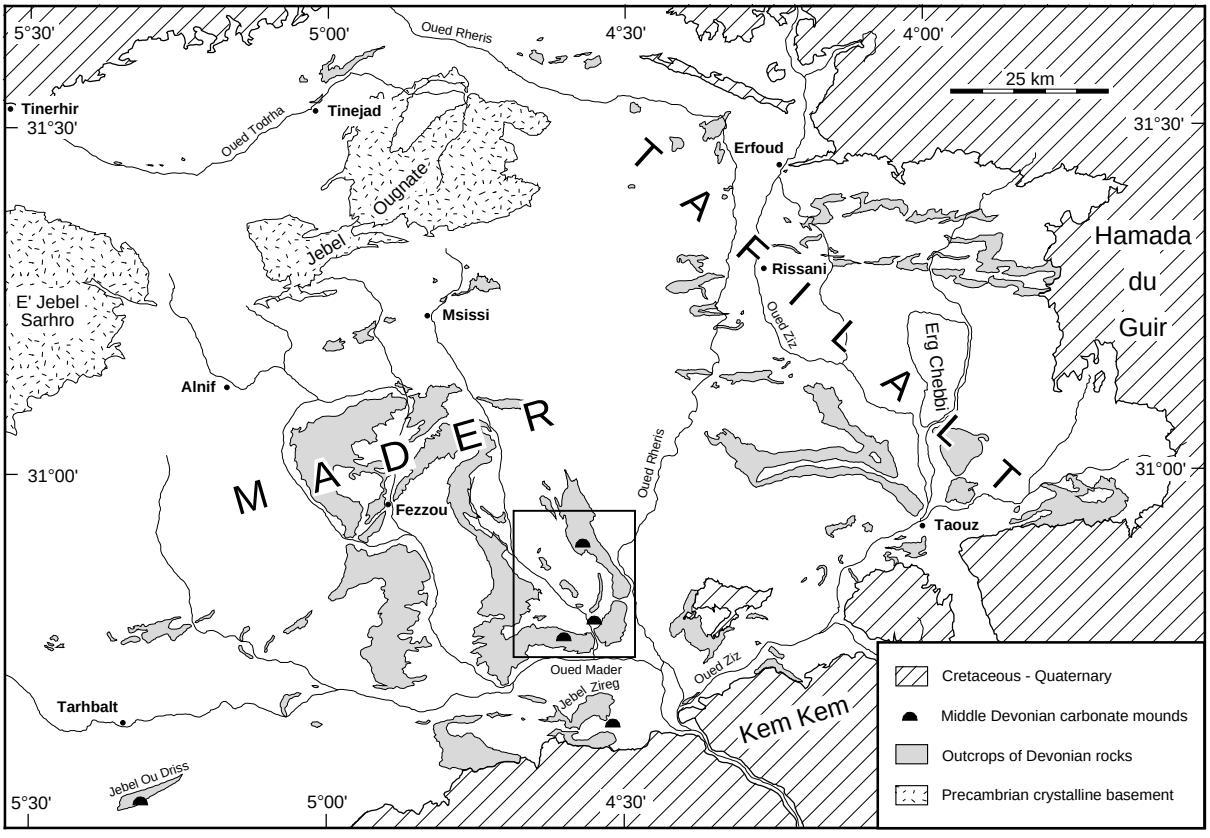

Fig. 2. Locality map of the eastern Anti-Atlas with locations of Middle Devonian carbonate mounds; boxed area indicates field of Text-fig. 9

northwestern edge of Erg Chebbi. The geological history of the Anti-Atlas between the Namurian and the continental Upper Cretaceous (Cenomanian) is unknown. Variscan folding and uplift was weak and probably took place during the Late Carboniferous (Westphalian) (BONHOMME & HASSENFORDER 1985).

LOWER TO MIDDLE DEVONIAN STRATIGRAPHY, FACIES PATTERN AND PALAEOGEOGRAPHY

The stratigraphy and sedimentology of the Lower to Middle Devonian succession in the eastern Anti-Atlas were studied by MASSA (1965) and HOLLARD (1967, 1974, 1981). Detailed biostratigraphical and palaeontological investigations of conodonts, goniatites, dacryoconarids and trilobites were made by BULTYNCK & HOLLARD (1980), BULTYNCK & JACOBS (1981), BENSAÏD & *al*. (1985), BULTYNCK (1985, 1987, 1989), WALLISER (1991), ALBERTI (1981b), and BECKER & HOUSE (1994). Previous studies by WENDT (1985, 1988, 1993, 1995) dealt with Middle Devonian mud-mounds and Middle to Late Devonian palaeogeography and palaeocurrent patterns. He subdivided the eastern Anti-Atlas into four distinct depositional areas (from W to E): Mader Platform, Mader Basin, Tafilalt Platform and Tafilalt Basin (Text-figs 4-5 and 7). These palaeogeographical units are characterized by contrasting facies distributions, different sediment thicknesses and palaeocurrent patterns. Tafilalt and Mader Platform probably merged into one another in an area which is now covered by Cretaceous deposits of the Kem-Kem (Text-figs 4-5).

Lower Devonian

The facies pattern of the Lower Devonian is developed rather uniformly in the eastern Anti-Atlas. However, significant thickness changes occur in individual lithological units which indicate, together with current directions, a palaeogeographical setting that follows a preexisting axis of uplift in Early Palaeozoic times (Middle Cambrian to Silurian) (DESTOMBES & *al*. 1985, WENDT 1985). Therefore, it anticipates the later Middle and Late Devonian basin and platform topography (WENDT 1985, 1988, 1995).

Lochkovian to Pragian

The Silurian-Devonian transition consists of shales intercalated with *Scyphocrinites* limestones, of which the youngest beds were already deposited in Lochkovian times (BRACHERT & *al*. 1992). They are succeeded by 70-200 m thick Lochkovian to lower Pragian shales ('Ihandar' of HOLLARD 1981), which contain graptolites (*Monograptus uniformis*, *M. hercynicus*) and dacryoconarids (*Paranowakia bohemica*, *P. intermedia*, *P. geinitziana*, *Nowakia acuaria*). Generally, these shales are poorly exposed because of Quaternary cover. A hiatus in the upper Lochkovian/Pragian transition is shown on the geological maps 1:200.000 (sheets 'Todrha-Ma'der' and 'Tafilalt-Taouz'), because several authors (JAEGER & MASSA 1965, MASSA 1965, MICHARD 1976) have suggested a temporary emergence of the NW-Sahara at that time. ALBERTI (1982) refuted this hypothesis by recognizing complete upper Lochkovian/Pragian successions of *Nowakia* zones in the Tafilalt and Béchar Basins (Algeria). In the upper Pragian, limestone deposition is common and these beds contain orthoconic nautiloids, trilobites (*Odontochile*, *Reedops*) and pelecypods (*Panenka*, *Hercynella*) (HOLLARD 1970, 1981; ALBERTI 1981b).

Volcanism, lasting from early Lochkovian until earliest Pragian times, is indicated by up to 100 m thick tuffites in the area of Hamar Laghdad (BRACHERT & *al*. 1992). There, the volcanic rocks are discontinuously overlain by up to 180 m thick crinoidal limestones (Kess-Kess formation) of Pragian to early Emsian age (BRACHERT & *al*. 1992).

Lochkovian to Frasnian strata are totally absent in the western and northern Mader area (Text-figs 3-5), where Silurian strata are overlain by Upper Devonian deposits. An even greater hiatus (Silurian to Frasnian) is found in the southern Tafilalt around Ouzina (Text-figs 3-5). It is possible that these gaps are due to a long interval of emergence of that area (Mader Platform, WENDT 1988, 1993, 1995), caused by tectonic uplift of the Precambrian basement (Jebel Sarhro, Jebel Ougnate). In the southwestern and southern Mader area (Jebel Oufatène, Rich Sidi Ali, Jebel Zireg), continued uplift during the Early to Middle Devonian resulted in the extension of the Mader Platform towards the west. This is sup-

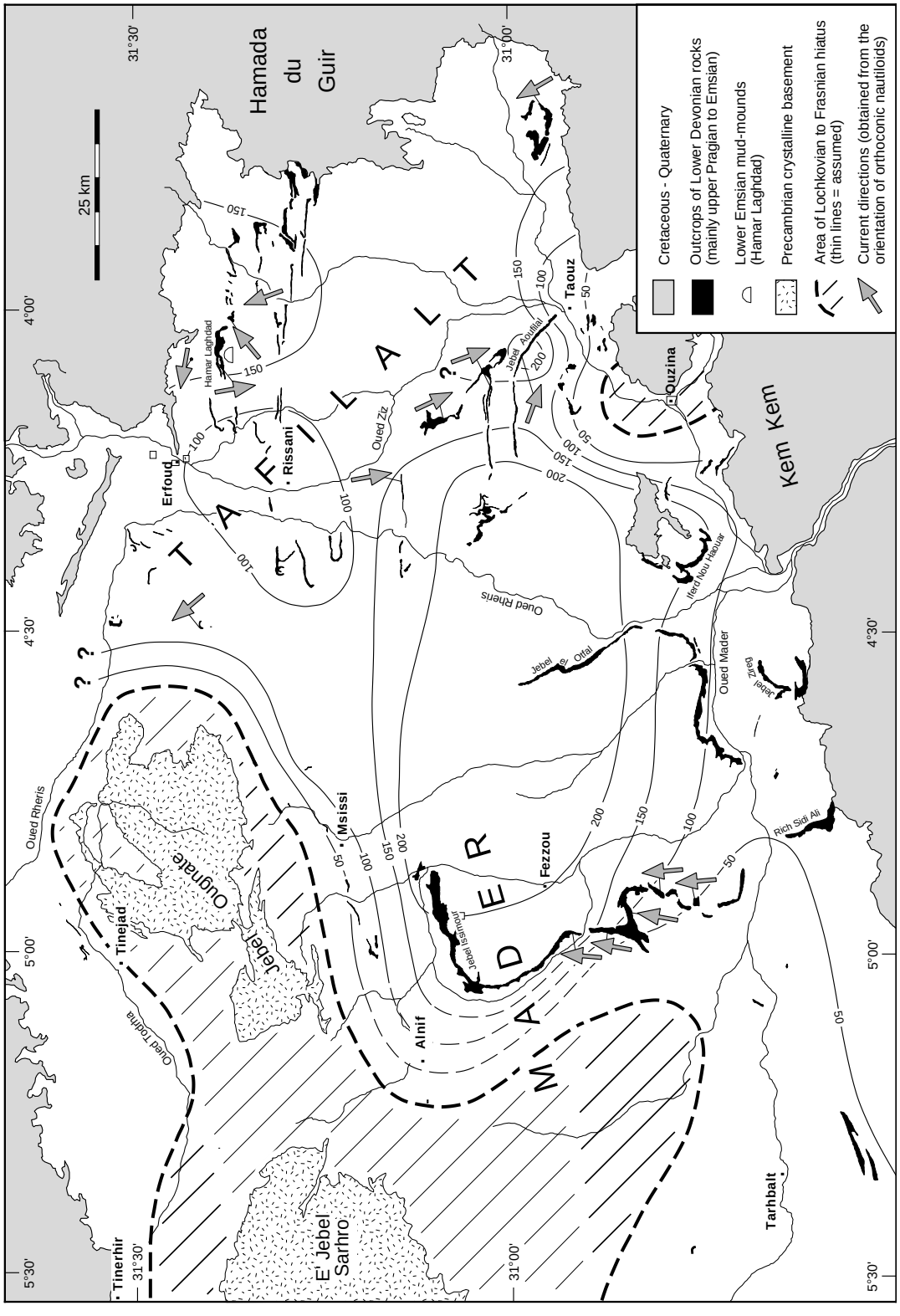

Fig. 3. Isopach map with Emsian thicknesses in metres and current directions; based on the geological map 1:200.000 (sheets 'Todrha-Ma'der' and 'Tafilalt-Taouz'), data in MASSA (1965), HOLLARD (1967, 1974), ALBERTI (1980, 1981b), BULTYNCK (1985), WENDT (1995) and own investigations

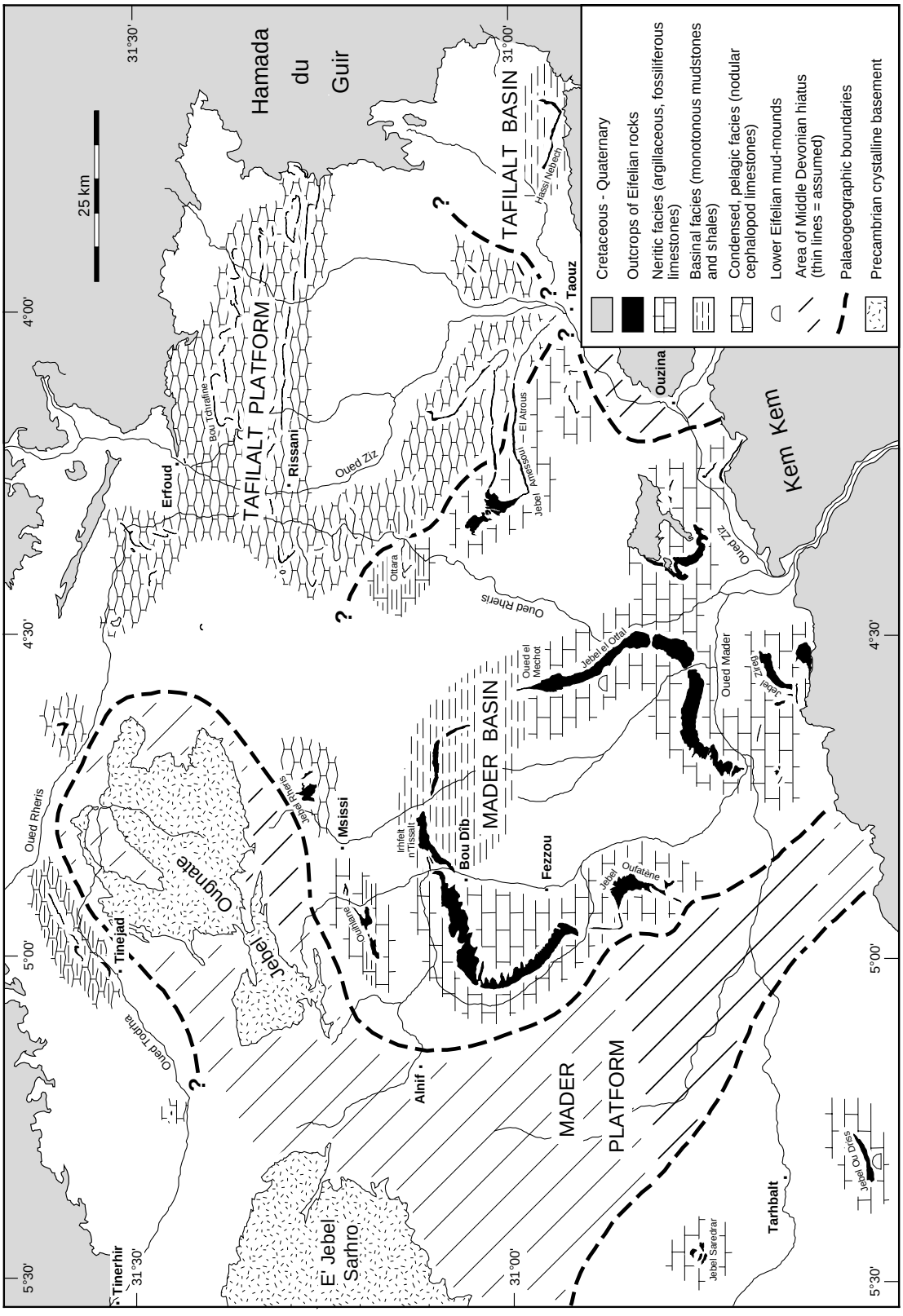

Fig. 4. Facies pattern and palaeogeography of the early Eifelian (*costatus* Zone); based on the geological map 1:200.000 sheets 'Todrha-Ma'der' and 'Tafilalt-Taouz'), data in HOLLARD (1974), WENDT (1988, 1993) and own investigations

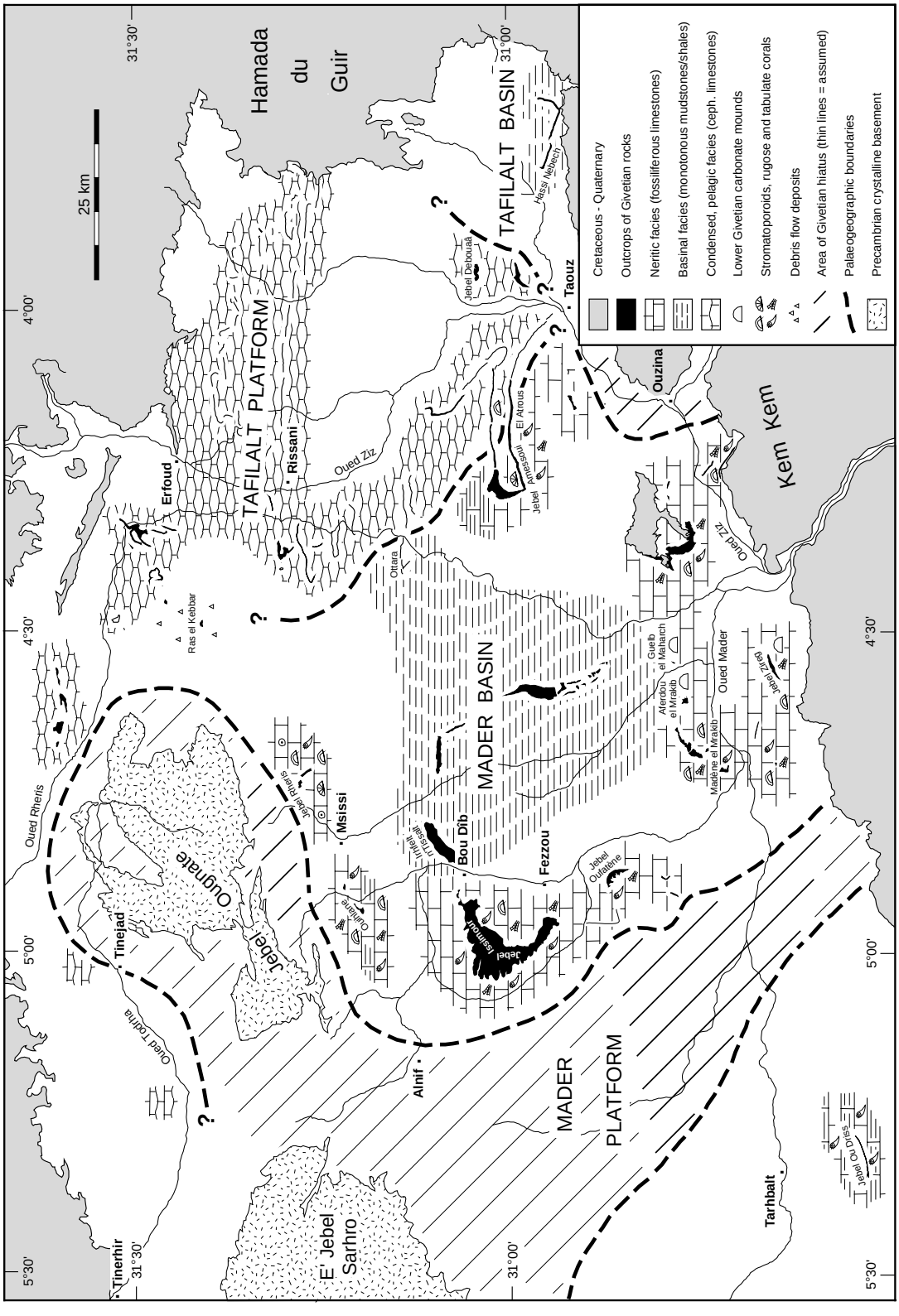

Fig. 5. Facies pattern and palaeogeography of the early Givetian (Lower *varcus* Zone); based on the geological map 1:200.000 (sheets 'Todrha-Ma'der' and 'Tafilalt-Taouz'), data in HOLLARD (1974), WENDT (1988, 1993) and own investigations

posed by the evidence of Upper Devonian strata overlying progressively younger deposits (geological map 1:200.000, sheet 'Todrha-Ma'der'). In Late Devonian times, the Mader Platform was flooded by early Frasnian (Lower *asymmetricus* Zone) and late Famennian (Lower *expansa* Zone) transgressions (WENDT & BELKA 1991).

Emsian

The lowermost part of the Emsian ('Emsien calcaire' of MASSA 1965, 'di 3.1' of HOLLARD 1974, 'Bou Tiskaouine' of HOLLARD 1981) consists of fossiliferous argillaceous limestones, containing numerous dacryoconarids (*Nowakia*, *Styliolina*), orthoconic nautiloids (*e.g. Jovelliana*), goniatites (*Anetoceras*, *Mimagoniatites*), trilobites (*e.g. Cornuproetus*), pelecypods (*Panenka*), crinoids and rare brachiopods. At Hamar Laghdad, mud-mounds were established on thick crinoidal limestones (*see* above). Thickness of the lower Emsian limestones ranges from 10-20 m in the Tafilalt and from 20-100 m in the Mader area (MASSA 1965, HOLLARD 1974, ALBERTI 1981b).

The calcareous lower Emsian is followed by thick green shales ('Emsien argileux' of MASSA 1965, 'di 3.2' of HOLLARD 1974, 'Er Remlia' of HOLLARD 1981), which contain dacryoconarids, brachiopods, trilobites, cephalopods, pelecypods and occasional tabulate and rugose corals. In the upper part of these shales, a famous fossiliferous horizon ('faune coblencienne de Haci-Remlia') with a highly diverse brachiopod fauna is found in the section of Iferd Nou Haouar (LE MAÎTRE 1944). Thickness of the Emsian shales varies considerably, obviously depending on seafloor topography. Maxima (130-220 m) in the areas of Jebel Issimour, Jebel el Otfal and Jebel Aoufilal indicate a depocentre, which subsequently developed into the Mader Basin (Text-fig. 3). Reduced thickness of the Emsian (< 100 m) in the northern Tafilalt (area around Rissani) suggest the persistence of a pelagic platform (Tafilalt Platform), which already existed in Silurian times (WENDT 1995) (Text-fig. 3).

The uppermost Emsian ('di 4' of HOLLARD 1974, 'Tazoulaït' of HOLLARD 1981) is characterized by 10-60 m thick, argillaceous limestones which contain cephalopods (*Sellanarcestes*, *Anarcestes*), pelecypods (*Panenka*), orthoconic nautiloids, dacryoconarids, trilobites and rare crinoids and corals.

Middle Devonian

Eifelian

In contrast to the rather uniform palaeogeography during late Silurian to early Devonian times, a more differentiated facies pattern developed in the eastern Anti-Atlas with the onset of the Middle Devonian (WENDT 1985, 1988). The following three facies belts can be distinguished during the Eifelian (Text-fig. 4):

1) Neritic facies. This facies occurs around the depocentre of the Mader Basin (Irhfelt n'Tissalt) and southwest of the Mader Platform (Jebel Saredrar, Jebel Ou Driss) (Text-fig. 4). It extends from the northern Mader area (Ouihlane) along the western margin of the basin into the southern Tafilalt (Jebel Amessoui) and consists of burrowed, argillaceous wackestones which contain crinoids, brachiopods, tabulate and rugose corals, bryozoans, trilobites, dacryoconarids and occasional pelecypods, gastropods and cephalopods. Lenses of coral-stromatoporoid floatstones occur in the upper Eifelian part of the Ouihlane section (LE MAÎTRE 1947, BULTYNCK 1985) in the northern Mader area. Mud-mounds were established during the early Eifelian at Jebel el Otfal (WENDT 1993, KAUFMANN 1995) and Jebel Ou Driss. Biostratigraphical correlation of these sections is difficult because of rapid lateral facies changes and thickness variations as well as scarcity of conodonts and goniatites. Thicknesses range from 30-50 m in the southern Tafilalt (El Atrous) up to 220 m in the northern Mader area (Ouihlane).

2) Basinal facies. This facies characterizes the central Mader Basin and extends from the northern Mader (Irhfelt n'Tissalt) to the southeast (Oued el Mechot) and towards the east into the western Tafilalt (Ottara) (Text-fig. 4). It consists of monotonous, sometimes laminated mudstones, limestone-marl rhythmites and shales. Similar lithologies occur in the southeastern Tafilalt (Hassi Nebech, Text-figs 4, 6), another area of stronger subsidence which subsequently developed into the Tafilalt Basin (WENDT 1988). Remarkable phenomena of folding in this facies are seen at Jebel Amessoui, Irhfelt n'Tissalt, Ouihlane, Jebel el Otfal and Hassi Nebech. They comprise several tens of metres thick rock piles, which are uniformly folded, suggesting a single

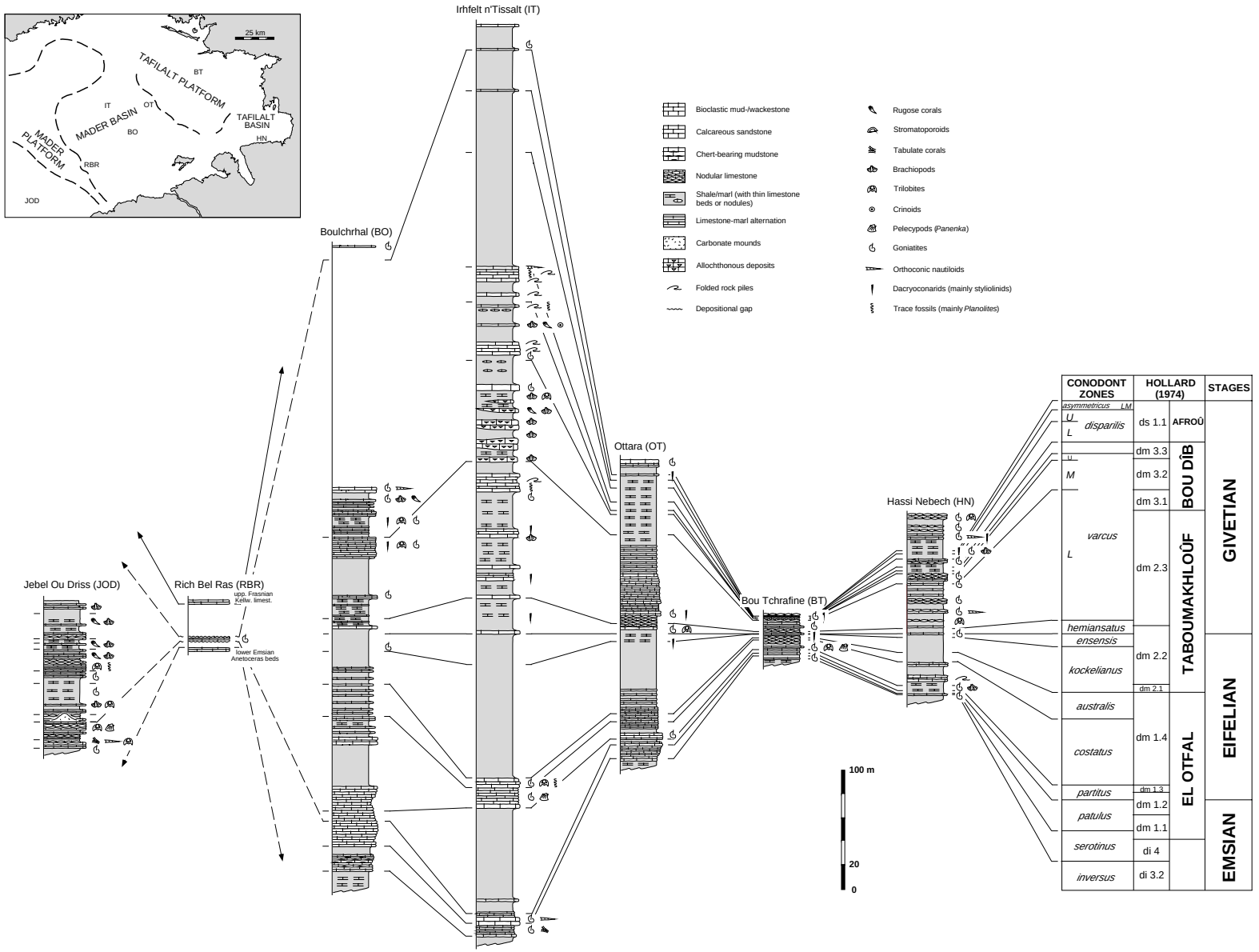

Correlation of typical upper Emsian to lower Frasnian sections of the eastern Anti-Atlas; correlation of HOLLARD's (1974) lithological units with the actual upper Emsian to Givetian conodont zonation after data in ALBERTI (1980, 1981a), BULTYNCK & HOLLARD (1980), BULTYNCK & JACOBS (1981) and own calculations; relative duration of conodont zones in the Eifelian and Givetian stage after BELKA & *al*. (in press) and HOUSE (1995) respectively; ottara and Boulchrhal sections modified and completed after HOLLARD (1974); Irhfelt n'Tissalt section modified and completed after HOLLARD (1974), BULTYNCK & JACOBS (1981) and WENDT (*written comm*.)

process of deformation, either synsedimentary (sliding/slumping) or tectonic in origin (*see* discussion further in this paper). The fauna of the basinal facies is sparse and consists of occasional goniatites, trilobites, orthoconic nautiloids, dacryoconarids and trace fossils (*Zoophycos*). Thickness varies from 50 m in the Tafilalt Basin up to 230 m in the central Mader Basin (Irhfelt n'Tissalt) (Text-fig. 6).

3) Condensed pelagic facies. Condensed nodular limestones and marls occur in the northern, northeastern and central Tafilalt (Text-fig. 4). They consist mainly of fossiliferous wackestones and contain a rich pelagic fauna with goniatites, orthoconic nautiloids, dacryoconarids and trilobites. Eifelian biostratigraphy is well documented by goniatites and conodonts at the famous Bou Tchrafine section (BULTYNCK & HOLLARD 1980; BULTYNCK 1985, 1987; BECKER & HOUSE 1994) (Text-fig. 6), about 8 km southeast of Erfoud. Thicknesses range from 6 to 20 m (MASSA 1965, BECKER & HOUSE 1994). The strong stratigraphic condensation suggests deposition on a submarine high (Tafilalt Platform) (WENDT 1988).

Givetian

During the Givetian, the differentiation of the facies pattern continued (Text-figs 5, 7). In the neritic facies belt, coral-stromatoporoid limestones, intercalated within argillaceous wackestones, extended from the northern Mader (Jebel Rheris, Ouihlane) across the western (Jebel Issimour, Jebel Oufatène) and southern Mader (Madène el Mrakib) to the southern Tafilalt (Jebel Amessoui) (Text-fig. 5). Generally, the coral-stromatoporoid limestones are lenses with a thickness of a half to a few metres. The frame-building organisms are predominantly not *in situ*, but undestroyed and therefore only slightly displaced. At Madène el Mrakib, 20 m thick stromatoporoid--coral-cyanobacteria-boundstones are developed, which contain abundant calcified cyanobacteria (*Rothpletzella*) and thus probably reflect the most shallow-water environment in the Mader Basin. A few small patch reefs occur in lower Givetian sections of the southern Tafilalt (Jebel Amessoui, MASSA 1965, Fig. 13) and flat *in situ* colonies of "*Phillipsastrea*" of late Givetian age are found in the western Mader area (Aït Ou Amar) (WENDT 1988). Accumulation of the coral-stromatoporoid limestones culminated in early Givetian times (Lower *varcus* Zone). Simultaneously, the carbonate mounds of Aferdou el Mrakib and Guelb el Maharch were established in the southern Mader area (WENDT 1993, KAUFMANN 1995). Generally, growth of coral limestones ceased during the middle to late Givetian, but in the southwestern Tafilalt (Iferd Nou Haouar) and the western Mader area (Bou Terga), the youngest reef debris limestones are of earliest Frasnian age (WENDT & BELKA 1991). Thickness of the Givetian neritic facies ranges from 100-200 m (Text-fig. 6).

Strong subsidence of the central Mader Basin extended the basinal facies from the depocentre (Irhfelt n'Tissalt) to the south (Text-fig. 5). Finally, in late Givetian to early Frasnian times, the neritic environment was drowned and the entire Mader Basin was covered with 100-400 m thick, monotonous shales, occasionally intercalated with calcareous sandstones (Text-fig. 6).

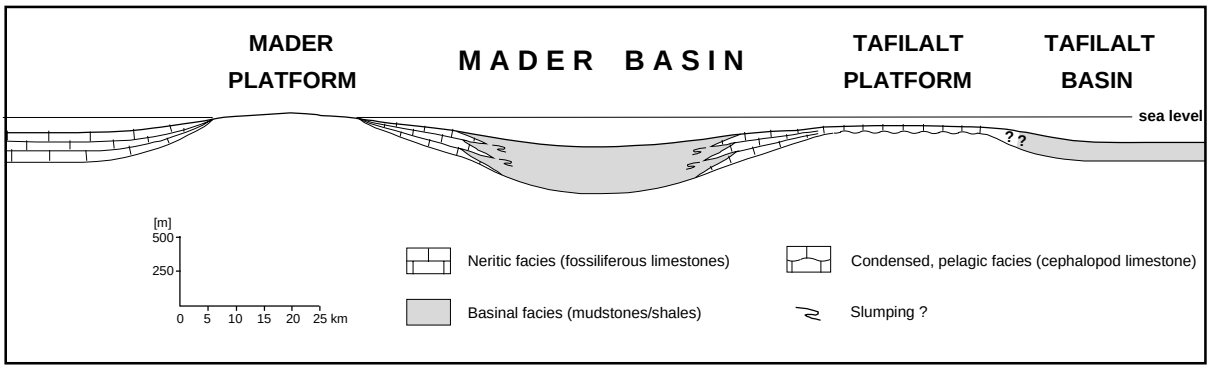

Fig. 7. Simplified lower Givetian (Lower *varcus* Zone) facies profile of the eastern Anti-Atlas, drawn along a line Tarhbalt – Fezzou – Jebel Amessoui – Jebel Debouaâ – Hassi Nebech (*see* Text-fig. 5)

As in Eifelian times, the Tafilalt Platform was covered by condensed, nodular cephalopod limestones (Text-fig. 7), ranging from 8 to 15 m in thickness (WALLISER 1991, BECKER & HOUSE 1994). At some localities near the western margin of the Tafilalt Platform (*e.g.* Ras el Kebbar), up to 30 m thick debris flows occur. They consist of redeposited cephalopod limestones interbedded with crinoidal limestones and have obviously been derived from the nearby Tafilalt Platform.

Early to Middle Devonian events and eustatic sea-level changes

Qualitative Early to Middle Devonian eustatic sea-level curves have been presented for Euramerica (JOHNSON & *al.* 1985, 1996) and for Australia and Southwest-Siberia (TALENT & YOLKIN 1987), but only very scarce data have been published from North Africa to date.

The distinct facies pattern in the eastern Anti-Atlas resulted from differential subsidence, leading to a platform and basin topography. The transgressive evolution of the Middle Devonian succession of the Mader Basin was caused mainly by rapid subsidence. Eustatic sea-level changes, superimposing the subsidence pattern are difficult to recognize. Local deepening events, *e.g.* termination of mound growth, cannot by correlated over the entire Mader area and hence do not reflect eustatic sea-level rises. Eustatic sea-level changes are developed rather clearly on the tectonically more stable shallow pelagic Tafilalt Platform, which reflect such fluctuations more precisely from faunal and sedimentary evidences.

Only three (the younger of the two intra-Ib deepening events = lower part of the *inversus* Zone, Ie = mid-*kockelianus* Zone and IIa = Middle *varcus* Zone) of eight Early to Middle Devonian major transgressive events (Ia to IIb) of JOHNSON's (1985, 1996) 'global' sea-level curve can be recognized in the eastern Anti-Atlas (Text-fig. 8). These events correlate with the Daleje, Kacak and Taghanic Events (HOUSE 1985) respectively. The remaining five major transgressions, however, cannot be recognized and clear evidences for these events from elsewhere in the world are so rare, that doubts arise about the general global applicability of JOHNSON's curve.

Other events, represented in Lower to Middle Devonian sections of the eastern Anti-Atlas are the end-*pesavis* Event (TALENT & *al.* 1993), the Chotec Event (CHLUPAC & KUKAL 1986) and the *pumilio* Events (LOTTMANN 1990). The end-*pesavis* and Chotec Events are possibly also related to global sea-level changes but they do not correspond to any change in JOHNSON's sea-level curve.

End-pesavis *Event*

ALBERTI (1981b) reported a conspicuous colour change from dark to light at the Lochkovian/Pragian boundary of some sections on the Tafilalt Platform and attributed it to a possible eustatic sea-level fluctuation. This change correlates with the end-*pesavis* Event of TALENT & *al.* (1993), a conspicuous reduction in conodont diversity at the end of the latest Lochkovian *pesavis* Zone. In eastern Australia, this reduction is related to a regional regression, but a global component of that regression is uncertain (TALENT & *al.* 1993).

Daleje Event

The Daleje Event (HOUSE 1985), typified from sequences in Bohemia (CHLUPAC & KUKAL 1986), corresponds to an apparently global transgression (younger of the two intra-Ib transgressions of JOHNSON & *al.* 1985, 1996) that occurred in the lower part of the *inversus* Zone. This event can be recognized in the entire eastern Anti-Atlas by a lithological change from fossiliferous limestones to basinal, green shales ('Emsien argileux' of MASSA 1965, 'di 3.2' of HOLLARD 1974, 'Er Remlia' of HOLLARD 1981), which are much poorer in fossils.

Chotec Event

The Chotec Event (CHLUPAC & KUKAL 1986) happened within the *partitus* Zone (early Eifelian), immediately prior to the first occurrence of *Pinacites jugleri* (*jugleri* Event, WALLISER 1985). It is well represented in the Tafilalt at Bou Tchrafine, Jebel Amelane, Jebel Mech Irdane, Hamar Laghdad and Gara Mdouard (ALBERTI 1980, BECKER & HOUSE 1994). The Chotec Event is characterized by a thin interval of dark calcareous shales and large black limestone concretions with masses of styliolinids (BECKER & HOUSE 1994). The dark

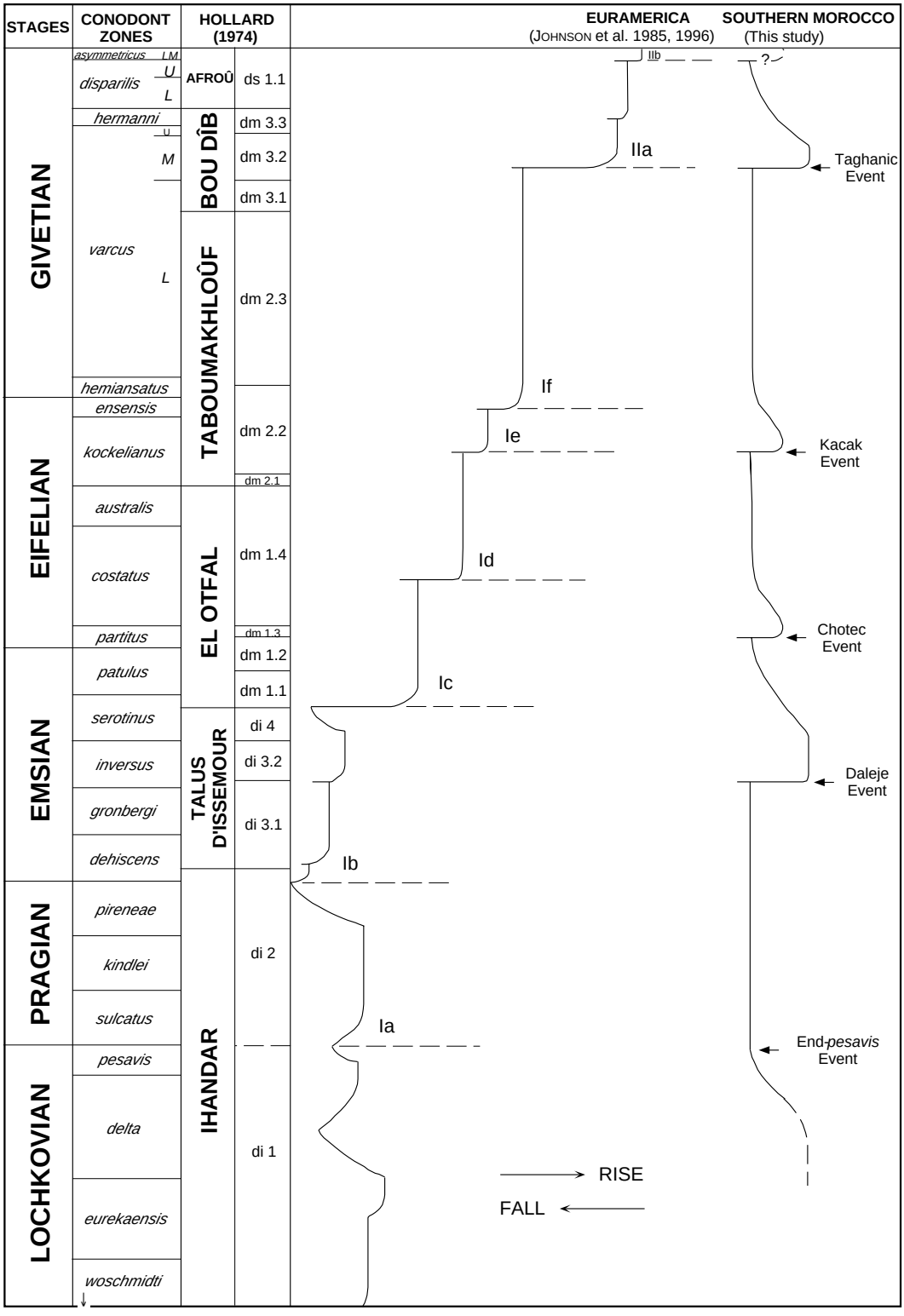

Fig. 8. Comparison of eustatic sea-level changes in Euramerica and Morocco; correlation of HOLLARD's (1974) lithological units with the actual Lower to Middle Devonian conodont zonation after data in ALBERTI (1980, 1981a), BULTYNCK & HOLLARD (1980), BULTYNCK & JACOBS (1981) and own calculations; relative duration of conodont zones in the Eifelian and Givetian stage *after* BELKA & *al*. (in press) and HOUSE (1995) respectively; relative duration of stages after JOHNSON & *al*. (1985)

sediments are generally interpreted as a hypoxic event (CHLUPAC & KUKAL 1986), probably related to an eustatic sea-level rise. Correlatable dark intervals at the same stratigraphic positions have also been reported from Bohemia (type locality, CHLUPAC & KUKAL 1986), Germany (REQUADT & WEDDIGE 1978) and Northern Spain (HENN 1985).

Kacak Event

The Kacak Event (HOUSE 1985) corresponds approximately to WALLISER's (1985) *otomari* and *rouvillei* Events and is marked by a facies change to dark sediments in late Eifelian times (mid-*kockelianus* Zone). In the Tafilalt, the event is represented by a black shale intercalation at Bou Tchrafine, Jebel Amelane and Jebel Mech Irdane (BECKER & HOUSE 1994, WALLISER & *al*. 1995). It can be correlated to sections in Germany (WALLISER 1985), Spain (TRUYOLS-MASSONI & *al*. 1990) and Bohemia (CHLUPAC & KUKAL 1986). Similar to the Chotec Event, it is inferred to a hypoxic perturbation, probably related to an eustatic sea-level rise (Text-fig. 8), which is also documented at this time from Euramerica (transgression Ie of JOHNSON & *al*. 1985, 1996).

Taghanic Event

The Taghanic Event (HOUSE 1985) happened in the middle Givetian (Middle *varcus* Zone) and was a major ammonoid extinction event of the Devonian. It also refers to the subsequent appearance of the genus *Pharciceras* (*Pharciceras* Event of WALLISER 1985) and is probably related to a major transgression, documented worldwide (transgression IIa of JOHNSON & *al*. 1985, 1996; TALENT & YOLKIN 1987). On the southern margin of the Tafilalt Platform (Jebel Aoufilal, Jebel Debouaâ), this event correlates with the onset of green shales overlying condensed cephalopod limestones. Possible evidence for a hypoxic character is a thin, dark styliolinite at Jebel Amelane (BECKER & HOUSE 1994). It is likely that this trangression event superimposed regional, subsidence-caused deepening events in the Mader Basin and caused the drowning of the neritic facies in this area.

Pumilio *Events*

The *pumilio* Events (LOTTMANN 1990) also happened in middle Givetian times (Middle *varcus* Zone) and are represented by two dark horizons, consisting mainly of small lenticular brachiopods ("*Terebratula*" *pumilio*). In the eastern Anti-Atlas, these events can be recognized in many areas of the Tafilalt. They are interpreted as tsunami deposits and can be correlated to sections of Algeria, France and Germany (LOTTMANN 1990).

MIDDLE DEVONIAN CARBONATE MOUNDS OF THE MADER AREA

With the exception of Hamar Laghdad, all Devonian carbonate mounds of the eastern Anti-Atlas are located in the Mader area (Text-fig. 2). They are intercalated within a 150-400 m thick Middle Devonian succession of bedded, fossiliferous limestones which contain crinoids, brachiopods, tabulate and rugose corals, trilobites, bryozoans, gastropods, pelecypods and, less common, pelagic elements, such as cephalopods (goniatites, orthoceratids) and dacryoconarids. The mounds, which are subject of this study, are exposed at the following five localities (x-, y-coordinates are Clarke ellipsoids 1880 from the topographical map of Morocco 1:100000):

Aferdou el Mrakib (Top): sheet 'Fezzou' (NH-30-XIV-3): x = 574.1; y = 417.8
Guelb el Maharch: sheet 'Fezzou' (NH-30-XIV-3): x= 580.2; y = 419.5
Jebel el Otfal (Mound 1): sheet 'Fezzou' (NH-30-XIV-3): x = 579.1; y = 432.7
(Mound 2): sheet 'Fezzou' (NH-30-XIV-3): x = 579.4; y = 432.8
(Mound 3): sheet 'Fezzou' (NH-30-XIV-3): x = 579.3; y = 432.0
(Mound 4): sheet 'Fezzou' (NH-30-XIV-3): x = 579.6; y = 431.8
Jebel Ou Driss: sheet 'Tarhbalt' (NH-30-XIII-4): x = 507.9; y = 391.0
SE' Jebel Zireg: sheet 'Fezzou' (NH-30-XIV-3): x = 583.6; y = 403.4

Aferdou el Mrakib

Geological and stratigraphical setting, off-mound succession

The Aferdou el Mrakib reef-mound is located at the northern flank of the 15 km wide, E-W-

trending Jebel el Mrakib (Text-fig. 9), a range forming the southeastern limb of a 40-50 km wide Variscan syncline, which is the largest tectonic structure of the eastern Anti-Atlas (Text-fig. 2). Here, a Lower to Middle Devonian (Emsian to lower Givetian) sequence is exposed (Text-fig. 31), dipping with 6° to the north. The uppermost 25 m (upper Eifelian to lower Givetian) of the succession are preserved only in the immediate surrounding of the Aferdou mound, where they form the mound basement; they were protected from erosion by the overlying mound (Pl. 1, Fig. 1; Pl. 2, Fig. 1).

The Eifelian interval at Jebel el Mrakib ('El Otfal Formation' of HOLLARD 1974, 1981) is about 75 m thick (Text-fig. 31) and exhibits a shallowing-upward sequence from deep-water unfossiliferous, chert-bearing mudstones with high siliciclastic influx over burrowed, bioclastic wackestones of moderate depth to relatively shallow-water crinoidal grainstones. The latter are 22 m thick and restricted to the site of the Aferdou mound.

The base of the Givetian is marked by a 2 m thick coral-stromatoporoid boundstone (Text-fig. 10; Pl. 3, Fig. 4), which directly underlies the Aferdou mound and probably served as a pioneer stage in mound development. It is overlain by crinoidal grainstones and, three metres above, these by a conspicuous, 30 cm thick trilobite wackestone (commercially exploited level with abundant *Drotops megalomanicus* STRUVE 1990) (Text-fig. 10). The section continues with 13 m of poorly fossiliferous mudstones which, in the middle part, contain a 3 m thick brachiopod lense (exclusively *Ivdelinia* sp., Pl. 13, Fig. 11). These mudstones are followed by 20 m of mound debris facies. The Aferdou mound interfingers with the off-mound strata (17 m in thickness), which overlie the initial coral-stromatoporoid bed and with the lower 5 m of the mound debris facies (Text-fig. 10). Unfortunately, the lateral transition of the mound debris facies to the coeval off-mound strata has been removed by erosion. The same applies to strata, which directly overlie the Aferdou mound. They are preserved only at two small areas on the northern flank of the Aferdou mound (Text-fig. 11), where they cap the mound debris facies. They consist of 2-3 m thick, slumped, blue-grey, poorly-fossiliferous mudstones (Pl. 1, Fig. 2; Text-fig. 10) which occasionally contain coarse mound debris.

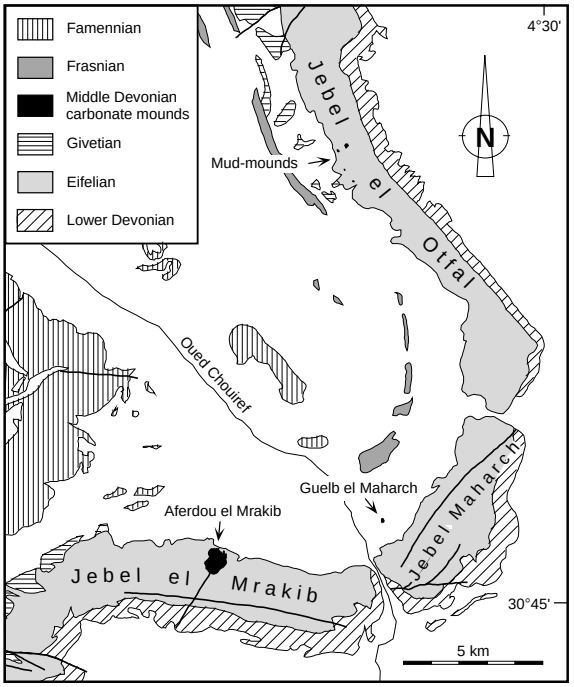

Fig. 9. Geological map of the southern central Mader area (*see* Text-fig. 2) with locations of the three most conspicuous mound occurrences (Aferdou el Mrakib, Guelb el Maharch, Jebel el Otfal); modified from the geological map 1:200.000, sheets 'Todrha-Ma'der' and 'Tafilalt-Taouz'

Size and geometry

Aferdou el Mrakib is the largest reefal structure of the eastern Anti-Atlas. It has an almost circular outline with a diameter of about 900 m (Text-fig. 11), a truncated cone-shape (Pl. 1, Fig. 1; Pl. 2, Fig. 1) and a height of 100-130 m (Pl. 1, Fig. 1). The mound has a rather symmetrical shape (after correction of the flank inclinations for rotation of underlying northward-dipping strata, Text-fig. 12) with a mean angle of flank inclination of 35°. By adding the eroded mound flank beds on the other mound sides, an original diameter of 1700-1800 m (including mound debris facies) can be reconstructed for the Aferdou mound (Text-fig. 13). Caused by northward Variscan tilting, the north side of the mound has been prevented longer from erosion and thus displays primary mound surfaces. On the top of the mound slopes, flank beds are cut discordantly (Pl. 1, Figs 2a, b), showing post-sedimentary erosion. According to WENDT (1993), the original height can be reconstructed

by extrapolation of the flank beds as about 250 m (Text-fig. 13). SCHWARZACHER (1961) found similar discordant cuts of mound tops in Lower Carboniferous mud-mounds of Ireland and suggested that mound growth was controlled by wave action. Because the upper mound surface of Aferdou el Mrakib is inclined in the same direction as the underlying strata (Pl. 2, Fig. 1), it cannot be excluded that a wave-related erosion took place prior to Variscan tilting.

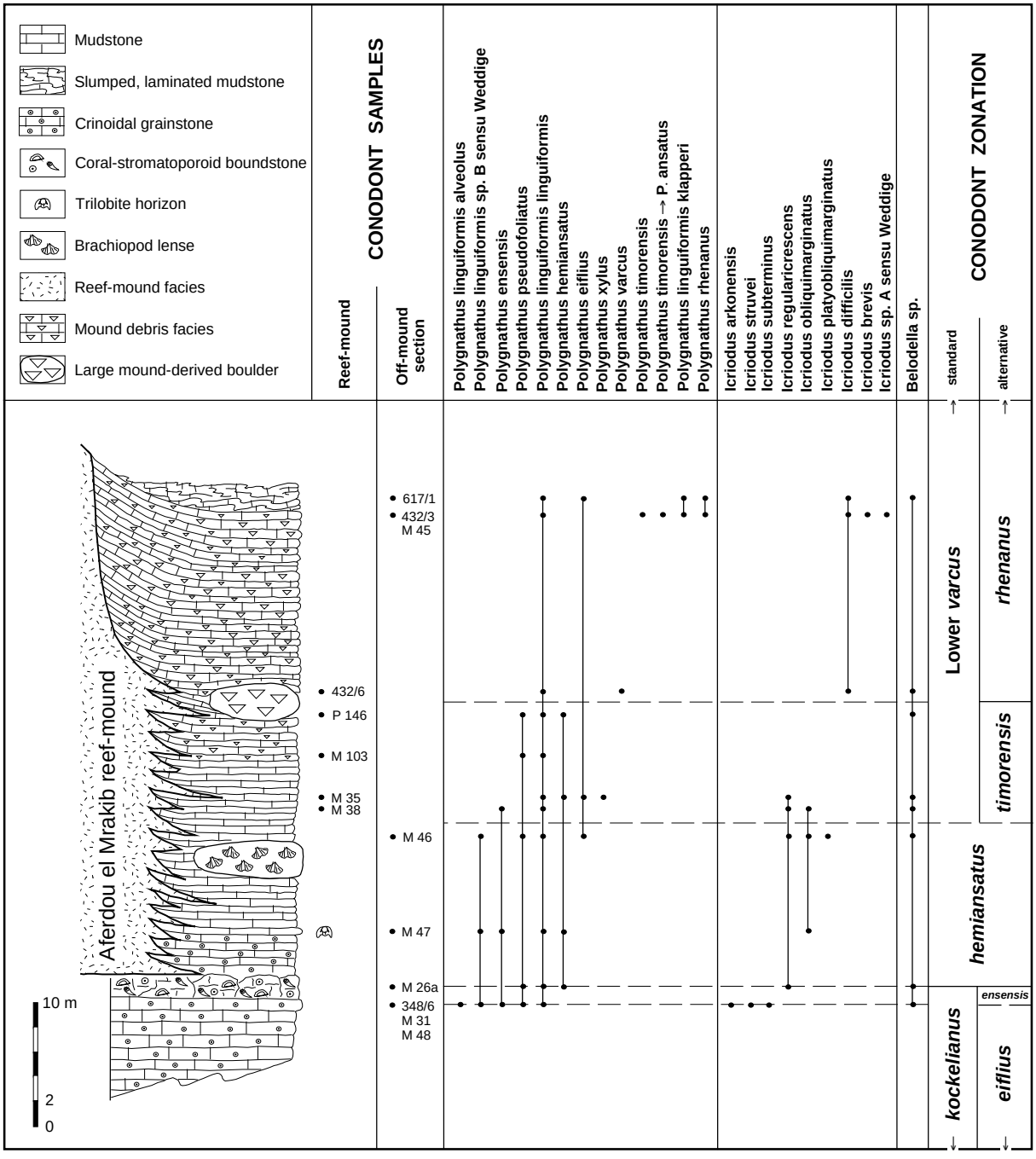

Fig. 10. Lithology of Aferdou el Mrakib off-mound section with conodont distribution; alternative conodont zonation *after* BELKA & *al*. (in press)

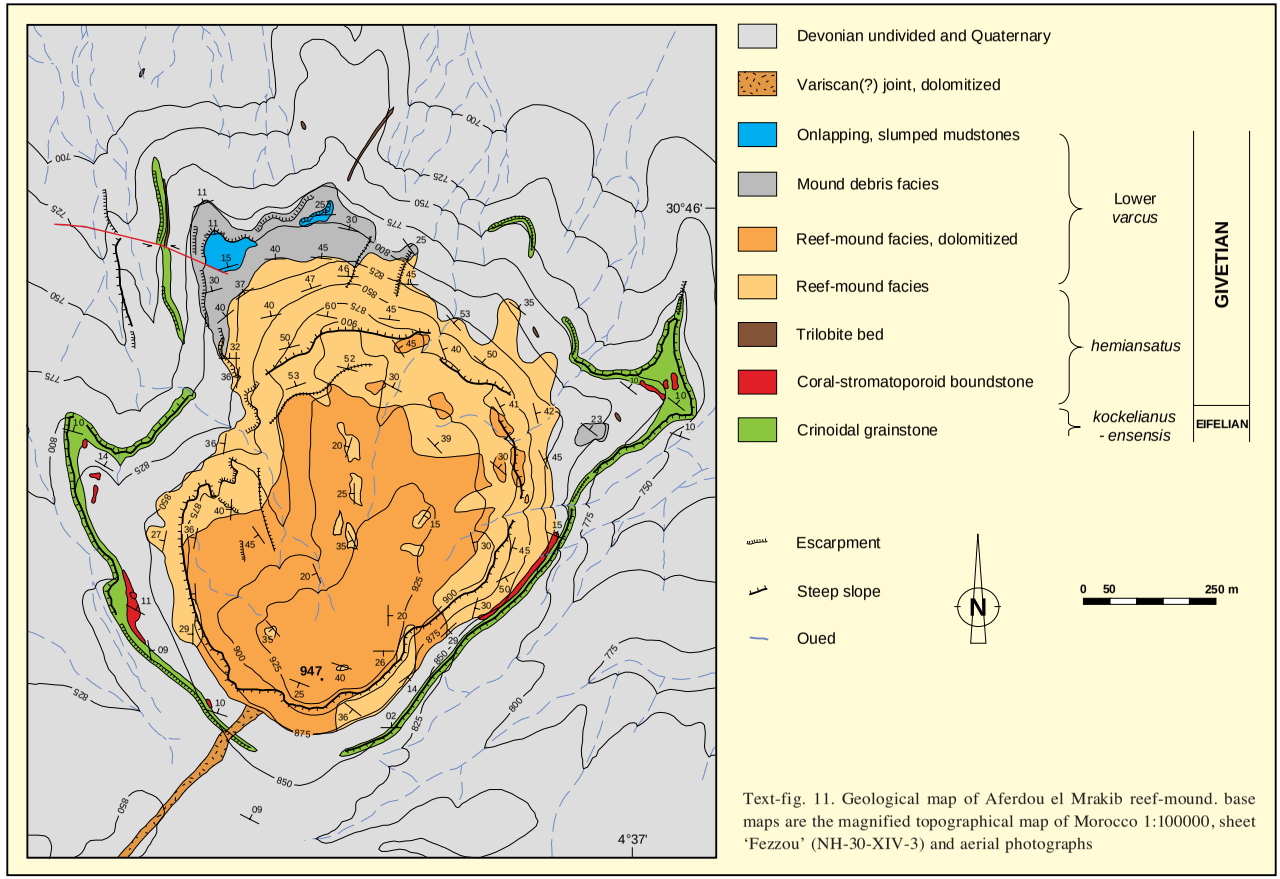

Text-fig. 11. Geological map of Aferdou el Mrakib reef-mound. base maps are the magnified topographical map of Morocco 1:100000, sheet 'Fezzou' (NH-30-XIV-3) and aerial photographs

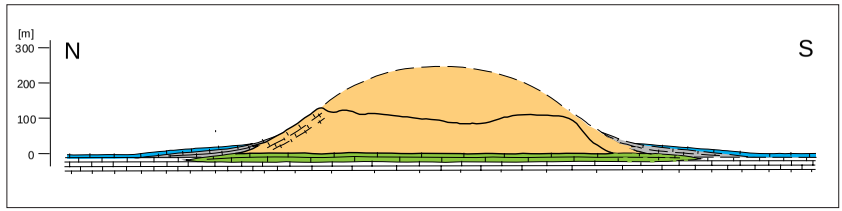

Text-fig. 13. Reconstruction of Aferdou el Mrakib reef--mound by extrapolation of discordantly cut mound flanks; thick black line is actual mound profile; legend as in Text-fig. 11

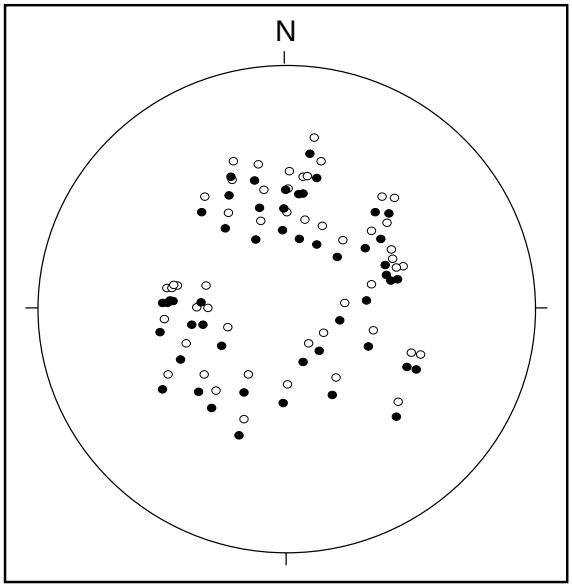

Text-fig. 12. Stereographic projection (upper hemisphere) of polar points of Aferdou el Mrakib mound flanks; empty points before, black points after correction for rotation of underlying strata to the horizontal (rotation axis: 106/06); note rather symmetrical flank inclinations after rotation

Lithology and sedimentary structures

The reef-mound facies is rather uniform and consists of indistinctly thick-bedded, stromatactoid boundstones (purely descriptive: wackestones and floatstones). A detailed descripition of stromatactis fabrics (of all Mader carbonate mounds) is given further in this paper. No distinction between flank- and core-facies can be made. A massive bedding with bed thicknesses of 0.5-1 m is ubiquitous, even in dolomitized areas. The beds dip away from the centre (Text-fig. 11), suggesting that the mound grew concentrically, both expanding laterally and vertically. Unfortunately, no informations about eventual ecological succession within the mound can be obtained, because the Aferdou mound is not cut by erosion and therefore does not exhibit its internal structure. Locally, coral boundstones occur, formed by few m^2-sized *in situ* colonies of distinct coral species [especially *Platyaxum* (*Platyaxum*) *escharoides* (STEININGER 1849) (Pl. 3, Fig. 3), cf. *Fletcheria* (Pl. 2, Fig. 7) and *Thamnophyllum ossalense* (JOSEPH & TSIEN 1975)].

The mound debris facies is only preserved on the northern flanks of the mound and in an isolated occurrence on the east side (Text-fig. 11). It consists of up to 20 m thick, mound-derived coral-stromatoporoid floatstones (Text-fig. 10) which contain large mound-derived boulders (Pl. 2, Fig. 2). Interfingering with the massive mound facies can be seen on the northwestern side of the mound (Pl. 1, Figs 2a, b). Originally, the mound debris facies probably formed an aureole surrounding the mound and was later largely removed by erosion.

The central part of the mound is pervasively dolomitized (Text-fig. 11) whereby both fossils and sedimentary structures have been obliterated. A dolomitized NE-SW-trending Variscan(?) joint runs into the south side of the mound and has obviously acted as a conduit for dolomitizing fluids.

Small scale fissures and neptunian dykes, only few centimetres wide and to be followed for 2-3 metres, have been found in the Aferdou mound. Generally, they are filled with dark mudstones or, in one case, with fine-grained sandstone which is similar to the Lower Carboniferous deltaic sandstones that overlie the Devonian sucession of the eastern Anti-Atlas (WENDT 1993).

Fauna

Aferdou el Mrakib is the mound with the most abundant and most varied fauna (Text-fig. 14). It is described as 'reef-mound' because the potential Devonian reef-builders (stromatoporoids, colonial rugose corals) are present but do not form a rigid framework.

Stromatoporoids occur mostly as undestroyed but slightly displaced or overturned individuals, but they occur also frequently *in situ* (Pl. 2, Fig. 5). Domical morphotypes (*Actinostroma* ?, *Stromatoporella* ?, *Clathrodictyon* ?), 20-80 cm in diameter, dominate; laminar forms are rare and dendroid forms are totally absent. According to JAMES & BOURQUE (1992), the relationship between external shape and internal growth banding geometry of stromatoporoids can be used to infer relative sedimentation rates and water roughness. In the Aferdou mound, the predominant growth forms with enveloping latilaminae without ragged margins indicate a relatively low sedimentation rate (compared with a 'true' reef) and low water roughness.

Siliceous sponge spicules (smooth hexacts; Pl. 13, Figs 9-10) of hexactinellids were found

frequently in insoluble residues and in thin sections. Coralline sponges are represented by rare chaetetids.

Solitary rugose corals are represented by *Heliophyllum halli moghrabiense* LE MAÎTRE 1947, *Cystiphylloides* sp. (Pl. 2, Fig. 6), *Acanthophyllum* sp., *Macgeea* cf. *minima* BRICE 1970, *Siphonophrentis* sp., *Stringophyllum normale* WEDEKIND, 1922, *Calceola sandalina* LAMARCK, 1799 (rare) and metriophyllids. *Thamnophyllum ossalense* (JOSEPH & TSIEN 1975) forms some m^2-sized, dendroid colonies. In addition, flat, disc-shaped colonies of "*Phillipsastrea*" (Pl. 2, Fig. 4) and, less common, "*Hexagonaria*", occur. Further colonial rugose corals belong to the bizarre group of *Fletcheria* MILNE-EDWARDS & HAIME (Pl. 2, Fig. 7).

The tabulate coral fauna displays a high taxonomic diversity. Fragments of branching striatoporids (cf. *Pachystriatopora*, Pl. 3, Fig. 7), "thamnoporids" (*Thamnopora germanica* BIRENHEIDE, 1985, *Thamnopora proba* DUBATOLOV 1955) and auloporids (*Bainbridgia* sp., *Cladochonus* sp., *Remesia* sp.) are ubiquitous in the mound facies. Favositids are represented by massive, fascicular colonies (mainly *Favosites* cf. *goldfussi* ORBIGNY, 1850) and by 3-10 mm thick and up to 20 cm wide, *in situ* crusts of alveolitids [mainly *Platyaxum* (*Platyaxum*) *escharoides* (STEININGER, 1849), Pl. 3, Fig. 3). Heliolitids (*Heliolites* cf. *porosus* (GOLDFUSS 1826)] occur rarely as spherical colonies.

Brachiopods are abundant in the Aferdou mound. The two big-sized, thick-shelled pentamerid genera *Ivdelinia* sp. (Pl. 13, Fig. 11) and *Devonogypa* sp. form conspicuous, monotypical, several m^2-sized *in situ* communities. GODEFROID & RACKI (1990) described similar reef-dwelling faunas from 'nests, lenses and bands' in Frasnian fore-reef limestones and attributed these brachiopods to semi-protected, intermittendly agitated habitats which would reflect the assumed moderate bathymetric position of the Aferdou mound. Other brachiopods belong to spiriferids (*Atrypa*?, *Planatrypa* sp., *Spinatrypa* sp., *Carinatina* sp., Spinatrypinae), orthids (*e.g.* *Schizophoria* sp.), athyrids and rare strophomenids (*Leptaena* sp.).

Crinoids are ubiquitous in the reef-mound. They are mainly disarticulated into single ossicles and rarely preserved as up to 20 cm long stems. Crowns and holdfasts have not been found.

Cephalopods (orthoconic nautiloids and goniatites) are extremely rare in the reef-mound facies.

Additionally, dacryoconarids (common styliolinids, rare *Nowakia* sp.), fragments of fenestellid bryozoans, trilobite carapaces, small gastropods, rare ostracods and microproblematica [*Rothpletzella devonica* (MASLOV 1956), Pl. 3, Fig. 8] were found in thin sections.

Rare findings of shark teeth (*Phoebodus fastigatus* GINTER & IVANOV, 1992; Pl. 13, Figs 1-4) in insoluble residues suggest that sharks belonged to the mound's ecosystem.

Guelb el Maharch

Geological and stratigraphical setting, off-mound succession

The cone of Guelb el Maharch (Pl. 4, Fig. 1) rises above the plain of Oued Chouiref in the southeastern quarter of the Mader syncline (Text-fig. 9). The mound basement with the off-mound and intermound transitions is covered by Quaternary deposits. The nearest off-mound strata are exposed 800 m southeast of the mound at the 7 km wide Jebel Maharch, which constitutes the continuation of the Jebel el Mrakib range towards NNE (Text-fig. 9). Stratigraphy, thickness of individual units and facies evolution of the Emsian to Eifelian succession at Jebel Maharch correspond to that of Jebel el Mrakib. Only the youngest bed at Jebel Maharch, a conspicuous, 50 cm thick cephalopod limestone of late Eifelian age (*kockelianus* Zone) could not be recognized at Jebel el Mrakib. If one projects the 6°-dipping cephalopod bed below the Guelb el Maharch mud-mound, about 80-90 m of thickness are concealed below the plain between the bed and the mound. The nearest overlying strata are bituminous styliolinid limestones (Kellwasser facies) of early Frasnian age (Lower *asymmetricus* Zone), exposed 2 km NNW of the mound (WENDT & BELKA 1991).

Size and geometry

Guelb el Maharch is the second largest mound of the Mader area. It has an exposed base-diameter of 120-180 m and a height of

Occurrence and relative abundance of fossils in Middle Devonian carbonate mounds of the Mader.

	Aferdou el Mrakib	Guelb el Maharch	Jebel el Otfal Mound 1	Jebel el Otfal Mound 2	Jebel el Otfal Mound 3	Jebel el Otfal Mound 4	Jebel Ou Driss
PORIFERA							
Domical stromatoporoids	●						
Hexactinnelids	□	□	●	□	△		
Chaetetids	△						
COLONIAL RUGOSE CORALS							
"Hexagonaria"	□						
"Phillipsastrea"	□						
SOLITARY RUGOSE CORALS			×	×	×		
Heliophyllum halli moghrabiense	□						
Cystiphylloides sp.	●						
Acanthophyllum sp.	△						
Macgeea cf. *minima*	△						
Siphonophrentis sp.	□						
Stringophyllum normale	□						
Calceola sandalina	△						
Thamnophyllum ossalense	□						
Amplexocarinia sp.				△			
cf. *Fletcheria*	□	□	□		□		
cf. *Neomphyma*							□
Metriophyllids	□	△		△			
TABULATE CORALS							
Striatoporids							
cf. *Pachystriatopora*	□	□	□		□	□	
cf. *Taouzia*			□				□
cf. *Crenulipora*		□					
cf. *Zenmmourella*		□					□
Dualipora preciosa						●	
Thamnoporids							
Thamnopora germanica	□						
Thamnopora proba	□						
Auloporids			×				
Bainbridgia sp.	□	●		●	□	□	
Cladochonus sp.	□	□				□	
Remesia sp.	△	□			□	□	
Aulocystis sp.		△			□		
Favositids							
Favosites cf. *goldfussi*	□						
Platyaxum (P.) escharoides	●						
Heliolitids							
Heliolites cf. *porosus*	△						
BRACHIOPODS							
Pentamerids			×	×	×	×	×
Ivdelmia sp.	●						
Devonogypa sp.	●						
Spiriferids							
Atrypa ?	●	□		×	×		
Planatrypa sp.	□			□			
Spinatrypa sp.	□						
Carinatina sp.	□	□					
Desquamatia sp.				□			
Spinatrypinae	□						
Orthids							
Schizophoria sp.	□	×					
Strophomenids							
Leptaena sp.	□						
Athyrids	□						
BRYOZOANS							
Fenestellids	□	□	△	□			
Fistuliporids		□		□			
MOLLUSCS							
Cephalopods	△	△			△		
Gastropods			△	□	□	△	△
Pelecypods				□			
CRINOIDS	●	□	□	●	□	□	□
TRILOBITES	□	△	□	□	□	●	□
DACRYOCONARIDS	□	□	□	□	□	△	□
OSTRACODES	□	□	△	□			△
AGGLUTINATED FORAMINIFERA		△	△	△	□	□	
MICROPROBLEMATICA							
Rothpletzella devonica	□			△			
CONODONTS							
Polygnathids	□	△	△	△	△	□	
Icriodids	□	△		△		△	△
Belodella sp.	□	□	△	□	△	△	
SHARK TEETH	△						

● = frequent □ = present △ = rare × = undetermined genera

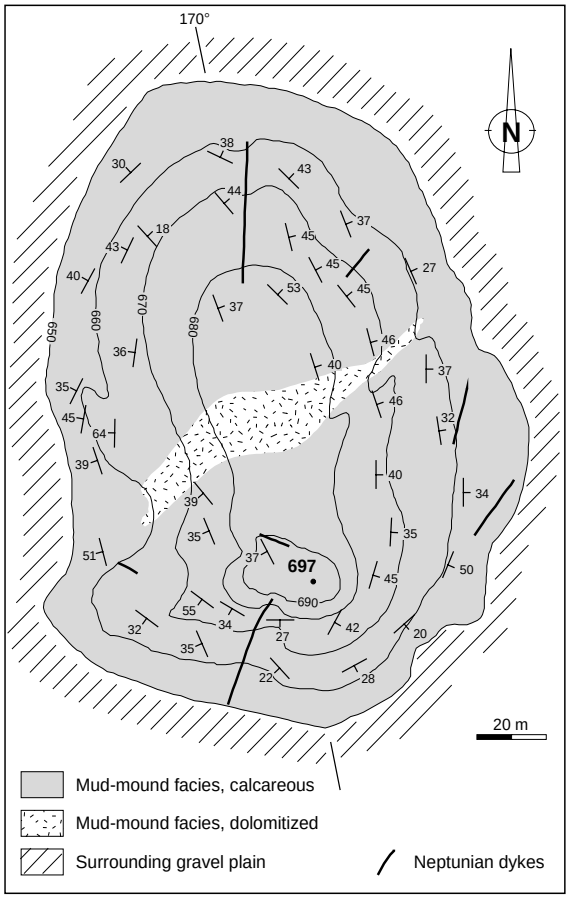

Fig. 15. Outline and topography of Guelb el Maharch mud-mound

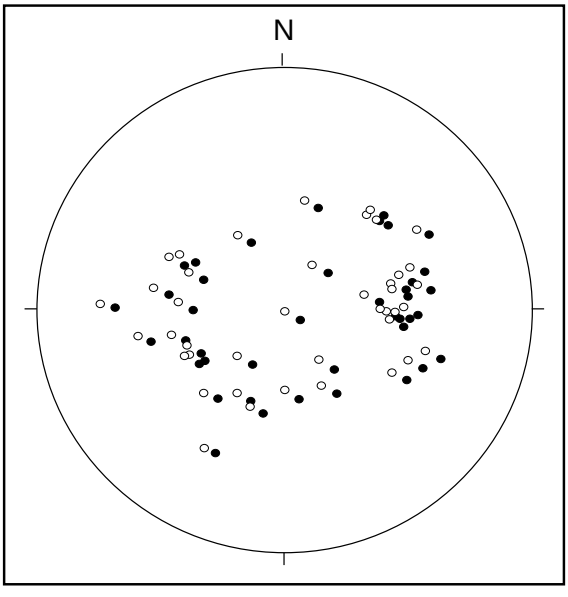

Fig. 16. Stereographic projection (upper hemisphere) of polar points of Guelb el Maharch mound flanks; empty points before, black points after correction for rotation of underlying strata to the horizontal (rotation axis: 029/06); note slight asymmetry with steeper eastern than western flanks.

about 45 m (Text-fig. 15). Though the contact to the directly underlying beds is covered, the original height is probably only a few metres more, because the inclination of the mound flanks becomes more gentle at the mound periphery. Additionally, the covered thickness of 80-90 m corresponds approximately to the same interval (*kockelianus* to Lower *varcus* Zone) at Jebel el Mrakib. The mound shape is conical with a slight elongation in N-S-direction (170°). After correction for rotation of the nearest underlying strata to the horizontal (Text-fig. 16), the mound displays a slight asymmetry with steeper eastern (mean angle of inclination: 43°) than western flanks (mean angle of inclination: 35°). Steep mound flanks represent primary accretionary surfaces as is evidenced by the horizontal alignments of brachiopod infillings and laminations of internal sediments.

Lithology and sedimentary structures

In contrast to the Aferdou mound, Guelb el Maharch consists exclusively of massive limestones with no bedding features. Microfacies analyses of polished hand specimens and thin sections from a great variety of mound positions show a very uniform lithology of stromatactis-bearing boundstones (Pl. 5, Figs 3-4). Pervasive dolomitization occurs along an up to 20 m wide band, which runs in NE-SW-direction through the centre of the mound (Text-fig. 15).

Neptunian dykes are common in this mound. Generally, they are 2-5 cm wide, filled with dark mudstones and can be followed for 6-20 m (Pl. 4, Fig. 2). On the southern flank, a 1 m wide dyke, filled with a dark, crinoidal-brachiopod rudstone (Pl. 5, Fig. 2), cuts the mound from base to top (Pl. 4, Fig. 1). The two prefered directions of the dykes are NNE-SSW and WNW-ESE. Because the infillings have yielded no conodonts, the age of the dykes is unknown. Their formation was probably caused by tensional movements prior to

Variscan folding though the main directions could not be related to any pre-orogenic tectonics so far.

In addition to stromatactis fabrics, irregular cavities, 5-20 cm in size and filled with dark, laminated internal sediments have been found (Pl. 4, Fig. 3; Pl. 5, Fig. 1). Cavity margins are lined with 5 mm thick, laminated cement rims (Pl. 5, Figs 1, 4) and infillings are often dolomitized (Pl. 4, Fig. 3; Pl. 5, Figs 3, 4). Because those cavities occur in the immediate neighbourhood of neptunian dykes and contain the same, dark internal sediments, their formation is probably related to the dyke formation.

Fauna

Though only 6 km apart from Aferdou el Mrakib, the Guelb el Maharch mud-mound contains an impoverished fauna (Text-fig. 14). Stromatoporoids and colonial rugose corals are absent, and solitary Rugosa are represented only by isolated metriophyllids and cf. *Fletcheria*. Though the diversity of the tabulate corals is also strongly reduced, they are the prevailing faunal elements, represented by auloporids (*Bainbridgia* sp., Pl. 5, Figs 3, 8; *Cladochonus* sp., *Remesia* sp. and *Aulocystis* sp.) and striatoporids (cf. *Crenulipora*, Pl. 5, Fig. 7; cf. *Zemmourella*, *Pachystriatopora* sp.). Crinoids are also very common, preserved mostly as isolated ossicles, but also as *in situ* disintegrations of longer stems. Brachiopods are mainly represented by small forms (5-10 mm in size), which could not be determined generically. Atrypids (*Atrypa*?, *Carinatina* sp.) occur rarely. Cephalopods are represented only by a few orthoconic nautiloids, oriented in their most stable position with their apices towards the mound top. As at Aferdou el Mrakib, hexactinellid sponges are found commonly as isolated spicules (smooth hexacts) in insoluble residues and thin sections, but also rarely as whole sponge bodies, about 5 cm in diameter. Insoluble residues contain occasionally agglutinated foraminifers (*Sorosphaera* sp., *compare* Pl. 13, Figs 5-8). In thin sections, dacryoconarids (common styliolinids, rare *Nowakia* sp.), fragments of fenestellid (Pl. 5, Fig. 6) and fistuliporid bryozoans (the latter mostly incrusting tabulate corals), small gastropods (1-2 mm-sized) and rare trilobite carapaces were observed.

Jebel el Otfal

Geological and stratigraphical setting, off-mound succession

The range of Jebel el Otfal constitutes the continuation of Jebel Maharch in NNW-direction (Text-fig. 9). It is 15 km wide and forms the eastern limb of the large Mader syncline (Text-figs 2, 4). Four mud-mounds are located in an area of 6 km^2 (Text-fig. 17) in the central part of the range (Text-fig. 9). HOLLARD (1974 pp. 23-28, Fig. 3) studied the stratigraphy of the Jebel el Otfal in detail, sampled several fossiliferous horizons, and provided the first informations about the mud-mounds. A more detailed description and maps of the mounds were presented by WENDT (1993). The Lower to Middle Devonian (upper Pragian to lower Givetian) succession is significantly different from those of Jebel el Mrakib and Jebel Maharch. Only the facies of the late Pragian to early Eifelian interval corresponds more or less to the sections farther south (Text-fig. 31), but individual units are thicker (especially the upper Emsian shales, Text-fig. 3) and more argillaceous. The lower Eifelian (*partitus* to lower part of the *costatus* Zone) consists of 55 m thick rather uniform argillaceous, burrowed, bioclastic wackestones, which contain crinoids, brachiopods, tabulate and solitary rugose corals, fenestrate bryozoans, gastropods, goniatites, orthoceratids, trilobites and trace fossils (common *Planolites*, Pl. 8, Fig. 6; rare *Zoophycos*) (Text-fig. 31). The top of the section is a 2 m thick crinoidal limestone, which thickens to the largest mud-mound (mound no. 2) of Jebel el Otfal (Pl. 6, Figs 1, 2a, b; Text-fig. 19). Similar to the crinoidal limestones, which underly the Aferdou mound, this level seems to be restricted to the mound surroundings, because it has not been found in the vicinity. Three metres above the crinoidal limestone bed, a conspicuous 50 cm thick cephalopod bed (TM 465 of HOLLARD 1974) with abundant goniatites (*Pinacites jugleri* (ROEMER; 1843), *Fidelites occultus* (BARRANDE, 1865), *Subanarcestes macrocephalus* SCHINDEWOLF, 1933) and orthoconic nautiloids, appears (Pl. 6, Fig. 1; Text-fig. 19). Above the cephalopod bed, the facies changes abruptly into a blue-grey limestone-marl alternation (Text-fig. 19; Pl. 6, Fig. 1) which contains an impoverished fauna, dominated by pelagic elements [rare goniatites, orthoconic nautiloids,

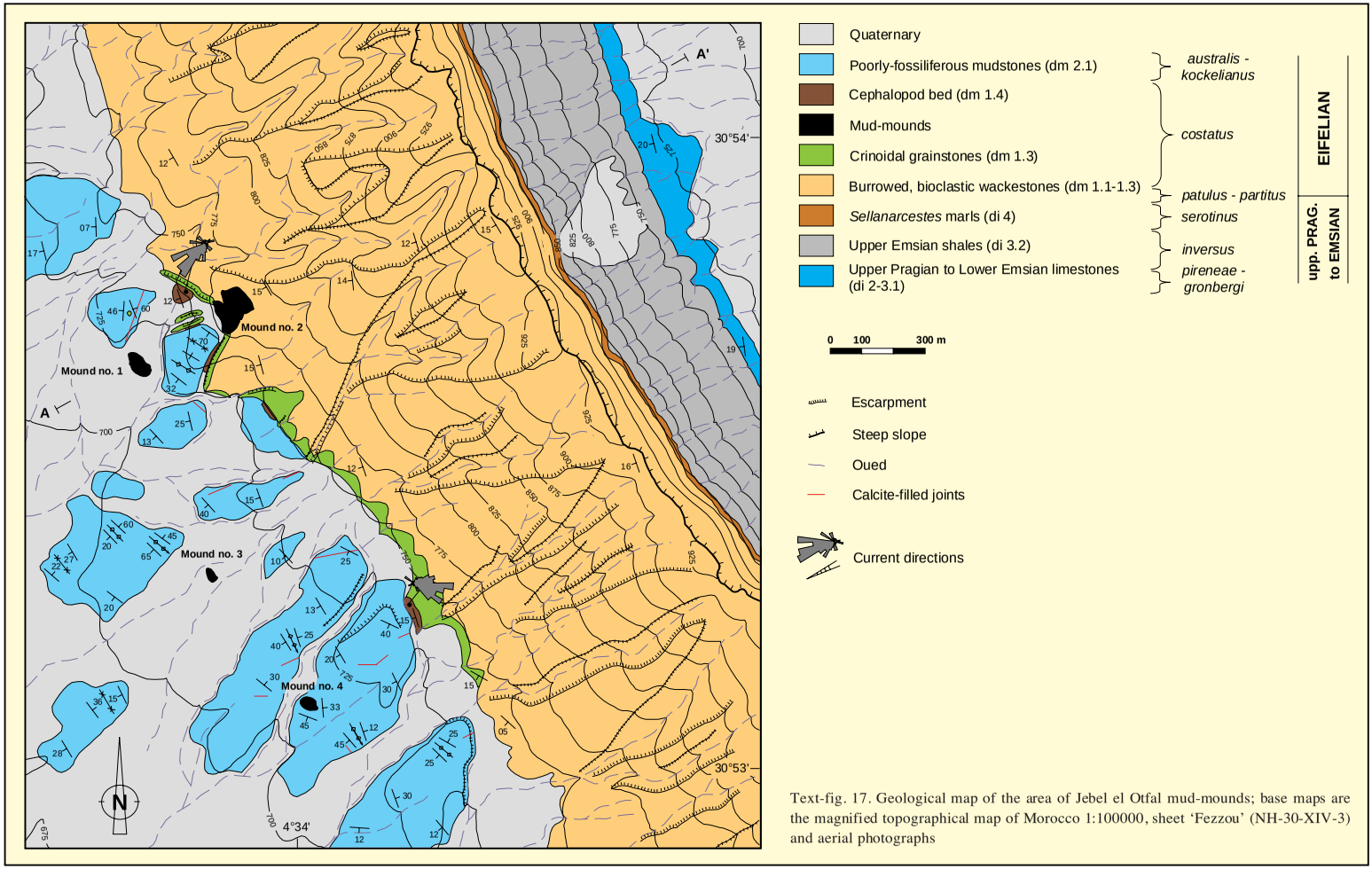

Text-fig. 17. Geological map of the area of Jebel el Otfal mud-mounds; base maps are the magnified topographical map of Morocco 1:100000, sheet 'Fezzou' (NH-30-XIV-3) and aerial photographs

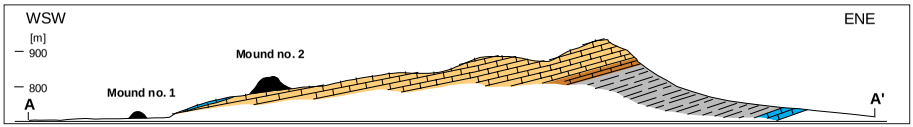

Text-fig. 18. Cross section of Jebel el Otfal; for line of section and legend *see* Text-fig. 17

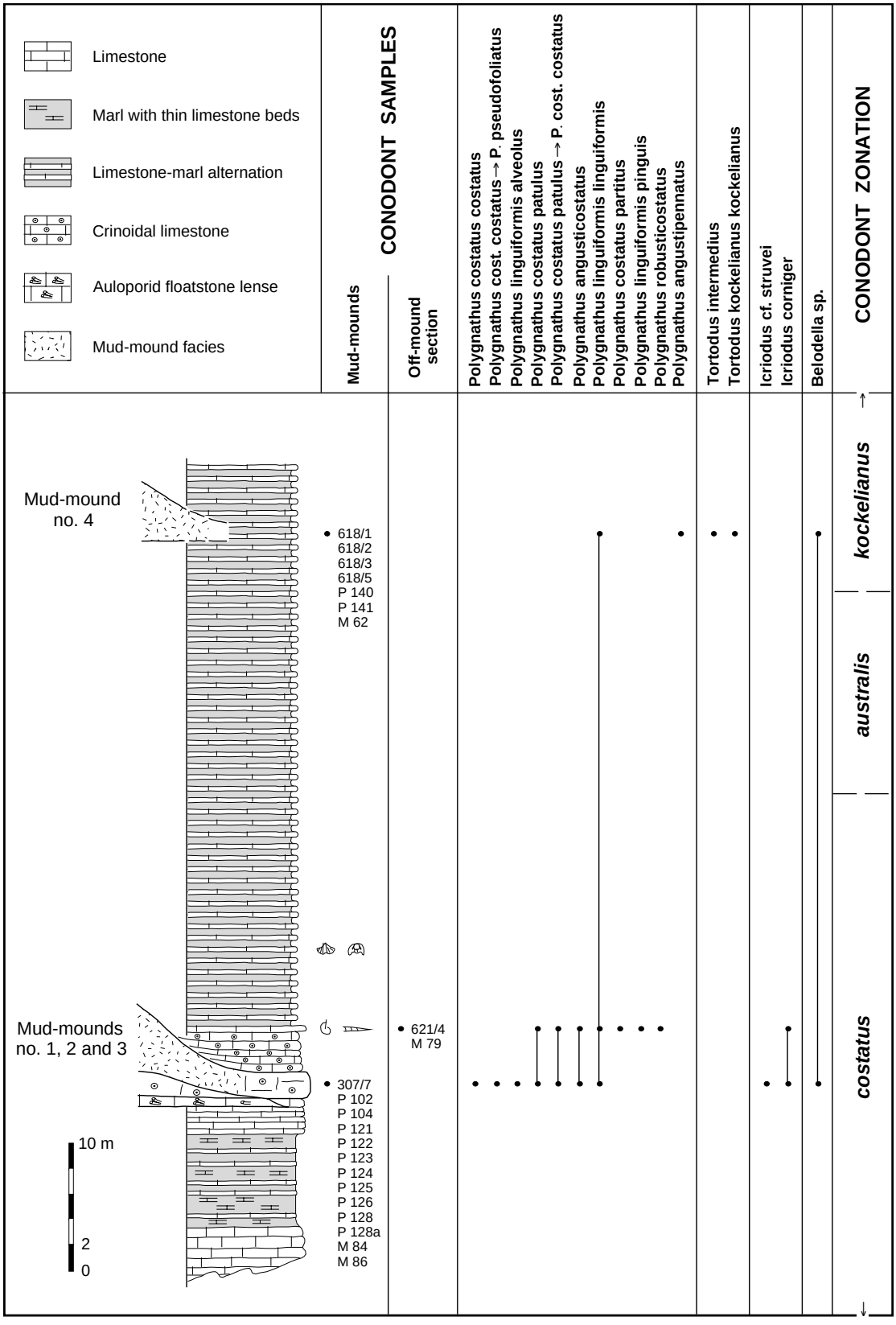

Fig. 19. Lithology of Jebel el Otfal off-mound section with conodont distribution

trilobites, styliolinids and trace fossils (common *Zoophycos*, rare *Planolites*)]. About 40 m above the cephalopod bed, mound no. 4 is intercalated within this basinal facies (Text-fig. 19), which has a total thickness of 90 m and continues up to the Eifelian-Givetian transition (Text-fig. 31), where the strata become more argillaceous and disappear below the gravel plain. The upper 80 m of this facies are folded uniformly, a phenomenon of controversial origin, which occurs at numerous localities in the eastern Anti-Atlas (*e.g.* Jebel Amessoui, Irhfelt n'Tissalt, Ouihlane, Hassi Nebech). WENDT (1988, 1993) suggested slumping processes as a cause, emphasizing the common basinward-directed faces of folds and completely undeformed over- and underlying strata. However, homogeneous folding of an 80 m thick rock pile suggests a single process of deformation which is difficult to explain by slumping. Moreover, the folds appear rather symmetrical after correction for rotation of the underlying Variscan-tilted strata to the horizontal. This suggests tectonic deformation prior to Variscan tilting but after burial at considerable lithification of the limestones. As mentioned above, the folding is restricted to the lithology of the limestone-marl alternation. Therefore, the limestone beds of this lithology, sandwiched between marl layers, probably could react more incompetent on deformation than the underlying relatively homogeneous limestones which are completely unfolded. Fractures within the folded rock pile are probably related to the deformation process and filled by ferroan blocky calcite cements. The oxygen isotope data of these cements can provide evidences for the burial depths of fracturing. $\delta^{18}O$ values of the ferroan calcite fracture fills range from –6.8‰ to –9.3‰ PDB and are thus depleted from the assumed marine seawater composition ($\delta^{18}O$ = –2.6‰ PDB) by 4.2‰ to 6.7‰. By simply using temperature as the main controlling factor for these negative $\delta^{18}O$ values, rough estimates for the burial depth of precipitation can be made (*e.g.* HURLEY & LOHMANN 1989, LAVOIE & BOURQUE 1993). From the isotopic fractionation curve of FRIEDMAN & O'NEIL (1977) and a geothermal gradient of 50°C/km (BELKA 1991), the depletion of 4.2‰ to 6.7‰ corresponds to a temperature increase of 21° to 33.5°C which calculates to 420 to 670 m of burial. Thus, based on stratigraphic reconstruction, precipitation of the ferroan calcite fracture fills at Jebel el Otfal, linked with the tectonic deformation of the limestone-marl alternation, took place in late Givetian to early Frasnian times.

Size and geometry

The largest mound of Jebel el Otfal (mound no. 2) resembles the Guelb el Maharch mud-mound in size and cone shape (Pl. 6, Fig. 1; Text-fig. 21a). It has a diameter of 100-150 m and rises 40 m above the underlying strata. After correction for rotation of the off-mound strata to the horizontal, the mound shows an asymmetrical shape with steeper southwestern than northeastern flanks (Text-fig. 21b; Pl. 6, Fig. 1). The mean angle of flank inclination is 39°.

The bases (and partly the bulk volumes) of the remaining three mounds (nos 1, 3 and 4) are covered by Quaternary deposits. Only their upper 10-20 m rise above the plain (Pl. 7, Figs 1-3; Text-figs 20a, 22a and 23), but it is likely that their original sizes and shapes are similar to mound no. 2 and that other mud-mounds are buried under the Quaternary cover W of Jebel el Otfal. As indicated by biostratigraphical data (Text-figs 19, 28) mounds nos 1, 2 and 3 are of the same age and therefore coeval to the crinoidal limestone bed, which passes into mound no. 2. By projecting this bed below mound nos 1 and 3, their original height can approximately be determined as 30 m and 50 m respectively.

The exhumed parts of mounds nos 1, 3 and 4 are elongated in outline, with northwest- and north-trending long axes, 45-105 m in length (Text-figs 20a, 22a and 23). Compared with mound no. 2, mounds nos 1 and 3 show inverted asymmetries with steeper northeastern than southwestern flanks (Text-figs 20b, 22b). These asymmetries are rectangular to the elongation of the mounds, suggesting different causes for each elongation and asymmetrical shapes. Because of the limited outcrops of mounds nos 1 and 3, one has to be careful with the interpretation of these features and investigations should focuse on the totally exhumed and non-elongate mound no. 2. WENDT (1993) reported uniform, even more significant asymmetries with 10-30° steeper eastern/northeastern than western/southwestern flanks from Guelb el Maharch as well as from all Jebel el Otfal mud-mounds. He obviously worked with higher angles of rerotation, possibly resulting in unilateral, exaggerated asymmetries.

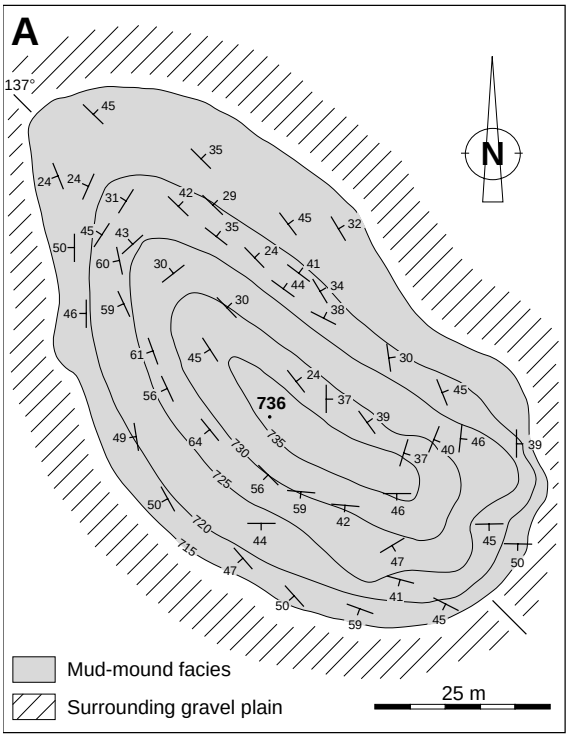

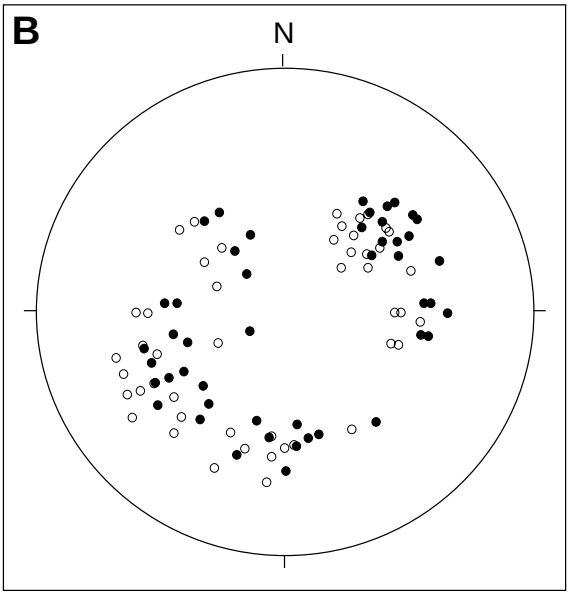

Fig. 20. Jebel el Otfal mud-mound no. 1. A) Outline and topography; B) Stereographic projection (upper hemisphere) of polar points of mound flanks; empty points before, black points after correction for rotation of off-mound strata to the horizontal (rotation axis: 158/12); note slight asymmetry with steeper northeastern than southwestern flanks

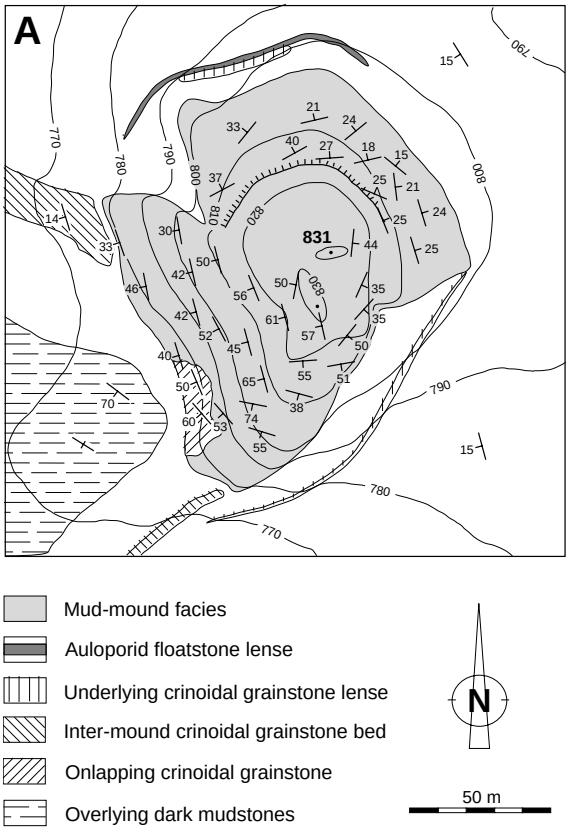

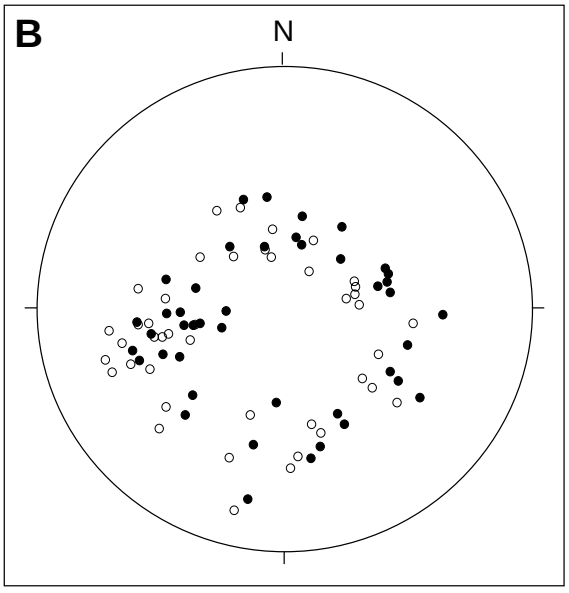

Fig. 21. Jebel el Otfal mud-mound no. 2; A) Outline, topography and surroundings; B) Stereographic projection (upper hemisphere) of polar points of mound flanks; empty points before, black points after correction for rotation of off-mound strata to the horizontal (rotation axis: 158/12); note distinct asymmetry with steeper southwestern than northeastern flanks

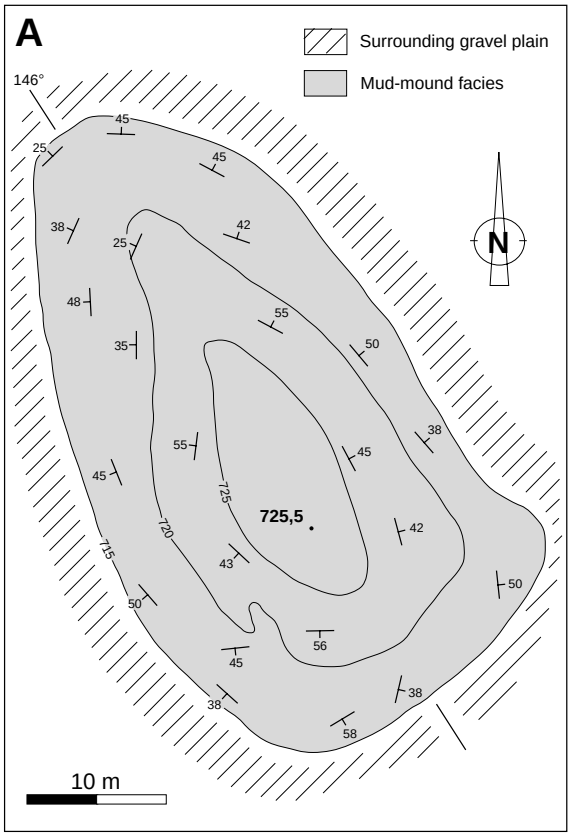

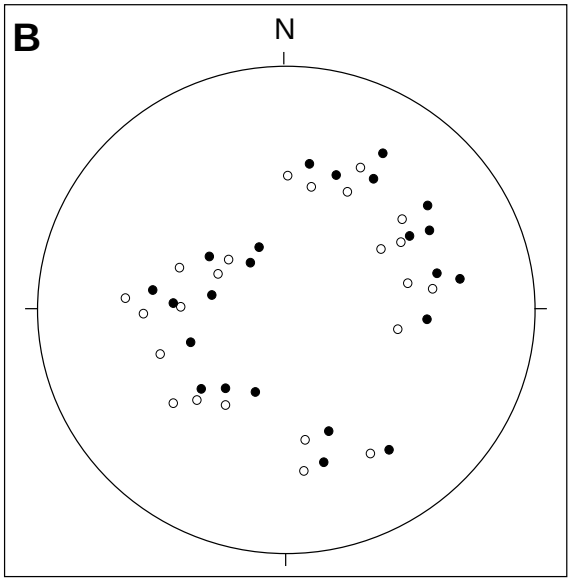

Fig. 22. Jebel el Otfal mud-mound no. 3; A) Outline and topography. B) Stereographic projection (upper hemisphere) of polar points of mound flanks; empty points before, black points after correction for rotation of off-mound strata to the horizontal (rotation axis: 158/12) note distinct asymmetry with steeper northeastern than southwestern flanks

The cause of mound asymmetries is uncertain. This phenomenon has also been found at the Hamar Laghdad mud-mounds (BRACHERT & *al*. 1992) and in Middle Devonian mud-mounds of the Algerian Sahara (WENDT & *al*. 1993, BELKA 1994). Generally, asymmetries are interpreted as a result of bottom currents, which accumulated sediment in the lee of the mounds, winnowing the mound-luves and leaving them

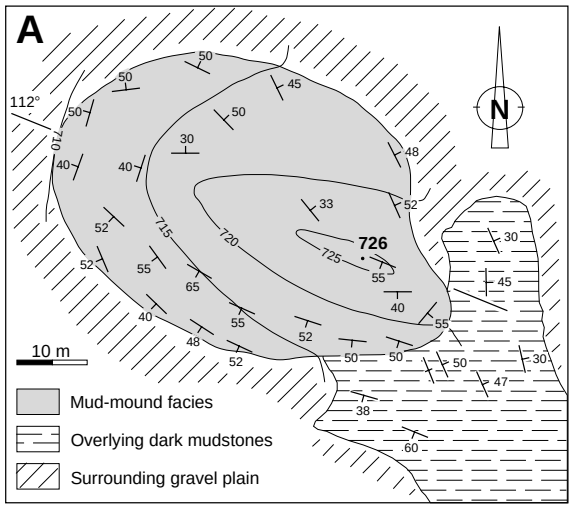

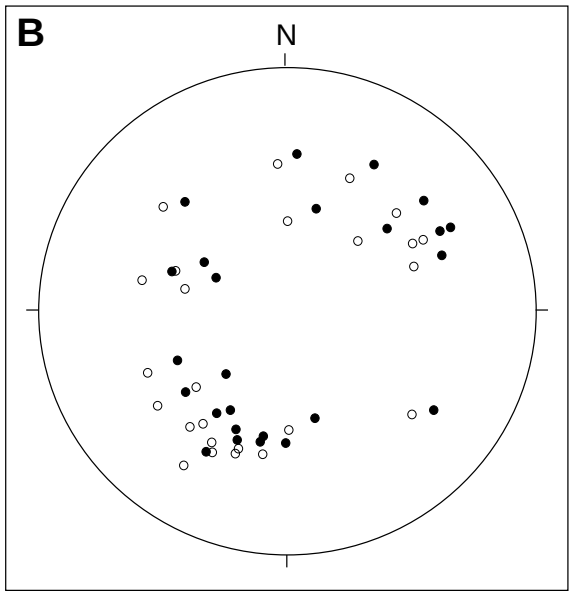

Fig. 23. Jebel el Otfal mud-mound no. 4; A) Outline, topography and surroundings; B) Stereographic projection (upper hemisphere) of polar points of mound flanks; empty points before, black points after correction for rotation of off-mound strata to the horizontal (rotation axis: 158/12); note rather symmetrical flank inclinations after rotation

consequently steeper (BRACHERT & *al*. 1992). A modern example for this fact are the current-formed, elongate lithoherms in the Straits of Florida (NEUMANN & *al*. 1977). Mound no. 2 at Jebel el Otfal has a steeper southwest-face which would correspond to a NE-directed bottom current measurement (301 values) obtained from orthoconic nautiloids in the vicinity (cephalopod bed, Text-fig. 17). Another measurement (100 values) from the same cephalopod bed, 1300 m farther southeast, yielded an almost opposite W-directed current. Other current measurements (207 values) in the vicinity of Guelb el Maharch provided no evidence for a current-related asymmetry of this mound. The same observation was made at the Middle Devonian mud-mounds of the Algerian Sahara, where no relation of mound asymmetries to bottom currents could be demonstrated.

Lithology, sedimentary structures and off-mound relations

The lithology of all Jebel el Otfal mud-mounds corresponds to that of Guelb el Maharch. They consist exclusively of massive, stromatactis-bearing boundstones without any zonation or bedding (Pl. 8, Fig. 1; Pl. 9, Fig. 1). Dolomite occurs only within cm- to dm-sized, irregular cavities, where a formerly laminated internal sediment was dolomitized, still preserving 'ghost lamination' (Pl. 8, Fig. 2). Neptunian dykes have not been found in the Jebel el Otfal mud-mounds.

The investigations of the Jebel el Otfal mud-mounds were focused on mound no. 2, where the lateral and vertical off-mound relations are clearly exposed (Pl. 6, Figs 1, 2). Three units of crinoidal limestones, underlying, coeval to and overlying the mound can be distinguished:

1) The mound is underlain by a flat, crinoidal grainstone lense (Pl. 6, Figs 2a, b), which is up to 2 m thick and is in turn underlain by a 50 cm thick auloporid floatstone lense (Text-figs 19, 21a). Both horizons are restricted to the immediate vicinity of the mound. Common preservation of articulated crinoid stems (Pl. 8, Fig. 4), poor sorting and the lack of outwash phenomena suggest a minimum transport and therefore to an autochthonous accumulation of the crinoidal limestone. Obviously, both auloporid floatstone and crinoidal limestone acted as pioneer phases of mound development. Similar phenomena occur at the mounds of Aferdou el Mrakib and Hamar Laghdad (BRACHERT & *al*. 1992), which are also underlain by crinoidal limestones. Thus, the local accumulation of crinoidal limestone lenses seems to precede (and trigger?) the growth of carbonate mounds in the eastern Anti-Atlas.

2) The mound wedges out into a 2 m thick crinoidal grainstone bed (Pl. 6, Figs 1, 2; Text-fig. 19), which is very similar in lithology to the underlying crinoidal limestone lense. The ratio of mound height to the thickness of the coeval bed is 20:1 and can be taken as an approximate difference in accumulation rate.

3) Poorly-sorted crinoidal grainstones onlap the base of the southwestern mound flank (Text-fig. 21a; Pl. 6, Figs 2a, b). Originally, these grainstones probably formed a debris aureole surrounding the mound and have subsequently been largely removed by erosion. They are interpreted as parautochthonous accumulations of mound-dwelling crinoids at the lower mound flanks after disarticulation.

Fauna

The faunal composition of all the Jebel el Otfal mud-mounds is similar to that of Guelb el Maharch (Text-fig. 14). Crinoids and tabulate corals prevail; the latter display an association, which resembles that of Hamar Laghdad (F. TOURNEUR, *written comm*.). Most abundant are auloporids (*Bainbridgia* sp., Pl. 9, Fig. 8; rare *Remesia* sp. and *Aulocystis* sp.) followed by striatoporids (*cf. Taouzia*; cf. *Pachystriatopora*, Pl. 8, Fig. 5). Less frequent are brachiopods (*Atrypa*?, small spiriferids (*e.g. Desquamatia* sp.) and orthids), hexactinellid sponges (Pl. 9, Fig. 5), fragments of fenestellid and fistuliporid bryozoans (Pl. 9, Fig. 6), dacryoconarids (mainly styliolinids, rare *Nowakia* sp.) and isolated gastropods, ostracods and rugose corals (*e.g. Amplexocarinia* sp.). Microproblematica (*Rothpletzella* sp.) occur rarely, encrusting auloporids (Pl. 9, Fig. 8). Agglutinated foraminifers (*Sorosphaera* sp., Pl. 13, Figs 5-8) have frequently been found in insoluble residues. In contrast to Aferdou el Mrakib and Guelb el Maharch, trilobites are common and very abundant in mound no. 4 (*Gerastos* sp., *Koneprusia* sp., *Radiaspis radiata*; Pl. 9, Fig. 3). The latter contains a reduced fauna which consists of tabulate corals (*Dualipora preciosa* TERMIER & TERMIER 1980, Pl. 9, Fig. 7; *Remesia* sp.; cf.

Pachystriatopora, *Cladochonus* sp., *Bainbridgia* sp.), crinoids and rare styliolinids.

Jebel Ou Driss

Geological and stratigraphical setting, off-mound succession

Jebel Ou Driss, the westernmost Devonian outcrop of the eastern Anti-Atlas, is an 8 km long ENE-WSW-trending narrow syncline, located in the Zagora Graben on the southwestern edge of the Mader region. The only mud-mound of this locality is of early Eifelian age and is situated in the western half of the southeastern synclinal limb. The Jebel Ou Driss consists of upper Emsian to lower Givetian rocks, which were studied in detail by HOLLARD (1974) and BULTYNCK (1985, 1989, 1991). The Middle Devonian part of the sequence is about 100 m thick and changes from the base to the middle part from burrowed, argillaceous mudstones in the lower Eifelian (mud-mound surroundings) to argillaceous wackestones which contain brachiopods, crinoids, goniatites and trilobites. In the upper part of the section (upper Eifelian to lower Givetian), significant trilobite horizons, followed by a conspicuous coral horizon, appear. The upper 20 m of the section are dominated by fossiliferous shales.

Size and geometry

The mud-mound of Jebel Ou Driss is rather inconspicuous. It rises 4 m above the surrounding bedded off-mound facies, but the bulk mound volume is still covered (Pl. 10, Fig. 1). Rotation of the underlying strata to the horizontal shows that erosion has exhumed only the southern mound flank, forming a NNW-SSE-trending outcrop, elliptical in outline, 50 m long and 25 m wide (Text-fig. 24a). Fortunately, the contact to the immediate under- and overlying strata is exposed, so that reconstructions of size and shape are possible. The original mound height was determined as about 25-30 m by projecting the underlying strata below the overlying beds (Text-fig. 24b). The inclination of the southern flank is up to 40° and the mound shape is assumed to have been conical (resembling the Guelb el Maharch and Jebel el Otfal mud-mounds) with a base diameter of about 80-90 m.

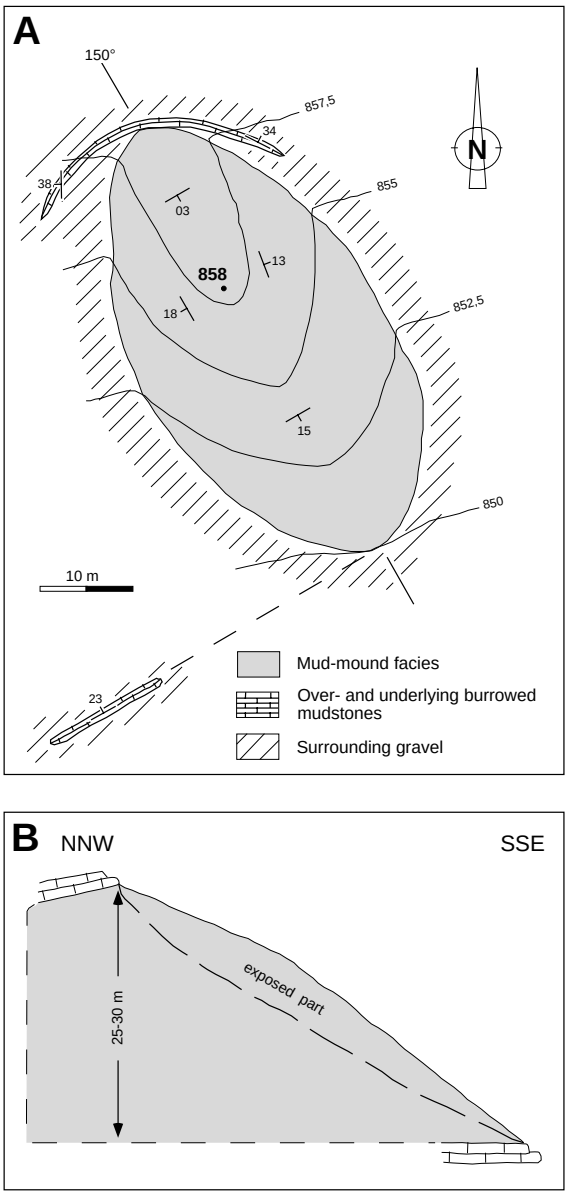

Fig. 24. Jebel Ou Driss mud-mound; A) Outline, topography and surroundings; B) Cross section of mound after rotation of underlying beds to the horizontal

Lithology

The mound consists mainly of stromatactoid, bioclastic boundstones (Pl. 10, Fig. 4) in which few dm^2-sized patches of coral boundstones (Pl. 10, Figs 3, 5) occur. A small lense of crinoidal grainstone is exposed at the mound base, indicating that mound growth started with a crinoidal limestone as at Jebel el Otfal mound no. 2.

Fauna

The mud-mound contains a varied fauna with respect to its surrounding off-mound facies, which consists of monotonous, burrowed mudstones. Tabulate corals are represented by striatoporids (dendroid colonies of cf. *Zemmourella* and cf. *Taouzia*, Pl. 10, Figs 3-4) and, less common, auloporids (mainly *Bainbridgia* sp.), solitary rugose corals by scattered *Neomphyma* sp. or *Sociophyllum* sp., (Pl. 10, Fig. 5). Crinoids, brachiopods, trilobites and dacryoconarids (common styliolinids, rare *Nowakia* sp.) are common. Gastropods and ostracods are rare.

SE' Jebel Zireg

Three small mounds occur about 2 km southeast of the Jebel Zireg monocline (Text-fig. 2). In shape, they are rather lenses than mounds, which have escaped erosion with respect to the argillaceous off-mound strata (Pl. 10, Fig. 2). They are 30-50 m long, 10-20 m wide and aligned in an E-W-trending row with 200-300 m space in between and rise from one southward-dipping bed. Pervasive dolomitization has obliterated all fossils and sedimentary structures that no informations about facies can be obtained, not even under cathodoluminescence light.

A concordant fault, located north of the three mounds, has probably brought them up to the surface and may have acted as a conduit for the dolomitizing fluids.

CONODONT FAUNA AND BIOSTRATIGRAPHY OF THE MADER CARBONATE MOUNDS

Based on goniatite stratigraphy, HOLLARD (1974), on the geological map 1:200.000, sheet 'Todrha-Ma'der', attributed the mounds of Aferdou el Mrakib, Guelb el Maharch and Jebel el Otfal to the late Eifelian ('édifice récifale', dm 1.3-4). WENDT (1993) provided the first conodont data of these mounds and showed that this age must be corrected. Results of conodont datings of Mader carbonate mounds are summarized in Text-fig. 25.

The conodont zonation of the Middle Devonian is very rough, with durations of individual zones of about 0.5-2 Ma. A more precise

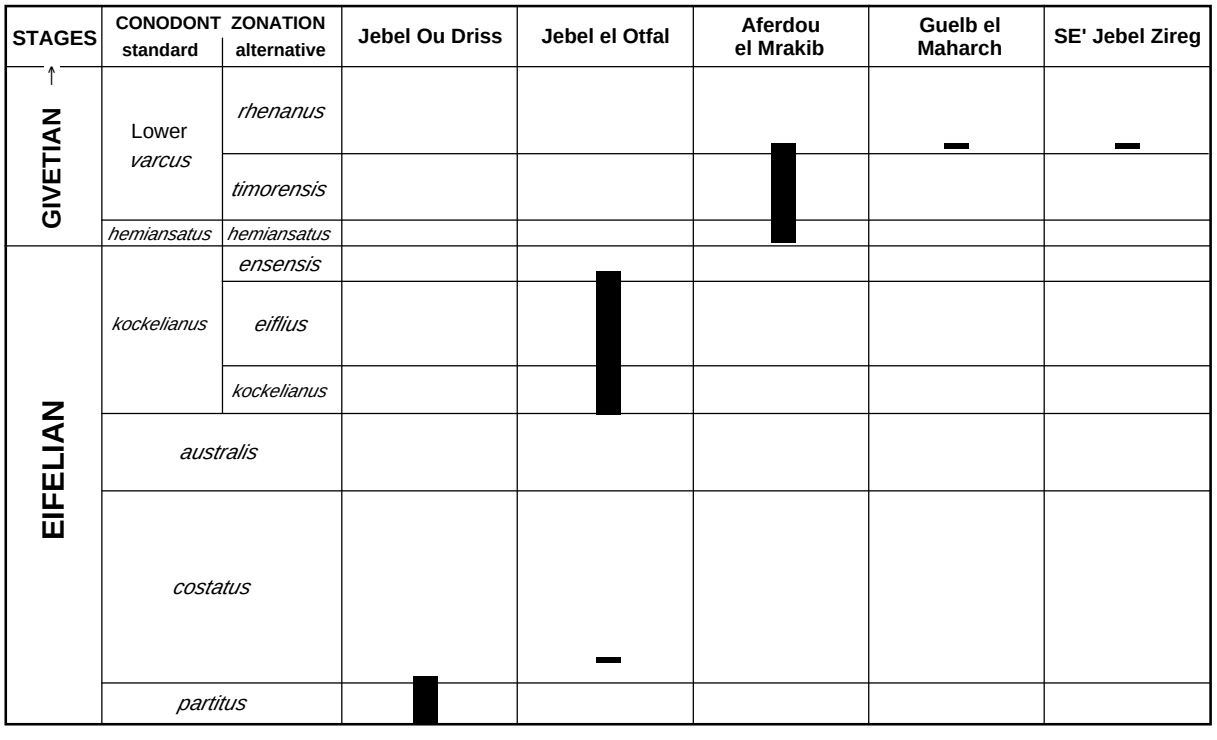

Fig. 25. Stratigraphical positions of the Mader carbonate mounds; note that vertical bars do not show growth times but maximum temporal ranges of conodont associations; relative duration of conodont zones and alternative zonation *after* BELKA & *al*. (in press)

stratigraphical calibration of mound growth can be achieved in applying the method of graphic correlation. BELKA & *al*. (in press) have assembled the measured stratigraphic ranges of 52 conodont taxa represented in seven upper Emsian to lower Givetian sections of the eastern Anti-Atlas by graphic correlation into a chronostratigraphic framework. By overlapping stratigraphic ranges of conodont taxa, intervals of mound growth can be determined with much higher resolution than with the conventional conodont zonation (Text-figs 26-30). Applying this method, an alternative conodont zonation of higher stratigraphic resolution for the late Eifelian to early Givetian has been proposed (BELKA & *al*. in press) (Text-figs 26-28, 30).

Aferdou el Mrakib

Conodont samples have been collected from the underlying upper Eifelian to lowermost Givetian succession, the massive mound facies, the mound debris facies and from the overlying strata (Text-fig. 10). As a result, the interval of mound growth could be precisely limited. Pectiniform elements prevail over ramiform elements. In the underlying strata, the *Polygnathus*/*Icriodus* ratio is 5.2:1 (average value of six 1-2 kg samples, containing a total of 140 conodonts), in the massive mound and mound debris facies it is 1.5:1 (average value of ten 1-2 kg samples, containing a total of 244 conodonts). In addition to polygnathids and icriodids, the stratigraphically insignificant genus *Belodella* sp. occurs frequently in the massive mound and mound debris facies and rarely in the off-mound strata.

Conodont samples from the top of the crinoidal grainstones and the coral-stromatoporoid boundstones, immediately mound-underlying, contain:

Polygnathus linguiformis linguiformis
Polygnathus linguiformis alveolus
Polygnathus linguiformis sp. B *sensu* WEDDIGE 1977
Polygnathus pseudofoliatus
Polygnathus ensensis
Polygnathus hemiansatus
Icriodus struvei
Icriodus regularicrescens
Icriodus arkonensis
Icriodus subterminus
Belodella sp.

They represent the time interval from the upper part of the *kockelianus* Zone to the lowermost part of the *hemiansatus* Zone [upper part of the *eiflius* Zone to lowermost part of the *hemiansatus* Zone after the alternative zonation of BELKA & *al*. (in press), Text-fig. 10]. Because *Polygnathus hemiansatus* appears for the first time in the coral-stromatoporoid boundstone, immediately underlying the mound, the Aferdou mound is believed to have started growing in the lower part of the *heminansatus* Zone (Text-figs 10, 26).

Conodont samples from the massive mound facies (M 35, M 38, M 103) contain:

Polygnathus linguiformis linguiformis
Polygnathus pseudofoliatus
Polygnathus eiflius
Polygnathus ensensis
Polygnathus hemiansatus
Polygnathus xylus
Icriodus regularicrescens
Icriodus obliquimarginatus
Belodella sp.

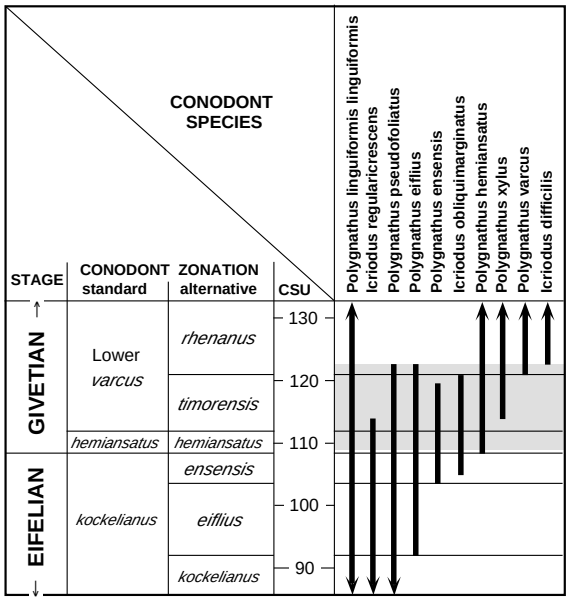

Fig. 26. Maximum temporal range (grey field) of Aferdou el Mrakib reef-mound, limited by overlapping conodont taxa ranges. CSU = composite standard units; alternative zonation, CSU and stratigraphic ranges of conodont species *after* BELKA & *al*. (in press)

The youngest conodont samples from the massive mound facies (432/6, P 146) were obtained from the primary mound surface of the northern slope of the mound. They contain:

Polygnathus linguiformis linguiformis
Polygnathus pseudofoliatus
Polygnathus hemiansatus
Polygnathus varcus
Icriodus difficilis.

This association represents a very short time interval in the middle part of the Lower *varcus* Zone (alternative: lower part of the *rhenanus* Zone, Text-fig. 26).

Strata (617/1), directly onlapping the mound yielded:

Polygnathus linguiformis linguiformis
Polygnathus linguiformis klapperi
Polygnathus eiflius
Polygnathus rhenanus
Icriodus difficilis
Belodella sp.

They indicate exactly the same short time interval as the youngest mound samples. The mound growth was thus terminated in the middle part of the Lower *varcus* Zone (alternative: lower part of the *rhenanus* Zone, Text-fig. 26).

Guelb el Maharch

Conodonts are rare in the Guelb el Maharch mud-mound. Nine 1-2 kg samples from the base, flanks and top yielded only 15 pectiniform elements (7 *Polygnathus*, 8 *Icriodus*), ramiform elements are completely missing. In comparison, *Belodella* sp. (69 specimens) is just as common as in the Aferdou mound. The conodont association of

Polygnathus pseudofoliatus
Polygnathus linguiformis linguiformis
Polygnathus aff. *P. kennettensis*
Icriodus difficilis
Icriodus brevis

can be assigned to the same short time interval in the middle part of the Lower *varcus* Zone (alternative: lower part of the *rhenanus* Zone, Text-fig. 27) as the youngest part of the Aferdou mound (Text-fig. 25).

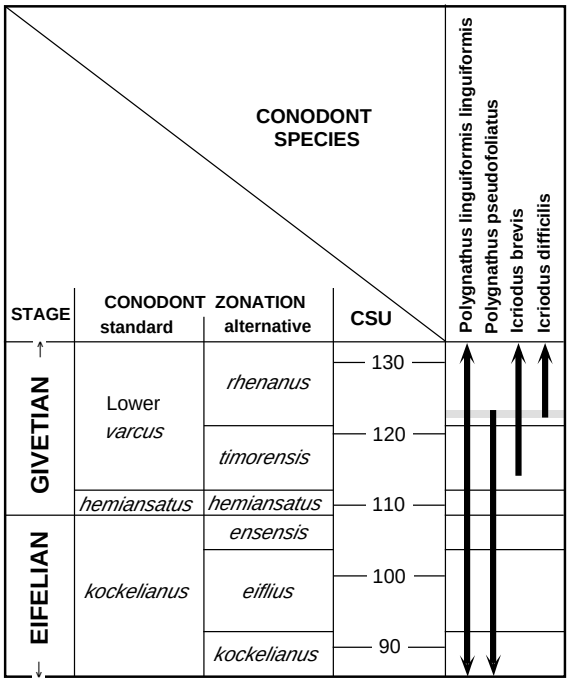

Fig. 27. Maximum temporal range (grey field) of Guelb el Maharch mud-mound; CSU = composite standard units; for further explanations, *see* Text-fig. 26

Jebel el Otfal

Conodont samples were collected from the four mud-mounds and the Eifelian off-mound section. Apart from the cephalopod bed, ten 1-2 kg samples of the off-mound facies contained no conodonts (Text-fig. 19). Twenty-five 1-2 kg samples, obtained from the mounds yielded a total of 85 conodonts, predominantly pectiniform elements. The *Polygnathus*/*Icriodus* ratio is 12.3:1 and *Belodella* sp. is represented by 30 specimens. Mounds nos 1, 2 and 3 contain:

Polygnathus costatus patulus
Polygnathus costatus costatus
Polygnathus angusticostatus
Polygnathus linguiformis linguiformis
Polygnathus linguiformis alveolus
Polygnathus costatus patulus → P. costatus costatus
Polygnathus costatus costatus → P. pseudofoliatus
Icriodus corniger
Belodella sp.

This fauna represents a very short time interval in the lower part of the *costatus* Zone (Text-fig. 28).

A 1-2 kg sample from the cephalopod bed yielded 81 conodonts, dominated by pectiniform elements. The fauna contains almost exclusively polygnathids, but only one icriodid. *Belodella* sp. is completely missing. The association of

Polygnathus angusticostatus
Polygnathus costatus patulus
Polygnathus costatus partitus
Polygnathus costatus patulus → *P. costatus costatus*
Polygnathus linguiformis linguiformis
Polygnathus linguiformis pinguis
Polygnathus robusticostatus
Icriodus corniger

also indicates the lower part of the *costatus* Zone.

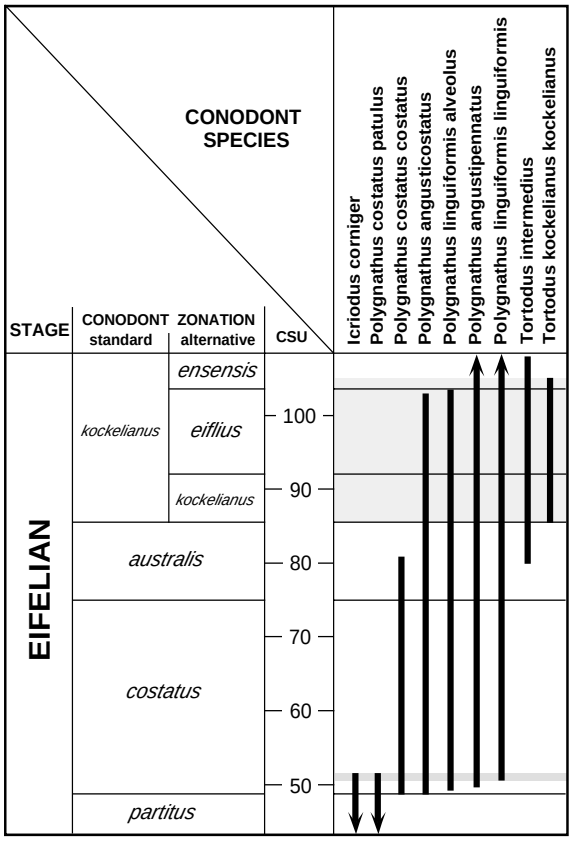

Fig. 28. Maximum temporal ranges (grey fields) of the Jebel el Otfal mud-mounds; lower grey field = Mounds no. 1, 2 and 3; upper grey field = mound no. 4; CSU = composite standard units; for further explanations, *see* Text-fig. 26

Mound no. 4 contains an association of

Polygnathus angustipennatus
Polygnathus linguiformis linguiformis
Tortodus kockelianus kockelianus
Tortodus intermedius

showing that this mound is the youngest of the Jebel el Otfal mounds [*kockelianus* Zone (alternative: *kockelianus* to lower part of the *ensensis* Zone), Text-fig. 28].

Jebel Ou Driss

Only one of three 1-2 kg samples from the mound yielded conodonts (3 specimens of *Icriodus corniger*). From the over- and underlying strata, an association of

Polygnathus costatus patulus
Polygnathus costatus partitus
Polygnathus linguiformis bultyncki
Icriodus corniger

were obtained which indicate the time interval from the *partitus* to the lowermost part of the *costatus* Zone (Text-fig. 29).

SE' Jebel Zireg

The only conodont-bearing sample, obtained from the dolomite lenses contained an association of

Polygnathus linguiformis linguiformis
Polygnathus pseudofoliatus ?
Icriodus difficilis ?
Icriodus cf. *struvei*

which probably indicate a short time interval in the middle part of the Lower *varcus* Zone (alternative: lower part of the *rhenanus* Zone, Text-fig. 30). These mounds are therefore coeval to Guelb el Maharch and the youngest parts of Aferdou el Mrakib (Text-fig. 25).

FACIES MODEL (CARBONATE RAMP)

The carbonate mounds of the Mader Basin (Aferdou el Mrakib, Guelb el Maharch, Jebel el

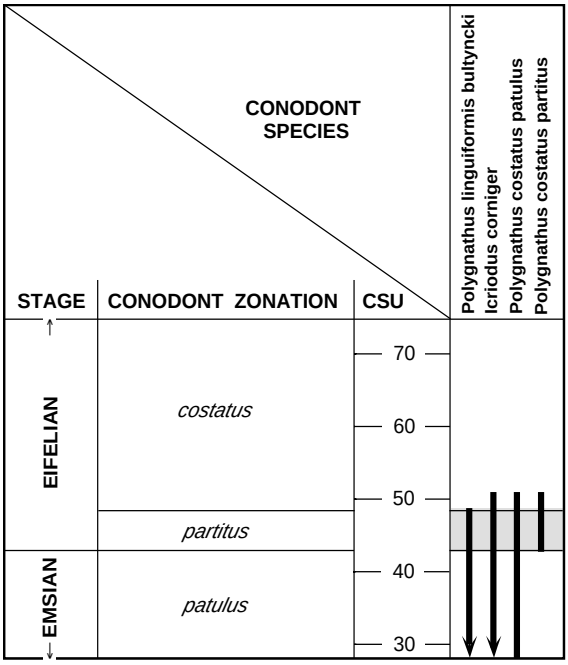

Fig. 29. Maximum temporal range (grey field) of Jebel Ou Driss mud-mound; CSU = composite standard units; for further explanations, *see* Text-fig. 26

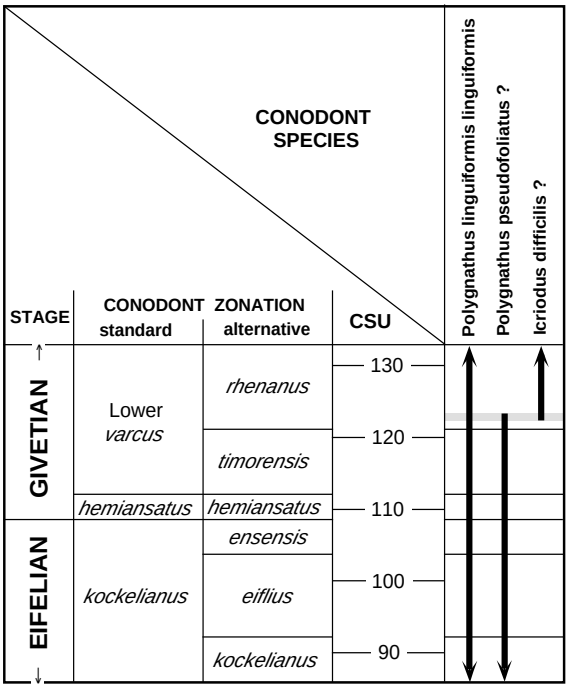

Fig. 30. Maximum temporal ranges (grey fields) of dolomitized mound lenses SE of Jebel Zireg; CSU = composite standard units; for further explanations, *see* Text-fig. 26

Otfal) are intercalated within a 200-400 m thick Middle Devonian succession, which was deposited along a 40 km wide, northward-dipping carbonate ramp. The ramp was tectonically-controlled and established between an area of uplift (Mader Platform) and an area of strong subsidence (depocentre of the Mader Basin).

Facies zones

In chapter on the Middle Devonian, I briefly introduced the two major facies belts, neritic and basinal, which characterize the Middle Devonian palaeogeography of the Mader area. They can be further subdivided into five depositional facies zones on the carbonate ramp, mainly based on fossil assemblages and different lithologies. In order of increasing water depths these are: shallow ramp, mid-ramp, outer ramp, transitional outer ramp to basinal and basinal facies. Text-fig. 32 illustrates a facies model and the spatial and temporal distribution of these facies zones on the southern Mader carbonate ramp.

Shallow ramp facies (stromatoporoid-coral-cyanobacteria boundstones)

This facies is represented in the lower Givetian (Lower *varcus* Zone) part of the Madène el Mrakib section by 20 m thick, dark, thick-bedded, stromatoporoid-coral-cyanobacteria boundstones (Text-fig. 31). The stromatoporoids are mainly domical morphotypes, 20-80 cm in diameter and are frequently found *in situ*. Ragged-type growth forms occur frequently and indicate high accumulation rates. Laminar forms are rare and dendroid forms are totally absent. Corals are dominated by Tabulata (large thamnoporids, alveolitids, heliolitids, favositids and auloporids), followed by Rugosa (*Heliophyllum halli moghrabiense* LE MAÎTRE, 1947, *Cystiphylloides* sp., *Acanthophyllum* sp., *Calceola sandalina* LAMARCK, 1799). Colonial rugose corals have not been found. Also common are large, conical gastropods, crinoids and siliceous sponge spicules (hexactinellids). Bioturbation is sparse. An enigmatic fossil with respect to its bathymetric significance is *Rothpletzella*, a microproblematicum, which is tentatively attributed to the cyanobacteria (RIDING 1991). Generally it is found in shallow subtidal or even backreef facies (MACHEL

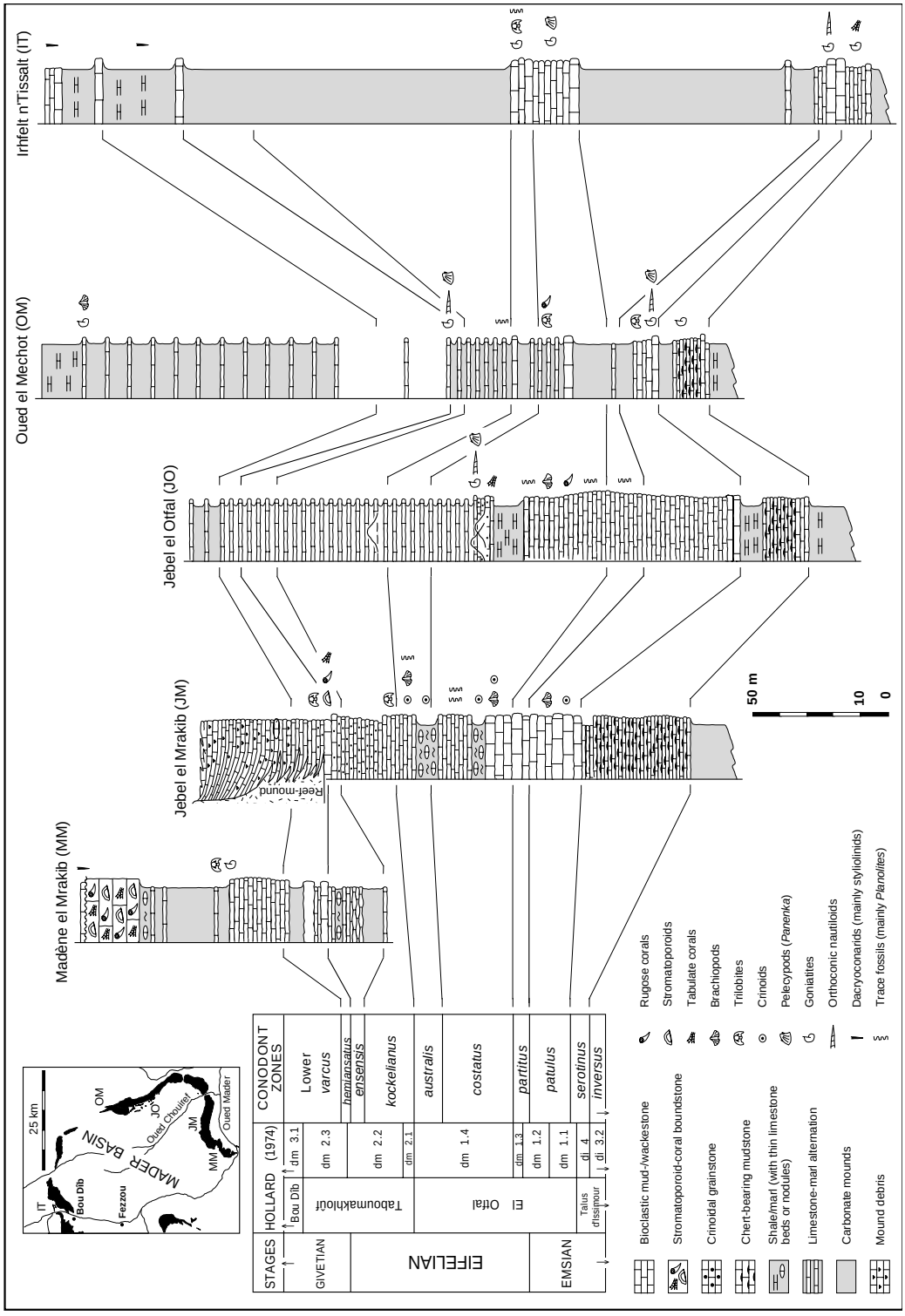

Fig. 31. Correlation of upper Emsian to lower Givetian carbonate ramp sections in the southern Mader area; correlation of HOLLARD's (1974) lithological units with the actual upper Emsian to lower Givetian conodont zonation after data in BULTYNCK & HOLLARD (1980) and ALBERTI (1980, 1981a); relative duration of conodont zones *after* BELKA & *al*. (in press). Madène el Mrakib section *after* M. KAZMIERCZAK (*written comm*.); Irhfelt n'Tissalt section (Bou Dïb) *after* HOLLARD (1974)

1990a). Therefore, the stromatoporoid-coral-cyanobacteria boundstones are regarded as the most shallow environments in the Mader Basin.

Mid-ramp facies (burrowed, skeletal wackestones)

The mid-ramp facies is typified by a 70 m thick interval in the upper Emsian to middle Eifelian (*patulus* to lower part of the *kockelianus* Zone) part of the Jebel el Mrakib section (Text-fig. 31). It consists of grey, medium- to thick-bedded wackestones with abundant *Planolites* burrows. The fauna is dominated by crinoids and brachiopods. Trilobites and small solitary rugose corals are rare and pelagic faunal elements are almost totally absent.

The burrowed, skeletal wackestones were deposited below fair-weather wave base, as is indicated by the general lack of wave- or current-generated sedimentary structures. Occasional brachiopod coquinas and layers of crinoid debris with sharp lower boundaries are interpreted as storm deposits. On the top of the mid-ramp interval in the Aferdou el Mrakib section, a 22 m thick crinoidal limestone lense forms the base of the Aferdou el Mrakib reef-mound. The mid-ramp facies grades basinward into the outer ramp facies.

Outer ramp facies (burrowed, argillaceous skeletal wackestones)

This facies is represented by a 90 m thick interval in the upper Emsian to lower Eifelian (*patulus* Zone to lower part of the *costatus* Zone) part of the Jebel el Otfal section (Text-fig. 31). It resembles the mid-ramp facies and is composed of brown, argillaceous wackestones with abundant *Planolites* burrows. In contrast to the mid-ramp facies the shale content is higher and storm deposits are absent. The fauna is still dominated by neritic elements (crinoids, brachiopods, solitary rugose corals, tabulate corals, bryozoans, gastropods, trilobites) but pelagic elements (cephalopods and dacryoconarids) are also common. The mud-mounds nos 1, 2 and 3 of Jebel el Otfal were established on top of the outer ramp interval.

Burrowed, argillaceous skeletal wackestones were deposited below storm wave base but still within dimly-lit conditions, as is evidenced by the presence of large-eyed trilobites (R. FEIST, *pers. comm.*). The outer ramp facies wedges out basinward.

Transitional outer ramp to basinal facies (blue-grey, laminated mudstones)

This facies abruptly overlies the Aferdou el Mrakib reef-mound and the outer ramp facies in the section of Jebel el Otfal (Text-fig. 31). It consists of blue-grey, poorly-fossiliferous, laminated mudstones and limestone-marl rhythmites. The fauna is strongly impoverished with respect to the mid-ramp and outer ramp facies. Only pelagic organisms, like cephalopods, styliolinids and trilobites occur sparsely. *Planolites* burrows are less common than in the mid-ramp and outer ramp facies and *Zoophycos* are occasionally seen. Mud-mound no. 4 at Jebel el Otfal is intercalated within the lower part of this facies.

Blue-grey, poorly-fossiliferous mudstones were deposited below storm wave base in the dysaerobic environment of a transitional zone between outer ramp and basinal facies. The decrease in bottom-water oxygen levels relative to the mid-ramp and outer ramp facies is indicated by the almost complete absence of benthic organisms and the depletion of trace fossils. The termination of mound growth at Aferdou el Mrakib, Guelb el Maharch and Jebel el Otfal is probably caused by the deterioriation of bottom conditions. Limestone-marl rhythmites probably reflect periodic changes of terrigenous influx into the marine environment (RICKEN 1991).

Basinal facies (monotonous, poorly-fossiliferous shales)

This facies is typified by the section of Irhfelt n'Tissalt (Text-fig. 31). It consists of thick, monotonous, poorly-fossiliferous shales, interbedded with thin limestone units and in the upper half with calcareous turbidites (brachiopod lumachelles) and sandstones.

Prevailing shale sedimentation, high sedimentation rates, scarcity of fossils and intercalated turbidites suggest deposition in a basinal environment, which was the depocentre of the Mader Basin.

Bathymetric positions of carbonate mounds

The northward-deepening bathymetric gradient of the carbonate ramp is also reflected by different faunal associations of the Mader Basin carbonate mounds (see chapters on faunal characteristics). The Aferdou el Mrakib reef-mound

contains abundant frame-builders (domical stromatoporoids, colonial rugose corals), suggesting formation in relatively shallow water, but indications for photic conditions, like calcareous algae and micritic envelopes are absent. Therefore, this mound must have grown in moderate water depths in the mid-ramp zone, possibly influenced by storm waves. Compared with the Aferdou mound, the fauna of the smaller mounds (Guelb el Maharch, Jebel el Otfal) is impoverished and dominated by crinoids and tabulate corals, indicating deeper bathymetric positions on the outer ramp.

Drowning of the ramp and its mounds

Termination of mound growth in the Mader Basin is connected with the drowning of the carbonate ramp. The latter coincides with a relative rise in sea level which is largely related to basin subsidence and exceeded carbonate production. Sedimentation rates in mid- to outer ramp zones in the Mader area were in the order of 20-40 m/Ma (BELKA & *al*. in press) suggesting that these areas could easily be drowned by tectonic subsidence. The drowning is expressed by the rapid upward transition from mid- and outer ramp to basinal facies in the Middle Devonian sections. Drowning of the carbonate mounds, however, appears to have been more complex. The most obvious reason, that sea-level rise was too rapid for the mounds to keep up, is unlikely. As pointed out in further in this paper, accumulation rates of the mounds were between 0.2-0.8 m/1000 a, suggesting that the mounds were generally able to keep pace with any subsidence-caused sea-level rise. The termination of mound growth could have been caused by influx of shale during drowning of the ramp. High depositional rates of fine-grained siliciclastics on the

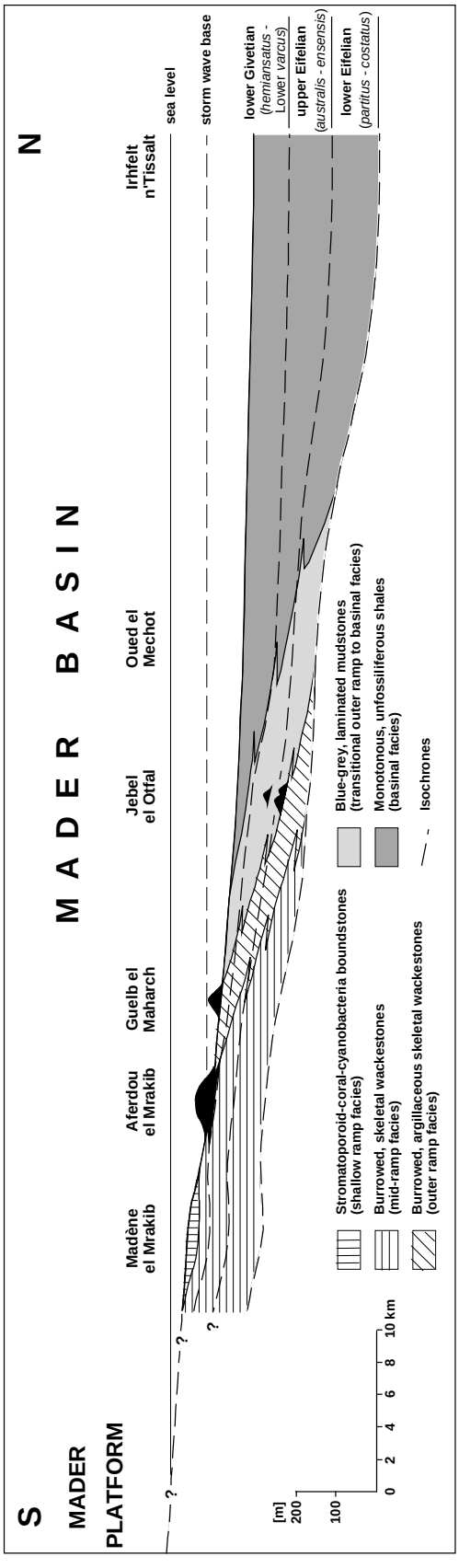

Fig. 32. Lower Givetian (Lower *varcus* Zone) facies model of the carbonate ramp in the southern Mader area, widths of mounds exaggerated; cross section shows distribution and diachrony of five different facies zones, illustrating the subsidence-related, southward extension of the Mader Basin depocentre; note that the section does not represent a Mader Basin cross section, but is drawn along a line, following the eastern bow of the Mader syncline (*see* inset of Text-fig. 31)

deepening ramp may have caused burial of mounds by onlapping basinal facies, but the direct cause for growth termination of Mader Basin carbonate mounds were probably changes in living conditions at the seafloor. All the mounds are overlain by laminated, basinal mudstones with a sharp contact to the underlying, fossiliferous, mid- to outer ramp wackestones. At this boundary the sedimentation becomes more argillaceous, the entire benthic fauna disappears and is substituted by a sparse pelagic fauna. This faunal change is certainly caused by a deterioriation of oxygenation conditions at the seafloor. Water depth probably increased below an oxygen level, at which a manifold benthos could not exist any longer, and mound growth consequently was terminated.

Termination of mound growth took place in early Eifelian times (*costatus* Zone) at Jebel el Otfal and in early Givetian times (Lower *varcus* Zone) at Guelb el Maharch and Aferdou el Mrakib. These deepening events cannot by correlated over the entire eastern Anti-Atlas and not even within the Mader Basin. Thus, they also cannot be related to eustatic sea-level rises. Strong subsidence, spreading out from the depocentre of the Mader Basin, resulted in the southward shift of the deeper water facies zones on the ramp, reaching and onlapping the more basinward Jebel el Otfal mounds in early Eifelian times (*costatus* Zone) and the more marginally situated Guelb el Maharch and Aferdou el Mrakib mounds in early Givetian times (Lower *varcus* Zone) (Text-fig. 32). The latter of these deepening events terminated not only mound growth at Aferdou el Mrakib and Guelb el Maharch but also drowned vast areas of the neritic facies belt, especially the coral-stromatoporoid limestones, which surround the depocentre of the Mader Basin. It cannot be excluded that this local, subsidence-caused deepening event is subsequently superimposed by an eustatic sea-level rise in the Middle *varcus* Zone, which is documented worldwide (Taghanic Event).

DIAGENESIS

Detailed diagenetic studies of Devonian carbonate buildups were made in Canada (WALLS & *al*. 1979, CARPENTER & LOHMANN 1989), Australia (KERANS & *al*. 1986, HURLEY & LOHMANN 1989) and Europe (SCHNEIDER 1977, MACHEL 1990b). Only very scarce data are known from North Africa to date.

Diagenetic studies of the Mader carbonate mounds were focused on Aferdou el Mrakib, Guelb el Maharch and Jebel el Otfal. The aim of these studies is to unravel the diagenetic history of the mounds applying transmitted light microscopy, SEM, staining techniques, cathodoluminescence and geochemical analyses (carbon and oxygen isotopes; Ca, Mg, Sr, Mn and Fe concentrations). Special objectives are: 1) to document and interpret the characteristic features of the complex cement succession in stromatactis fabrics and intraskeletal pores, 2) to establish the carbon and oxygen isotopic signatures of the Middle Devonian Mader Basin seawater and to compare these data with other Middle Devonian values, 3) to interpret the diagenetic environment of significant cathodoluminescence patterns, 4) to estimate the precipitation temperatures and burial depths of late blocky calcite cements, 5) to examine the recrystallization of the fine-grained mound carbonates and 6) to document the processes of dolomitization.

Methods

Petrographic investigations of calcite cements, microspar matrix and skeletal components were undertaken with light microscope combined with potassium ferricyanide staining (DICKSON 1966). A comparison of staining tests with microprobe analyses of the same samples yielded a sensitivity of potassium ferricyanide staining of about 1000 ppm Fe (0.18 mole% $FeCO_3$).

Cathodoluminescence (CL) was conducted on a CITL Cold Cathode Luminescence 8200 mk3 operating under 15-18 kV accelerating voltage, 200-300 μA beam current and a beam diameter of about 4 mm.

Microsamples of 0.8-3.1 mg for stable isotope and geochemical analyses were obtained from polished hand specimens using a drilling bit and a binocular microscope.

Stable isotope ratios have been measured in 23 Eifelian and 56 Givetian calcite microsamples. They were prepared with unhydrous phosphoric acid in an automatic carbonate reaction device (Carbo-Kiel) attached to a Finnigan MAT 251 mass spectrometer. Isotopic ratios were corrected for ^{17}O contribution (CRAIG 1957) and are

Table 1. CL and geochemical characteristics of calcite cements, skeletal components and dolomites of the Mader Basin carbonate mounds

	Staining Test [1]	Cathodoluminescence	$\delta^{18}O$ PDB	$\delta^{13}C$ PDB	mole% $MgCO_3$	Sr [ppm]	Sr/Mg	Fe [ppm]	Mn [ppm]
Radiaxial calcite, Eifelian (Jebel el Otfal)	non-ferroan	non / dull, mottled	-2.2 (±0.4)	+2.2 (±0.5)	1.4 (±0.2)	206 (±43)	0.063 (±0.015)	200 (±100)	300 (±100)
Radiaxial calcite, Givetian (Guelb el Maharch)	non-ferroan	non / dull, mottled	-2.5 (±0.1)	+2.2 (±0.9)	–	–	–	–	–
Radiaxial calcite, Givetian (Aferdou el Mrakib)	non-ferroan	non / dull, mottled	-2.6 (±0.3)	+3.0 (±0.2)	0.9 (±0.4)	171 (±27)	0.082 (±0.013)	150 (±100)	200 (±100)
Syntaxial cement	non-ferroan	non	–	–	–	–	–	–	–
Scalenohedral cement	non-ferroan	non	–	–	0.6 (±0.1)	–	–	400 (±250)	b.d.l[3]
Banded-luminescent cement	non-ferroan	alternating bright/moderate	–	–	0.7 (±0.4)	–	–	bright: 294 (mean) mod.: 770 (mean)	bri.: 1038 (mean) mod.: 294 (mean)
Blocky spar I	non-ferroan	moderate	-3.5 (±1.0)	+2.8 (±0.2)	0.2 (±0.1)	–	–	b.d.l	b.d.l
Blocky spar II	strong ferroan	dull	-8.9 to -6.8	+1.0 to +2.2	0.4 (±0.1)	–	–	3300 (±300)	290 (±90)
Blocky spar III	moderate ferroan	dull to moderate			0.5 (±0.1)	–	–	1900 (±900)	b.d.l
Blocky spar IV	moderate ferroan	bright			–	–	–	–	–
Calcite fracture fills	strong ferroan	dull	-7.6 (±1.7)	+0.5 (±1.4)	–	–	–	–	–
Microspar matrix	non-ferroan	dull to moderate, mottled	-6.9 (±2.1)	+2.1 (±1.1)	1.2 (±0.2)	232 (±57)	0.077 (±0.022)	1400 (±300)	170 (±70)
Crinoid ossicles	non-ferroan	non[2]	-3.3 (±0.5)	+2.0 (±0.8)	1.6 (±0.6)	219 (±65)	0.056 (±0.019)	880 (±400)	b.d.l
Brachiopod shells, Givetian (Aferdou el Mrakib)	non-ferroan	non	-2.6 (±0.2)	+2.7 (±0.2)	0.1 (±0.1)	394 (±27)	3.9 (±3.0)	–	–
Replacement matrix dolomite	moderate ferroan	alternating dull/moderate	-1.6 (±3.0)	+0.6 (±2.5)	46.5 (±3.1)	20 (±27)	–	4200[4]	1900[4]
Idiotopic mosaic dolomite (Ankerite)	strong ferroan	non	-5.1 (±3.9)	+1.1 (±4.2)	32.2 (±1.7)	–	–	82559 (±5000)	1335 (±529)

[1] potassium ferricyanide, [2] excepting microdolomite inclusions, [3] b.d.l = below detection limit, [4] one value only

reported in ‰ relative to the PDB standard. Precision was monitored through analyses of the NBS 18, 19 and 20 calcite standards and is better than 0.1‰ (σ) for both carbon and oxygen isotope compositions.

Cation compositions (Ca, Mg, Sr, Fe and Mn) of calcite cements, microspar matrix and skeletal components were determined with a SPECTO ICP-AES (Spektoflame Modula). Additional analyses of Ca, Mg, Fe and Mn were made by electron microprobe analyses of polished thin sections, using a CAMECA SX 50 Elektron Microprobe (accelerating voltage: 15 kV, beam current: 400 nA, beam diameter: 10 μm, counting time: 20 s). Microprobe detection limits were approximately 800 ppm for Mg and 100 ppm for Fe and Mn.

Scanning electron microscopy (SEM) of microspar matrix has been carried out by examining polished (1 μm alumina) and slightly etched surfaces (0.15% formic acid, 15-20 s). During SEM investigations of radiaxial calcites, microdolomite inclusions have been identified by an EDAX device.

Calcite cements

Petrography, CL and geochemical characteristics of calcite cements are summarized in Table 1.

Radiaxial calcite

Radiaxial calcite (RC) is the earliest cement phase, forming 1.0-4.0 mm thick, isopachous rims (Pl. 14, Fig. 1a) of large, bladed crystals on the walls of stromatactis cavities. The crystals diverge away from the cavity walls and display the characteristic undulose extinction (Pl. 14, Fig. 1b). Commonly, curved twins (Pl. 14, Fig. 1a) are well developed. RC of the Mader Basin mounds consists of cloudy (= rich in inclusions; Pl. 14, Fig. 1a; Pl. 15, Figs 1a, 2a) low-Mg calcite (LMC) with Mg concentrations of 1758-3959 ppm (0.8-1.8 mole% $MgCO_3$) and Sr concentrations from 172-249 ppm (bulk RC samples, Table 1). The Sr/Mg ratios vary from 0.048-0.095. Inclusions are mainly microdolomites (1.0-3.2 vol.%), which are subhedral to euhedral in shape and range from 1.5 to 15 μm in size (Pl. 16, Fig. 5). In areas of high inclusion density and at crystal terminations and intercrystalline boundaries, RC mostly exhibits a mottled, dull to moderate CL (Pl. 14, Fig. 1c; Pl. 15, Figs 1b, 2b). RC has not been found in intraskeletal pores, probably due to their restricted diagenetic environment and lower permeability in contrast to the more open stromatactis cavities. The development of RC is thus obviously dependent on high amounts of percolating seawater.

Since the first description of RC by BATHURST (1959), its origin has been a matter of debate. KENDALL & TUCKER (1973) had suggested that RC was neomorphosed from a fibrous aragonite precursor. KENDALL (1985) revoked this interpretation and concluded that most of the features of RC are primary, with the characteristic fabric of convergent optic axes produced by a process of asymmetric growth as the calcite crystals were undergoing split growth. This interpretation was confirmed by SANDBERG (1985) and SALLER (1986), who discovered RC in relatively young rocks (Pleistocene of Japan and Lower Miocene of the Enewetak Atoll in the Pacific respectively). As carbon and oxygen isotopic compositions and Mg contents were consistent with the marine composition, SALLER (1986) interpreted RC as a marine cement, directly precipitated from percolating seawater during shallow burial. However, microdolomite inclusions and partly mottled CL in RC of the Mader Basin mounds indicate that some diagenetic overprint must have occurred. The microdolomites and the low Sr/Mg ratios suggest a high-Mg calcite (HMC) precursor, which stabilized to low-Mg calcite (LMC) and dolomite (LOHMANN & MEYERS 1977). Several authors (LAND 1967, TOWE & HEMLEBEN 1976) pointed out that the transformation of HMC to LMC is a process of incongruent dissolution whereby $MgCO_3$ is lost into solution without any destruction of the calcite lattice. During this process, microdolomite crystals have been precipitated within the calcite crystals. The low total Mg contents (0.8 to 1.8 mole% $MgCO_3$) of RC may either be the result of original low magnesium concentrations (= low degree of carbonate supersaturation) of seawater or the transformation of HMC to LMC must has taken place in an open system, whereby the precursor HMC lost most of its Mg. The second alternative is preferred, because the total Mg concentrations as well as the Sr/Mg ratios of RC strongly resemble those of adjacent crinoid ossicles (Table 1), which were certainly of HMC composition.

Microdolomites have also been found in crinoid ossicles (Pl. 16, Fig. 1). In contrast to the RC

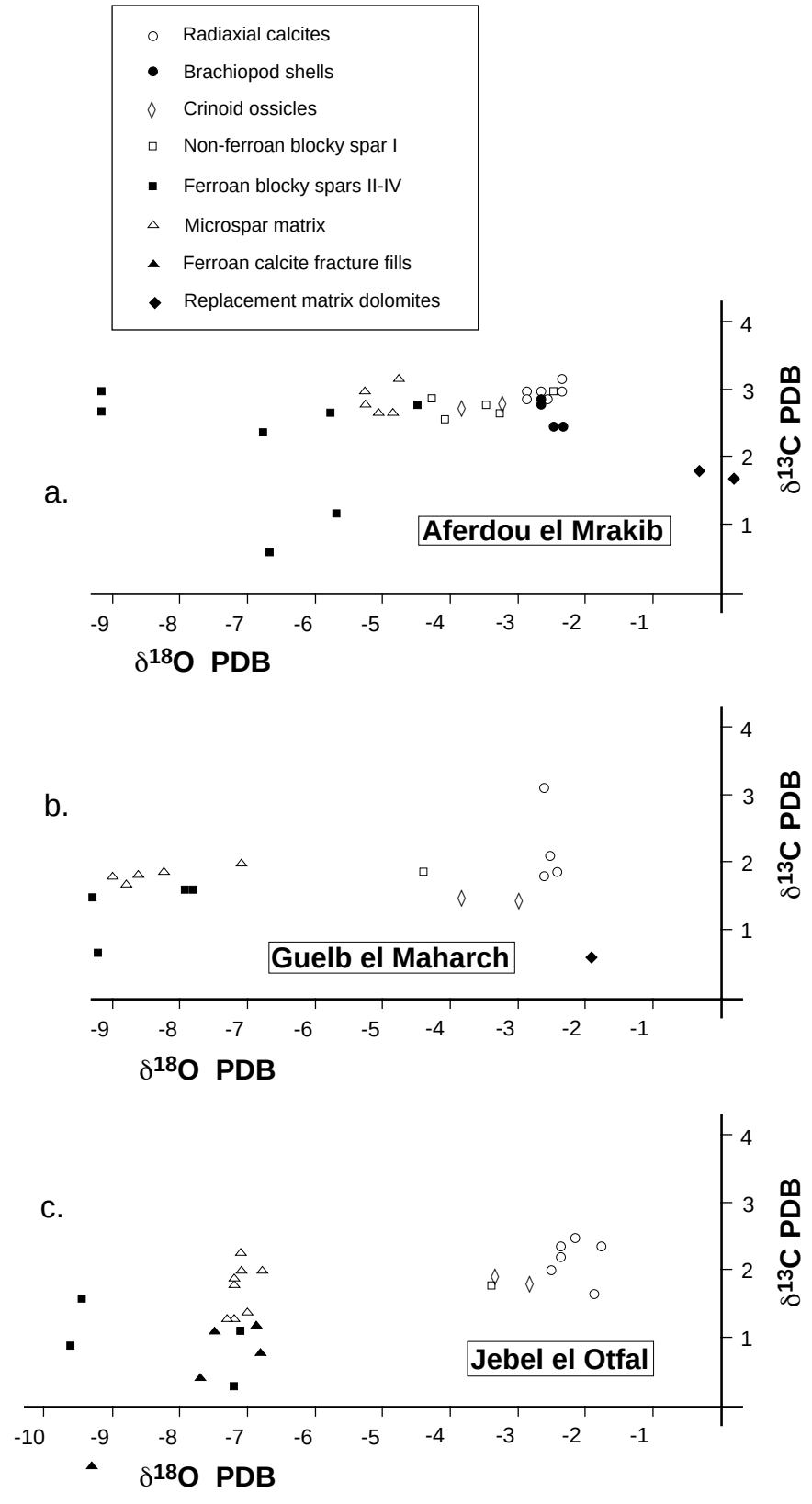

Fig. 33. $\delta^{18}O$ and $\delta^{13}C$ plots of calcite cements, skeletal components and dolomites of the Mader Basin carbonate mounds

microdolomites, the crystals are larger (10-20 μm) and display a moderate orange-red CL. Thus, the transformation of HMC to LMC probably happened under slightly reducing redox conditions during early burial diagenesis as is indicated by significant amounts of Mn^{2+} in the microdolomites.

Stable isotopic analyses of RC have been made from six samples each of Jebel el Otfal (lower Eifelian) and Aferdou el Mrakib (lower Givetian) and from four samples of Guelb el Maharch (lower Givetian). Jebel el Otfal values are in the range between $\delta^{18}O$ = –1.8 to –2.5‰ (mean: –2.2‰) and $\delta^{13}C$ = +1.7 to +2.5‰ (mean: +2.2‰) (Text-fig. 33c, Table 1). Isotopic analyses from Aferdou el Mrakib disperse only slightly around mean values of $\delta^{18}O$ = –2.6 (±0.3)‰ and $\delta^{13}C$ = +3.0 (±0.2)‰ (Text-fig. 33a, Table 1). RC from Guelb el Maharch displays $\delta^{18}O$ values of –2.5 (±0.1)‰ and $\delta^{13}C$ values of +2.2 (±0.9)‰ (Text-fig. 33b, Table 1).

Scalenohedral cement

Scalenohedral cement (dog-tooth cement) is the first cement generation in intraskeletal pores (mainly corals and brachiopods, Pl. 14, Fig. 3) and shelter cavities (*e.g.* trilobites, Pl. 14, Fig. 2). In stromatactis fabrics, it overgrows syntaxially the RC (Pl. 14, Fig. 1c; Pl. 15, Figs 1b, 2b) and marks a major change in crystal habit. The crystals are clear (= inclusion-free), non-ferroan and have lengths of 0.15 to 0.5 mm, rarely up to 0.8 mm (Pl. 14, Fig. 2). These crystal sizes are too small to obtain samples for stable isotopic analyses by conventional preparation methods. To aggravate the situation, this cement is usually only visible under CL (Pl. 14, Figs 1c, 2 and 3; Pl. 15, Fig. 1b). Scalenohedral cement typically exhibits a non-luminescent core and bright-luminescent or banded-luminescent margins (Pl. 14, Figs 1c, 2; Pl. 15, Figs 1b, 2b), which are treated here separately (see next chapter).

Microprobe analyses from the non-luminescent cores yielded mean cation concentrations of 1500 (±300) ppm Mg (0.6 ±0.1 mole% $MgCO_3$), 400 (±250) ppm Fe and below detection limit (< 50 ppm) for Mn (Table 1).

Bright-luminescent and banded-luminescent cements

As mentioned above, non-ferroan, bright- and banded-luminescent cements form the outer margins of the scalenohedral cements. The bright-luminescent cement consists of a single, 5-70 μm wide growth zone (Pl. 14, Fig. 1c), whereas banded-luminescent cement is concentrically zoned, consisting of several, irregularly alternating, 5-40 μm thick, bright- and moderate-luminescent zones with sharp boundaries (Pl. 15, Figs 1b, 2b). Additionally to concentric zoning, 'oscillatory zoning' (*sensu* REEDER & *al*. 1990) can be seen within moderate luminescent growth zones (Pl. 15, Fig. 1b), exhibiting regularly alternating, about 2-4 μm thick zones.

Syntaxial cement

Syntaxial calcite cement is often developed on crinoid ossicles (Pl. 16, Fig. 1). It is clear (= inclusion-free), non-ferroan and non-luminescent and therefore petrographically similar to the scalenohedral cement.

Blocky calcite cements

Clear, equant, non-ferroan and ferroan, blocky calcite cements fill the centres of the stromatactis cavities and intraskeletal pores. A combination of potassium ferricyanide staining and CL was used to distinguish four types of this cement. These are from oldest to youngest (Table 1): I) non-ferroan, moderate-luminescent spar (Pl. 14, Figs 1c, 3; Pl. 15, Fig. 1b), II) strong ferroan, dull-luminescent spar (Pl. 14, Figs 1c, 3; Pl. 15, Figs 1b, 2b), III) moderate-ferroan, dull- to moderate-luminescent spar (Pl. 14, Fig. 3; Pl. 15, Fig. 1b) and IV) moderate-ferroan, bright-luminescent spar (Pl. 14, Fig. 3). In most cavities and intraskeletal pores, only the cement generations I and II are found to occlude the pore space. Therefore, the latest generations III and IV are developed only in the largest stromatactis cavities.

Interpretation

Marine signature of radiaxial calcites and brachiopod shells

One aim of this study was to determine the isotopic composition for marine cements and brachiopod shells that formed in equilibrium with Middle Devonian seawater of the Mader Basin. These values can be compared to marine

Devonian isotopic records from other parts of the world. Generally, isotopic compositions from ancient seawater are obtained either from pristine marine cements (*e.g.* CARPENTER & LOHMANN 1989, LAVOIE & BOURQUE 1993) or from unaltered brachiopod shells (*e.g.* WADLEIGH & VEIZER 1992, LAVOIE 1993). The RC in the Mader Basin carbonate mounds is regarded as a marine cement, which has preserved the isotopic composition of the Middle Devonian Mader Basin seawater. This cement escaped neomorphism, but the open system transformation from a formerly HMC to a more stable LMC probably altered the original isotopic composition to some degree. Nevertheless, evidences for the preservation of a pristine isotopic signature in Mader Basin RC are: 1) the low variability of $\delta^{18}O$ and $\delta^{13}C$ values, 2) exceptional high $\delta^{18}O$ values and 3) the accordance of the stable isotopic compositions with those of unaltered brachiopod shells (*see* below) (Text-fig. 33a, Table 1).

Ten isotopic analyses of lower Givetian RC (Aferdou el Mrakib, Guelb el Maharch) and four brachiopod shell analyses of non-luminescent, fabric-retentive pentamerid shells (*Devonogypa* sp.) (Text-fig. 33a, b; Table 1) yielded mean values of $\delta^{18}O = -2.6$ (±0.2)‰ and $\delta^{13}C = +2.7$ (±0.5)‰. These values are believed to represent the Middle Devonian stable isotopic signature of the Mader Basin seawater. Mean $\delta^{18}O$ values from Jebel el Otfal RC (lower Eifelian) are slightly heavier (+0.4‰) than those of Aferdou el Mrakib and Guelb el Maharch. They indicate either a slight positive shift in $\delta^{18}O$ from early Eifelian to early Givetian times, or, more likely, lower temperatures associated with their deeper water setting within the Mader Basin. The latter explanation is supported by investigations of BATES & BRAND (1991), who found that brachiopods from deeper water settings within the Appalachian Basin (North America) have higher $\delta^{18}O$ values (+1‰) compared with shallower water occurrences of the same species.

Most other Middle Devonian isotopic signatures are reported from North America and were obtained either from brachiopod shells (POPP & *al*. 1986, BRAND 1989, BATES & BRAND 1991) or from pristine marine cements (LOHMANN 1988). They display a variability in $\delta^{18}O$ from –5.5 to –3.7‰ and in $\delta^{13}C$ from –0.5 to +5.0‰. LAVOIE (1993, 1994) has proposed a $\delta^{18}O$ curve for late Silurian to Middle Devonian times (Text-fig. 34), using the heaviest $\delta^{18}O$ values of previous studies (VEIZER & *al*. 1986, POPP & *al*. 1986, LOHMANN 1988, BRAND 1989, BATES & BRAND 1991, WADLEIGH & VEIZER 1992, GAO 1993). Even the heaviest Middle Devonian oxygen isotopic values from North America ($\delta^{18}O = -3.7$‰ PDB, POPP & *al*. 1986, BRAND 1989) are still 1.0‰ lighter than those of the Mader Basin RC, which are the heaviest $\delta^{18}O$ values documented for the Middle Devonian to date. Two explanations are possible for this phenomenon: 1) diagenetic alteration and 2) special environmental conditions.

Diagenetic alteration of RC (transformation of HMC to LMC, formation of microdolomites) almost always results in ^{18}O depletion (GIVEN & LOHMANN 1985, HURLEY & LOHMANN 1989, CARPENTER & *al*. 1991), because alteration commonly occurs in the presence of ^{18}O-depleted meteoric water or, as is assumed in this case, under slightly elevated temperatures at shallow marine burial conditions. Therefore, it is unlikely that diagenetic alteration would have enriched ^{18}O in the Mader Basin RC. I interpret the high $\delta^{18}O$ values as nearly primary marine signals of Middle Devonian seawater of the Mader Basin, which are probably due to particular environmental conditions. Two marine depositional settings can result in higher $\delta^{18}O$ values relative to other 'normal' Middle Devonian signatures. These are 1) restricted evaporative conditions (^{18}O-enriched seawater) and 2) colder water environments. The Middle Devonian sediments of the Mader Basin do not show any evidence for evaporative conditions. The highly diverse fauna of crinoids, brachiopods, tabulate and rugose corals, trilobites, dacryoconarids and some pelecypods, bryozoans, gastropods and cephalopods indicates normal, open marine conditions. Therefore, the high $\delta^{18}O$ values are probably related to latitude-dependent lower water temperatures. The North American stable isotopic data for the Middle Devonian (POPP & *al*. 1986, LOHMANN 1988, BRAND 1989, BATES & BRAND 1991) were all obtained from shallow marine seas near to the equator and are therefore thought to represent a well-mixed Middle Devonian ocean. The palaeolatitudinal position of the eastern Anti-Atlas during the Middle Devonian, however, was about 35° south of the equator (SCOTESE & MCKERROW 1990). In these temperate latitudes, lower water temperatures

must be assumed. In addition to the palaeolatitudinal effect, deeper (= colder) marine settings below wave base (no mixing with warmer surface waters) have been suggested for the Mader Basin carbonate mounds (WENDT 1993, KAUFMANN 1995). According to FRIEDMAN & O'NEIL (1977), a +1.0‰ shift in $\delta^{18}O$ corresponds roughly to a temperature decrease of 5°C. Based on this assumption, the higher $\delta^{18}O$ values obtained from the Mader Basin would correspond to about 5°C lower water temperatures compared to the low-latitude values from North America. If this assumption is correct, the stable isotopic compositions of the Mader Basin represent particular, special depositional conditions and not the global marine isotopic signature of the Middle Devonian ocean. Integration of these data into LAVOIE's (1993, 1994) $\delta^{18}O$ curve (Text-fig. 34) must take into account the palaeoenvironmental effect. The Mader Basin oxygen isotopic data (Text-fig. 34) must therefore be corrected by +5°C (= –1.0‰ $\delta^{18}O$) to $\delta^{18}O$ = –3.7‰ and are thus close to Middle Devonian low-latitude values of POPP & *al*. (1986), BRAND (1989) and BATES & BRAND (1991).

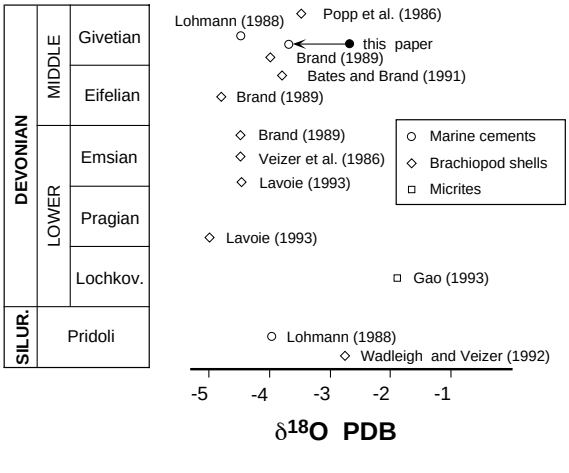

Text-fig. 34. Plot of $\delta^{18}O$ evolution during late Silurian to Middle Devonian times (*modified from* LAVOIE 1994); the $\delta^{18}O$ values plotted are the heaviest of each study (excepting LOHMANN 1988); data of BATES & BRAND (1991) are those of shallow-water brachiopod faunas; values of this study are corrected for the palaeoenvironmental effect (= –1.0‰ $\delta^{18}O$) of colder water settings (arrow)

Marine shallow burial origin of scalenohedral cement, bright- and banded-luminescent cement and blocky spar I

The succession of 1) scalenohedral cement, 2) bright- or banded-luminescent cement and 3) dull-luminescent blocky spar is documented from many studies (*e.g*. MEYERS 1978, STOW & MILLER 1984, CARPENTER & LOHMANN 1989, ZEEH & *al*. 1995). It exhibits the typical non-bright-dull CL sequence, which is interpreted either as meteoric (MEYERS 1978, CARPENTER & LOHMANN 1989) or as marine burial (STOW & MILLER 1984, ZEEH & *al*. 1995). According to previous studies (*see* above and reviews of MACHEL & BURTON 1991 and MEYERS 1991), hydrogeochemical conditions (redox reactions, $CaCO_3$ saturation, Mg^{2+}, Fe^{2+} and Mn^{2+} concentrations), under which non-bright-dull CL sequences develop, can obviously be the same in marine-phreatic as well as in freshwater diagenetic environments. The interpretation of a marine or meteoric origin of the scalenohedral/banded-luminescent cement/dull-luminescent blocky spar I sequence must therefore take into account the petrographic and geochemical evidences as well as the depositional setting. In the Mader Basin, the cement succession is thought to reflect a progressive marine shallow burial because the cement sequence exhibits no visible interruption or corrosion surfaces, which might be expected under the influence of meteoric water. A further criterion is the lack of a negative $\delta^{13}C$ shift, which usually appears when meteoric water passes through vadose environments and incorporates soil gas, which contains ^{12}C-enriched CO_2 (ALLAN & MATTHEWS 1982). It should be borne in mind that, in the Mader Basin carbonate mounds, there is no depositional evidence for meteoric influence like exposure surfaces, karst phenomena or vadose cements. As stated above, the mounds were established in subtidal mid- to outer ramp environments far from any recharge areas and were not exposed to intermittent periods of meteoric diagenesis. Moreover, the Mader Basin subsided rapidly in Middle and Late Devonian times and the mounds were drowned and covered by 2000-3000 m of Upper Devonian and Lower Carboniferous marine siliciclastic deposits. Under such conditions the input of meteoric water can be ruled out.

Scalenohedral cement. Scalenohedral cement was probably precipitated as stable LMC, as is

indicated by the unaltered crystal habit, the low Mg contents and the absence of microdolomite inclusions. Non-luminescence and low Fe^{2+} concentrations indicate oxydizing marine to shallow burial conditions. As pointed out by GIVEN & WILKINSON (1985), crystal morphology, composition and mineralogy are essentially controlled by $CaCO_3$ saturation and rates of fluid flow. Lower surface nucleation of scalenohedral cement relative to the predating RC (Pl. 14, Fig. 1c; Pl. 15, Fig. 1b) as well as the LMC composition and the significant change in crystal habit, indicates precipitation under stagnant conditions with lower $CaCO_3$ saturation and lower rates of fluid flow. According to KERANS & *al*. (1986), such conditions probably originate from former occlusion of the cavity systems by the predating RC.

Syntaxial cement. Because the petrographical features of syntaxial cements (lack of microdolomite inclusions, low Fe^{2+} concentrations and non-luminescence) resemble those of the scalenohedral cement, an original LMC mineralogy is suggested. Therefore, it is thought to have formed under oxydizing, but stagnant marine to shallow burial conditions.

Bright- and banded-luminescent cements. Bright- and banded-luminescent cements represent a marked increase of Mn^{2+} incorporation into the calcite lattice without a change of crystal habit (Pl. 14, Fig. 1c; Pl. 15, Figs 1b, 2b). In previous publications (*see* review above), the non/bright CL transition is generally interpreted as a decrease in redox potential (Eh) leading to a reduction of Mn^{4+} to Mn^{2+}. Decreasing Eh is usual under progressive marine burial conditions (DREVER 1982) and therefore probably also responsible for the non-bright CL transition in the Mader Basin calcite cements. Banded-luminescent cements with alternating bright-luminescent and moderate-luminescent zones are due to different Mn^{2+} concentrations and/or variations in the Fe/Mn ratio in successive growth zones. In previous studies (GROVER & READ 1983, BARNABY & RIMSTIDT 1989, EMERY & DICKSON 1989, HORBURY & ADAMS 1989), similar banded-luminescent cements have been interpreted as a reflection of fluctuating redox conditions, mostly related to meteoric aquifers. Changing redox potential (Eh) has often been explained by using pH/Eh diagrams, assuming chemical equilibrium (open systems) in porewaters (FRANK & *al*. 1982, BARNABY & RIMSTIDT 1989). However, chemical equilibrium is uncommon in natural environments (LINDBERG & RUNNELLS 1984). For instance, bright- and banded-luminescent cements in the Mader Basin carbonate mounds precipitated in pores, which were formerly nearly occluded by predating cements (RC, scalenohedral cements). Such restricted diagenetic environments represent closed or partly closed systems far from chemical equilibrium. As suggested by MACHEL & BURTON (1991), trace element partitioning in closed systems can determine Fe^{2+} and Mn^{2+} concentrations in solutions and therefore in precipitating cements. Diagenetic processes, like recrystallization and carbonate cementation in closed or partly closed systems generally lead to depletion of trace elements with distribution coefficients (D) > 1 (*e.g*. Mn^{2+} and Fe^{2+}) in solution and to their enrichment in the solid phase (PINGITORE 1978, MACHEL & BURTON 1991). In addition, the Mn/Fe ratio can change, because D_{Mn} is usually larger than D_{Fe} (DROMGOOLE & WALTER 1990). As shown in Textfig. 35, the CL intensities within banded-luminescent cements are dependent on both absolute Mn concentrations and Mn/Fe ratio. In contrast, changing redox conditions would result in an increase or a decrease of Mn as well as Fe concentration. Thus, the pattern of alternating bright- and moderate-luminescent zones within banded-luminescent cements of the Mader Basin carbonate mounds is

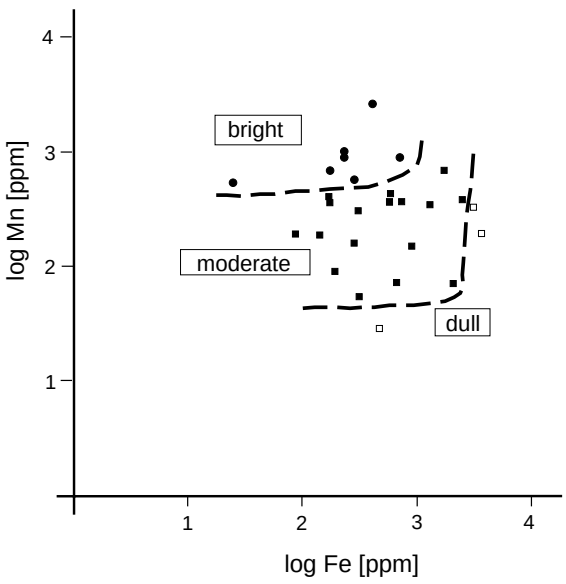

Fig. 35. Log Mn [ppm] and log Fe [ppm] plot of calcite cement values, obtained from a microprobe traverse across banded-luminescent cement of Pl. 15, Fig. 1b

interpreted as a result of varying Mn/Fe ratio, related to Mn and Fe distribution coefficients in semi-closed or closed systems. Also the common 'oscillatory zoning' seems to be related to closed system conditions. According to REEDER & *al*. (1990) this type of zoning developes from periodic fluctuations in growth rate in systems of chemical disequilibrium.

Individual zones of banded-luminescent cements can be correlated only within the same cavity. Cavities of the same size, only a few centimetres apart, can lack banded luminescence and display only a thin bright-luminescent outer rim on the predating scalenohedral cement. Though the overall cement succession in cavities and intraskeletal pores always shows a progressive reducing Eh trend (non-bright-dull CL sequence), small-scale changes in luminescence patterns are interpreted as a result of individual diagenetic environments in cavities, mainly concerning their degree of 'openness'.

Blocky spar I. The mean stable isotopic composition of blocky spar I exhibits a slight depletion in oxygen (-0.9‰) and rather constant values in $\delta^{13}C$ relative to the assumed early Givetian marine composition [$\delta^{18}O$ = –2.6 (±0.2)‰ PDB; $\delta^{13}C$ = +2.7 (±0.5)‰ PDB] (Text-fig. 33a-c, Table 1). The negative $\delta^{18}O$ shift presumably results from slightly elevated temperatures (about 5°C according to FRIEDMAN & O'NEIL 1977) during shallow marine burial. However, dull to moderate luminescence and Mg, Fe and Mn contents similar to the preceding banded-luminescent cements (Table 1) indicate no significant change in the diagenetic environment.

Deeper burial origin of ferroan calcite cements

The ferroan blocky calcite cements (blocky spars II, III and IV) are of deeper burial origin. The high Fe^{2+} content is usually the result of strongly reducing redox conditions and Fe^{2+} in solution is derived from clay minerals. On average, oxygen isotopic ratios are 4.2‰ (Aferdou el Mrakib) to 6.7‰ (Jebel el Otfal) (Text-fig. 33) lighter than the assumed marine composition, whereas the carbon isotopic values are only slightly depleted (–0.8 to –1.2‰). Many isotopic studies emphasize relatively constant or slightly depleted carbon and decreasing oxygen isotopic ratios in successive inferred burial cements (*e.g.* DICKSON & COLEMAN 1980, HURLEY & LOHMANN 1989). This trend is attributed to increasing temperatures and an isotopic change of porewaters during burial. By simply using temperature as the main controlling factor for the negative $\delta^{18}O$ values of the ferroan calcite cements, estimates for the precipitation temperature and the burial depth can be made (*e.g.* HURLEY & LOHMANN 1989, LAVOIE & BOURQUE 1993). According to FRIEDMAN & O'NEIL (1977), each 10°C increase in temperature causes a negative $\delta^{18}O$ shift of about 2.0‰. Assuming a seawater temperature of about 15°C, the observed shift of –4.2 to –6.7‰ would correspond to precipitation temperatures of 36 to 48.5°C. Additionally postulating a pre-orogenic geothermal gradient of about 50°C/km in the Mader Basin (BELKA 1991), 420 to 670 m of sediment overburden are required for the oxygen isotopic values of the ferroan calcites. These values can only serve as rough estimates because the isotopic evolution of porewaters is influenced by factors other than temperature, *e.g.* salinity and dewatering of clay minerals. If the above assumption is correct, the precipitation of the latest cements would have taken place during the Late Devonian, as can be inferred from the burial history of the Mader Basin carbonate mounds.

The slight negative shift in $\delta^{13}C$ (–0.8 to –1.2‰) is probably due to thermocatalytic decarboxylation of organic matter in burial depths of several hundred metres (IRWIN & *al*. 1977), releasing ^{12}C-enriched CO_2 into porewaters.

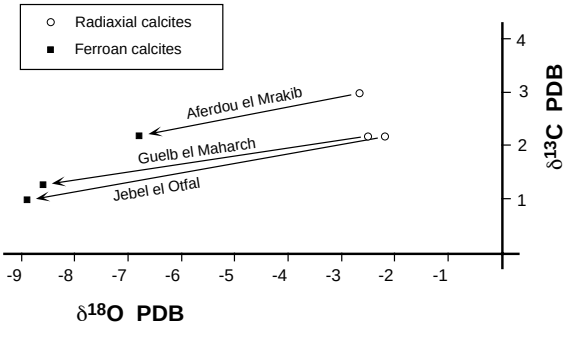

Fig. 36. Plot of $\delta^{18}O$ and $\delta^{13}C$ decreases from the assumed marine isotopic signatures (mean values of radiaxial calcites) to the latest deep burial calcite cements (mean values of ferroan calcites); note that ^{18}O and ^{13}C depletion is stronger towards the center of the Mader Basin

Text-fig. 36 shows the negative $\delta^{18}O$ and $\delta^{13}C$ shifts from RC to the late ferroan calcites for Aferdou el Mrakib, Guelb el Maharch and Jebel el Otfal. Depletion increases from Aferdou el Mrakib over Guelb el Maharch to Jebel el Otfal, corresponding to their progressively more central position within the Mader Basin. Conodont colour alteration indices (CAI), increasing from 4 to 5 in the same direction (BELKA 1991), correlate with the $\delta^{18}O$ and $\delta^{13}C$ depletion and indicate stronger subsidence and higher heat flow towards the basin centre.

Cement sequence

The cement succession in the Mader Basin carbonate mounds is interpreted to have developed under progressive marine burial conditions. It fits BRAITHWAITE's (1993) definition of a 'cement sequence' as a 'succession of syntaxial overgrowths having a crystallographic continuity unbroken by dissolution, renucleation, or other growth limiting events'. The shift from non-luminescence (RC, scalenohedral cement) over bright and moderate luminescence (banded-luminescent cement, blocky spar I) to dull luminescence (ferroan blocky spars II and III) is due to progressively decreasing redox conditions with increasing burial. This means that any single non-luminescent scalenohedral cement formed simultaneously with a banded-luminescent cement in a deeper burial level, which in turn was synchronous with dull, ferroan cement precipitation in a still deeper burial level. In the same way, the negative $\delta^{18}O$ shift from early to late cements reflects increasing temperatures with progressive burial. Thus, all cement types of the Mader Basin carbonate mounds are suggested to be diachronous, with no time-equivalence between two similar cement zones of two mounds and even between two samples of one and the same mound. Therefore, a correlatable cement stratigraphy (*e.g.* MEYERS 1978, KAUFMAN & *al.* 1988) cannot be established in the Mader Basin. The cement sequence is very similar to comparable cement sequences from elsewhere in the world (*e.g.* HURLEY & LOHMANN 1989, LAVOIE & BOURQUE 1993), which probably developed also under progressive marine burial conditions.

Pressure solution

Stylolites are common in the Mader Basin carbonate mounds and generally aligned almost horizontally. After WANLESS (1979) they can be classified as 'large amplitude, single sutured seams'. Stylolite teeth are arranged vertically (Pl. 16, Fig. 2), indicating pressure from sediment overburden. Their width does not exceed 0.4 mm and amplitudes are up to 2 mm. Sprouting dolomite rhombs, 50-200 μm in size, are often associated with these stylolites (Pl. 16, Fig. 2). Pressure solution by sediment overburden leads to compaction and decrease of porosity in limestones, because $CaCO_3$ is dissolved along stylolites and reprecipated in the available pore space. Stromatactis cavities and intraskeletal pores, partly occluded by marine and shallow burial cements, bear a 'rest porosity', which is required for pressure solution. If there is no pore space, stylolites are absent, as in the bedded off-mound limestones. Speculations about the depth of burial (= thickness of sediment overburden) required to initiate the pressure-induced stylolitization is controversial. DUNNINGTON (1967) has suggested a minimum overburden of 600-900 m but later studies (BUXTON & SIBLEY 1981, MEYERS & HILL 1983) point out that stylolites can also form at significantly shallower burial depths.

Timing of pressure solution is possible if stylolites pre- or postdate calcite cements (*e.g.* LAVOIE & BOURQUE 1993). Unfortunately, stylolites which cross-cut cement-filled cavities have not been found though a large number of thin sections have been examined. Therefore it is not possible to determine the exact timing of stylolitization in the Mader Basin carbonate mounds. It may have occurred before the final occlusion of the 'rest porosity', possibly coeval with the precipitation of the late ferroan calcites (Text-fig. 37).

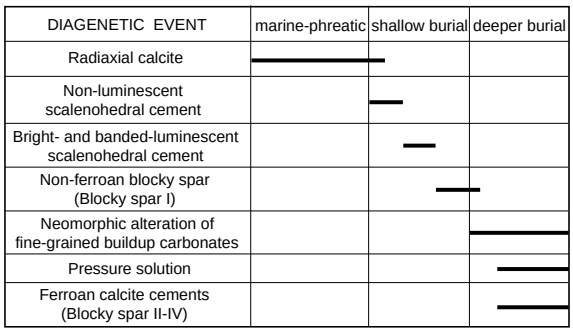

Fig. 37. Timing and environments of diagenetic events

Recrystallization of fine-grained mound carbonates

Recrystallization is the most pervasive and volumetrically important diagenetic process in the Mader Basin carbonate mounds because fine-grained carbonates constitude 80-90% of their rock volume. The matrix of the stromatactis-bearing, bioclastic mound boundstones consists exclusively of microspar. This term is prefered here rather than micrite, because the grain-size ranges from 4-12 μm (mostly 8-10 μm) and therefore falls in the microspar range of FOLK (1965, 4-30 μm). The fabric is a mosaic of equant, anhedral crystals and clay minerals between the irregular intercrystalline boundaries (Pl. 16, Fig. 6). Microspar exhibits a mottled, dull to moderate CL, indicating significant amounts of Mn. Surprisingly, no peloidal structures or clotted textures, often reported from Palaeozoic mud-mounds (MONTY & *al*. 1995), were found in the Mader mounds, not even under CL light. That means that either recrystallization has obliterated these primary microfabrics or, more likely, they have never been present.

Generally, microspar is interpreted to result from 'aggrading neomorphism' (FOLK 1965) of a formerly finer grained carbonate mud (micrite). This assumption is supported by the patchy mosaic of anhedral crystals, which have probably grown at the expense of previous micrite grains. Clay minerals between the irregular intercrystalline boundaries were obviously pushed aside during the growth of the microspar crystals. In addition, recrystallization is indicated by the mottled CL pattern, resulting from incorporation of Mn.

The importance of aggrading neomorphism (recrystallization) in ancient limestones was later questioned (STEINEN 1982, LASEMI & SANDBERG 1984). LASEMI & SANDBERG (1984) found abundant aragonite relics in ancient microspars as old as Ordovician. As an alternative to aggrading neomorphism of micrite, which itself replaced the aragonite needles, they suggested a one-step process of aragonite-calcitization leading to microspar. In addition, they proposed a subdivision of micrites and microspars into those with aragonite-dominated precursors (ADP) and others with calcite-dominated precursors (CDP), confirmed by FEIGL stain, X-ray and electron diffraction and Sr concentrations. However, no aragonite relics have been found in microspars from the Devonian Mader Basin carbonate mounds (Pl. 16, Fig. 6), a first indication for CDP. In addition, Mg and Sr concentrations provide an evidence for a pristine mineralogical composition though recrystallization certainly altered the geochemical composition of the precursor carbonates. Microspars have high Mg and low Sr concentrations (*see* above) resulting in Sr/Mg ratios of 0.061-0.099 (Table 1). Such low Sr/Mg ratios are a further evidence against ADP. In addition, these values strongly resemble those of radiaxial calcites and crinoid ossicles (Table 1), suggesting a Mg-calcite dominated precursor carbonate which origin is discussed further in this paper.

Stable isotope data provide evidence for temperature and burial depths of recrystallization. The carbon isotopic values of microspars (Text-fig. 33) are either quite similar (Aferdou el Mrakib) or slightly depleted (Guelb el Maharch, Jebel el Otfal) with respect to the assumed marine composition, whereas the oxygen isotopic ratios are 2.5 to 5.8‰ lighter. Applying the same temperature and burial calculations as used for the ferroan calcite cements (*see* above), recrystallization has taken place at temperatures of 27.5 to 44°C corresponding to burial depths of 250 to 580 m.

Dolomitization

Dolomitization is common in the Mader Basin carbonate mounds, especially at Aferdou el Mrakib (Text-fig. 11) and Guelb el Maharch (Text-fig. 15), where the mound cores are pervasively dolomitized. Apart from these larger areas, dolomite occurs only as cavity fillings at Guelb el Maharch (Pl. 4, Fig. 3; Pl. 5, Figs 3, 4) and Jebel el Otfal (Pl. 8, Fig. 2).

Petrographic types of dolomite

Three petrographic types of dolomite can be distinguished: 1) replacement matrix dolomite, 2) idiotopic mosaic dolomite and 3) isolated dolomite rhombs.

1) Replacement matrix dolomite. This is the most common dolomite type in the Mader Basin carbonate mounds. The dolomitized cores of Aferdou el Mrakib and Guelb el Maharch consist exclusively of this type. The prefered dolomitization of these mounds with respect to

their surrounding off-mound strata resulted from their higher permeability for the dolomitizing fluids. On the southwestern margin of Aferdou el Mrakib, a dolomitized Variscan(?) joint runs into the mound core (Text-fig. 11), a fact, which suggests post-orogenic funneling of dolomitizing solutions into this mound. Replacement matrix dolomite can also be found along Variscan faults and joints in the entire Mader area.

Generally, replacement matrix dolomite obliterates both fossils and sedimentary structures. It consists of anhedral to subhedral crystals in a xenotypic mosaic with crystal sizes from 0.1-1.0 mm (Pl. 16, Fig. 3). Individual crystals often display a slight undulose extinction. In thin sections from Guelb el Maharch, crystals with cloudy centres and clearer rims have been found. Replacement matrix dolomite exhibits a dull to moderate, concentrically zoned CL with several, irregularly alternating, 5-30 μm thick, dull- and moderate-luminescent zones (Pl. 16, Fig. 3).

A total of five analyses of stable isotopes have been made from samples of Aferdou el Mrakib (2), Guelb el Maharch (1) and SE' Jebel Zireg (2). Values fall in the range of $\delta^{18}O$ = +0.2 to –4.6‰ (mean: –1.6‰) and $\delta^{13}C$ = +1.8 to –1.9‰ (mean: +0.5‰) (Text-fig. 38, Table 1). Cation concentration analyses (ICP-AES) yielded a non-stoichiometric composition of 50.4 to 55.6 mole% $CaCO_3$ (mean: 52.4 mole%) and 43.4 to 48.6 mole% $MgCO_3$ (mean: 46.5 mole%). Fe and Mn concentrations (each one value only) are about 4200 ppm and 1900 ppm respectively, and Sr values range from below detection limit (< 10 ppm) to 47 ppm (mean: 20 ppm).

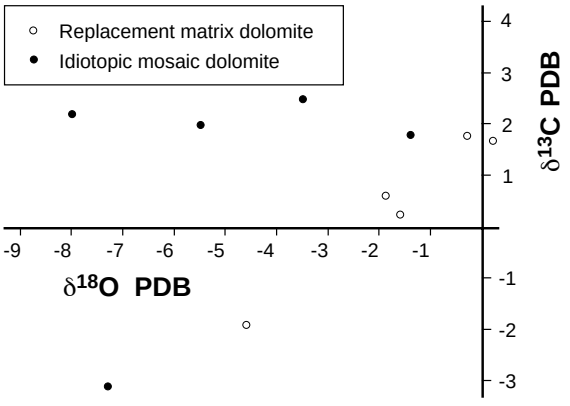

Fig. 38. $\delta^{18}O$ and $\delta^{13}C$ plots of replacement matrix dolomites and idiotopic mosaic dolomites of the Mader Basin carbonate mounds

2) Idiotopic mosaic dolomite. This type of dolomite occurs as central fillings in 3-20 cm-sized cavities at Guelb el Maharch and Jebel el Otfal (Pl. 4, Fig. 3; Pl. 5, Figs 3, 4; Pl. 8, Fig. 2). Commonly, it is a replacement of fine-grained internal sediments, as is indicated by occasional 'ghost laminations' (Pl. 8, Fig. 2). These internal sediments were obviously most susceptible for dolomitizing solutions. Idiotopic mosaic dolomite consists of strong ferroan, non-luminescent, loosely packed, sub- to euhedral rhombs with crystal sizes of 100-200 μm (Pl. 16, Fig. 4). Individual crystals are impure as is revealed by mottled potassium ferricyanide staining. Crystal rims and the matrix between the rhombs are brown and opaque and display moderate luminescence.

Five stable isotope analyses yielded values of $\delta^{18}O$ = –1.4 to –8.0‰ (mean: –5.1‰) and $\delta^{13}C$ = –3.1 to +2.2‰ (mean: +1.1‰) (Text-fig. 38, Table 1). Extremely high Fe concentrations (78296 to 87525 ppm corresponding to 14.2 to 15.3 mole% $FeCO_3$) characterize the idiotopic mosaic dolomite as ankerite. Mg values range from 75971 to 84760 ppm (corresponding to 30.6 to 33.9 mole% $MgCO_3$) and Mn values from 1013 to 1864 ppm (mean: 1335 ppm).

3) Isolated dolomite rhombs. Isolated dolomite rhombs have been found only in thin sections of the Aferdou el Mrakib reef-mound. They consist of non-ferroan, non-luminescent, sub- to euhedral crystals (Pl. 16, Fig. 2), ranging from 0.1-1 mm in size and occur in the matrix of the mound boundstones. Skeletal grains are not affected by dolomitization, suggesting that dolomitization began preferentially in the fine-grained matrix, which was obviously more permeable for dolomitizing solutions. In thin sections from samples close to the completely dolomitized mound cores, isolated dolomite rhombs mark the initial stage for a pervasive dolomitization (by replacement matrix dolomite). Dolomite rhombs have also been observed sprouting along stylolites (Pl. 16, Fig. 2), suggesting that stylolites locally acted as conduits for the dolomitizing fluids. Microprobe analyses sometimes revealed dedolomitization, indicated by LMC composition of individual rhombs.

Interpretation

As inferred from field investigations, petrographic evidences and stable isotope data, dolomites (especially replacement matrix dolomites) of the Mader Basin carbonate mounds formed after moderate to deep burial, after the Variscan compression and possibly after uplift and erosion of the overlying strata. This is indicated by 1) the postdating of stylolitization, 2) the relation of replacement matrix dolomites to Variscan faults and joints and 3) heavy $\delta^{18}O$ values, possibly indicating low precipitation temperatures near the surface.

Stable isotope data of the Mader Basin mound dolomites are still too scattered to allow precise conclusions about burial depths and formation temperatures of dolomites. Replacement matrix dolomites, however, display significant high $\delta^{18}O$ values (*see* above), even heavier than the assumed Middle Devonian stable isotopic signature of the Mader Basin seawater [$\delta^{18}O$ = –2.6 (±0.2)‰ PDB; $\delta^{13}C$ = +2.7 (±0.5)‰ PDB]. Three explanations are possible for these heavy values: 1) Replacement matrix dolomites represent synsedimentatry Devonian marine dolomites, 2) they precipitated from fluids derived from carbonates with heavier $\delta^{18}O$ or 3) they precipitated at low temperatures near the surface. As mentioned above, replacement matrix dolomites postdate stylolitization and are mostly related to Variscan faults and joints, ruling out a Devonian marine seafloor origin. Refering to point 2), it cannot be excluded, that Upper Devonian (or younger) brines, heavy in $\delta^{18}O$, may have circulated downwards and became involved in the formation of the replacement matrix dolomites. Though little is known about the stable isotope compositions of the overlying Upper Devonian marine limestones, it seems extremely improbable that they could yield values around $\delta^{18}O$ = –1.6‰. Explanation 3) involves Devonian brines that migrated upwards along the Variscan fault and joint system after erosion of the overlying Upper Devonian and Lower Carboniferous deposits. More thorough sampling and additional stable isotope data are required to solve the problem of these ^{18}O-enriched dolomites.

Dolomitizing fluids were probably derived from modified seawater and related to burial-compaction processes of Devonian Mader Basin shales and argillaceous limestones. Mg^{2+} is released into porewater by clay mineral changes (especially the smectite-illite transformation) at increased burial and rised temperatures (McHarque & Price 1982, Sternbach & Friedman 1986). Fluids probably migrated out of the shales and argillaceous limestones by compactional dewatering during the Late Devonian and Early Carboniferous subsidence and were subsequently expelled along Variscan faults and joints. Dolomitization related to faults is a common phenomenon, *e.g.* in the Devonian of Alberta, Canada (*e.g.* Machel & Anderson 1989, Kaufman & *al.* 1991, Mountjoy & Halim-Dihardja 1991).

Dolostone porosity

Dolomitization produced a secondary porosity in mound limestones of Aferdou el Mrakib and Guelb el Maharch. Mouldic porosity is developed in pervasively dolomitized limestones (replacement matrix dolomites) at Aferdou el Mrakib (Pl. 2, Fig. 8) and Guelb el Maharch. Fossils, especially stromatoporoids and brachiopods, which resisted dolomitization were dissolved selectively. Depending on the size of the organism remains, mouldic pores are a few cm in size (Pl. 2, Fig. 8). They are often enlarged, suggesting that subsequent leaching affected the matrix surrounding the bioclasts. Intercrystalline porosity, ranging from 5-10%, is represented only in idiotopic mosaic dolomites.

DISCUSSION

Origin of fine-grained mound carbonates

The origin of the fine-grained carbonates is the main problem in the formation of mud-mounds. The fine-grained host carbonates (microspars) of the Mader carbonate mounds are the product of recrystallization of a formerly finer-grained Mg-calcitic carbonate, a process, which has obliterated primary microfabrics and complicates interpretations of the origin of the primary carbonate. The following sources for the carbonate can be imagined:

(i) Baffling of lime mud by mound-dwelling organisms, like crinoids and tabulate corals

(ii) Trapping and binding of lime mud by cyanobacteria
(iii) Disintegration of calcareous skeletons, *e.g.* crinoids
(iv) Abiogenic precipitation of micritic cements
(v) Autochthonous carbonate production by microorganisms (cyanobacteria/bacteria)

Several authors have suggested sediment baffling by benthic invertebrates, like crinoids and bryozoans, as a cause for the accumulation of fine-grained carbonate (*e.g.* PRAY 1958, LEES 1964, WILSON 1975). It is unlikely, however, that a mere baffling effect could have caused the obvious disproportion of accumulation rates between the mounds proper and adjacent coeval off-mound areas (see further in this chapter). For the same reason, sediment supply by simple trapping and binding mechanisms by cyanobacteria (PRATT 1982) is improbable. Moreover, the mound facies consists of almost pure carbonate (> 95% $CaCO_3$) in contrast to the marly inter- and off-mound facies (50-70% $CaCO_3$). The only possible conclusion of these facts is that the carbonate fraction of the mounds must have been produced *in situ*. According to their Mg-calcite composition, the fine-grained carbonate could have been derived from the disintegration of crinoids. However, their ossicles are always well preserved and show no traces of micritization, dissolution or mechanical breakdown. Another possible interpretation is that the fine-grained mound carbonates are anorganic precipitated micritic cements. Generally, such cements are of Mg-calcite composition (*e.g.* LAND & MOORE 1980) and it is difficult to distinguish them from lime mud, especially after their recrystallization. But because skeletal components 'float' in the mound microspars, it is unlikely that the latter were cements.

Thus, no other origin rather than microbial activity seems possible for the origin of the fine-grained carbonates in the Mader carbonate mounds. Many authors have explained mound accretion by the activity of microbial communities (*e.g.* MONTY & *al.* 1982, 1995; LEES & MILLER 1985; TSIEN 1985a; BRIDGES & CHAPMAN 1988; CAMOIN & MAURIN 1988). Though microbial activity is difficult to recognize in ancient carbonates, several authors (*e.g.* MAURIN & NOL 1977, MAURIN & *al.* 1981, CAMOIN & MAURIN 1988, MONTY 1995) have found traces of microbes, *e.g.* filaments of cyanobacteria enclosed in micritic or microsparitic crystals. In spite of thorough examination, no traces of microbial activity, like stromatolitic or thrombolitic structures or peloidal textures, could be found in the Mader Basin mound microspars. Indications for microbial activity have been found, however, in the immediate neighbourhood of stromatactis fabrics. These are: 1) rare specimens of calcified cyanobacteria [*Rothpletzella devonica* (MASLOV 1956); Pl. 3, Fig. 8] and 2) thin, dark crusts, which are probably of cyanobacterial origin (R. RIDING, *pers. comm.*) (Pl. 3, Fig. 5). These crusts surrounding stromatactis fabrics suggest that cyanobacteria were cavity-dwellers and hence were involved in the formation of stromatactis (see next chapter). Evidences for cavity-dwelling cyanobacteria have also been reported by MONTY (1982, 1995) who found filaments enclosed in stromatactis-filling radiaxial calcite cements of several ancient mud-mounds.

Photosynthetically-enhanced production of fine-grained carbonates by cyanobacteria is known from modern lakes (THOMPSON & FERRIS 1990) and from the Bahama Platform (ROBBINS & BLACKWELDER 1992) as 'whiting events'. The assumed bathymetrical positions of the Mader carbonate mounds in dysphotic conditions are still compatible with photosynthetic cyanobacteria, because living species are known to exist down to considerable water depths. They are able to use particular pigments to achieve a chromatic adapdation, which enables them to use dimly-lit conditions for photosynthesis (MONTY 1995). However, high assimilation rates and hence large volumes of precipitated carbonate, as found in 'whitings' (ROBBINS & BLACKWELDER 1992), are unlikely under such conditions.

The processes of non-photoautotrophic microbial carbonate precipitation have recently been summarized by MONTY (1995). He emphasized that cyanobacterial/bacterial carbonate precipitation is not essentially dependent on photosynthesis, but is mainly the result of two microbial processes: active and passive precipitation. Active precipitation by cyanobacteria is related to the properties of their sheaths, which offer substrates for the nucleation of carbonate crystals. Cyanobacterial membranes and sheats consist essentially of polysaccharides, a material that tends to support carbonate precipitation (COSTERTON & *al.* 1981), regardless if bacteria are dead or alive (CHAFETZ & BUCZINSKY 1992).

Formation of carbonate nuclei in turn triggers the subsequent passive precipitation. Bacterial degradation of cyanobacteria and their surrounding mucilages induces passive carbonate precipitation (MONTY 1995). It is related to the metabolism of anaerobic, heterotrophic bacteria (nitrate reduction, sulphate reduction and ammonification), which alters the physico-chemical environment towards increased alkalinization and so leads to carbonate precipitation. Similar microenvironments may have existed in the Mader carbonate mounds, where uncalcified cyanobacteria and their surrounding mucilages have been progressively degraded by bacteria and have later been obliterated by recrystallization. Even if their occurrence, due to their low potential of fossilization, could be only poorly documented, I suggest that bacteria and cyanobacteria were present in large volumes and responsible for production of fine-grained mound carbonates in the carbonate mounds of the Mader area.

In chapter on Aferdou el Mrakib, I described the lithology of the Mader carbonate mounds as boundstones, following JAMES & BOURQUE (1992), who suggested this term for *in situ* accumulated microbial buildups. In a purely descriptive manner, the mound lithologies are stromatactoid, bioclastic wackestones and floatstones.

Stromatactis

Stromatactis fabrics are common in carbonate mounds of the Mader area. Generally, they fit the definitions of DUPONT (1881), HECKEL (1972) and BATHURST (1982) as spar-filled cavities in fine-grained limestones with flat to smoothly curved bases and irregular roofs (Pl. 2, Fig. 3; Pl. 3, Figs 2, 6; Pl. 8, Fig. 1; Pl. 9, Fig. 1; Pl. 10, Fig. 4). Often they are sheet spars (Pl. 3, Fig. 5) which lack irregular tops and be better termed stromatactoid. Lateral extension of these voids ranges from 2 mm (Pl. 3, Fig. 6) to 20 cm; the latter attain a height of up to 4 cm and form layered swarms (Pl. 2, Fig. 3; Pl. 8, Fig. 1). As an average, stromatactis fabrics constitute 5-10% (locally up to 20%; Pl. 2, Fig. 3; Pl. 8, Fig. 1) of the rock volume. When seen in three dimensions, these voids show extensions and interconnections. A reticulated network, which has been proposed as another criterion for stromatactis by LECOMPTE (1937), BATHURST (1982) and BOURQUE & BOULVAIN (1993), is rarely developed. In the Mader carbonate mounds, stromatactis bases are always aligned parallel to the accretionary surface of the mounds, even on the steep mound flanks, suggesting a close relationship between stromatactis and mound formation. If internal sediments are present, there tops are horizontally aligned, resulting from incomplete filling of the former cavities. Internal sediments consist of homogeneous, sometimes laminated mudstones, which are almost devoid of bioclasts and darker than the surrounding matrix. The transition to the host rock below the cavities is gradual without sharp boundaries (Pl. 3, Fig. 6).

Since the initial description of stromatactis by DUPONT (1881), the ideas about its formation have been controversial. About 20 hypotheses have been proposed for their origin (summary in FLAJS & HÜSSNER 1993). Without the intention to contribute another theory, I consider it appropriate to discuss some of these hypotheses. Because stromatactis fabrics occur mainly in Palaeozoic mud-mounds, a link between the origin of stromatactis and mud-mound formation seems feasible. The two major points of stromatactis formation are: 1) How were the cavities formed and 2) what is the cause of the irregular stromatactis shape. Most studies focused on the first question and came to the conclusion that stromatactis in different environments with different faunal compositions offer several possibilities for their origin. Two main groups of explanations can be distinguished:

1) Organic causes. The theories, which take into account organic causes deal with the presence of soft-bodied organisms or organism communities which left behind cavities in early lithified carbonate after their death and decay. BOURQUE & GIGNAC (1983), BOURQUE & BOULVAIN (1993) and WARNKE & MEISCHNER (1995) found sponge spicules in the immediate vicinity of stromatactis and interpreted the cavities as caused by the degradation of sponge tissues. Sponges do occur occasionally in the Mader carbonate mounds, but they are far too rare to play an important role in stromatactis formation. In addition, peloidal textures, often interpreted as originating from microbially decaying and/or calcifying sponges (BOURQUE & GIGNAC 1983, REITNER 1993, WARNKE & MEISCHNER 1995), are totally absent. LECOMPTE (1937) considered stromatactis as voids of decomposed, non-skeletal algae. Several authors

(*e.g.* BATHURST 1959, LEES 1964) thought that the cavities were formed by the decay of unknown soft-bodied organisms. TSIEN (1985b) questioned the presence of a formerly cavity system and suggested stromatactis as a replacement of microbial accretions by calcite cements. FLAJS & HÜSSNER (1993) attributed layered stromatactis fabrics to cyclic propagation of microbial mats at times of low sedimentation, which digitated and decayed after sediment covering.

2) Inorganic causes. BATHURST (1982) explained the cavities by winnowing of unconsolidated sediment between lithified crusts. In the carbonate mounds of the Mader area, no evidences for crusts, like brittle fractures, have been found. On the contrary, a homogeneous, firm gel-consistency is assumed for the fine-grained carbonate (see next chapter). After HECKEL (1972), the cavities, especially the digitated roofs, were formed by water-escape after collapse of sediment in thixotropic muds. As mentioned above, the primary carbonates are considered as firm, early lithified substrates and not water-rich and thixotropic. WALLACE (1987) imagined primary cavities of uncertain origin, whose roofs collapsed, leading to an upward migration of the cavities and so leaving below a trail of internal sediment. During this process, skeletal components often acted as a barrier for upward migration, creating shelter porosity. The same explanation of internal reworking and erosion was proposed by MATYSZKIEWICZ (1993), who described one of the rare examples of Mesozoic (Jurassic) stromatactis. He suggested that the primary cavities were of cyanobacterial origin.

In my opinion, the theory of WALLACE (1987) explaines best the typical stromatactis shape with irregular tops and, if internal sediments are present, flat, horizontal bases. As seen in the Mader carbonate mounds, horizontal bases are obviously a result of incomplete infilling, which has probably been derived from the cavity roofs. However, this process still bears the question how the primary cavities originate. In this point, LECOMPTE (1937) was probably right in considering the cavities to result from decaying algae. This idea was accepted by several authors (*see* above), who attributed stromatactis to non-preserved soft-bodied organisms or microbial communities. As pointed out in former chapter, the Mader carbonate mounds are suggested to originate from the activity of microbial (cyanobacterial/bacterial) communities, which flourished on the mound surfaces and precipitated actively the fine-grained mound carbonates. Once embedded, the communities decayed by heterotrophic bacterial degradation, leaving behind cavities, in which spar grew at the expense of the mucilages. This explanation matches closely TSIEN's (1985b) idea of successive replacement of microbial communities by calcite cements. The link between the origin of stromatactis and carbonate mound formation is evidenced by the alignment of stromatactis fabrics parallel to the accretionary surface of the mounds. In addition, the sparse traces of microbial activity have been found almost exclusively in the immediate neighbourhood of stromatactis fabrics (see former chapter).

Stability of steep mound flanks

The steep flanks (35-40°) of the Mader carbonate mounds are only possible with firm mound surfaces. Several textural indications suggest a firm gel-consistency of mound carbonates: 1) lack of compaction features, 2) absence of bioturbation in contrast to the highly bioturbated off-mound facies (Pl. 8, Fig. 6), 3) lack of mechanical reworking, 4) open intra- and interskeletal voids and 5) presence of neptunian dykes. According to ZANKL (1969), such a consistency of pure, fine-grained carbonates is caused by early lithification (cementation and recrystallization), which takes place at or near the surface. Additionally, mound flanks were probably stabilized by mucilages of microbial communities, which flourished on the mound surfaces.

Ecological succession

Faunal compositions, diversity and organization of carbonate mounds commonly change with growth. This is due to both intrinsic biological interactions, which lead to ecological succession or autostratigraphy and to external environmental controls, which result in allostratigraphy (JAMES & BOURQUE 1992). Stages of succession in reefs and mounds are stabilization, colonization, diversification and domination (WALKER & ALBERSTADT 1975). Following the concept of succession, only the first two stages, stabilization and colonization are developed in the carbonate mounds of the Mader area. Stabilization commu-

nities are composed mainly of crinoids, which are preserved as flat *in situ* lenses of crinoidal grainstones. These, in turn, served as substrates for the colonization of microbial communities, which formed stromatactis-bearing cone- and dome-shaped mud-mounds.

According to COPPER (1988), mounds fit the concept of a pioneer community, which is succeeded by a so-called climax community with ongoing growth, forming a 'true' reef. The Mader mounds were prevented from developing into such climax communities by drowning caused by rapid subsidence ('arrested successions' of COPPER 1988). The gradational development from a mound to a reef is partly achieved in the Aferdou mound, where domical stromatoporoids (= reef-builders) are already present but do not form a rigid framework. Examples for a complete ecological succession of mud-mounds, which developed into reefs are envisaged for the formation of the Middle Devonian reefs of former Spanish Sahara (DUMESTRE & ILLING 1967).

Accumulation rates and growth times

Accumulation rates of the Mader Basin carbonate mounds can be approximated from thickness ratios to the coeval off-mound strata. At Jebel el Otfal, the 40 m high mound no. 2 wedges out into a 2 m thick crinoidal grainstone bed with a thickness ratio of 20:1. At Aferdou el Mrakib, the originally 250 m thick reef-mound interfingers with 20-25 m of the coeval off-mound facies, indicating a ratio of about 10:1. Sediment accumulation rates in the off-mound facies of the Mader area were 20-40 m/Ma (BELKA & *al*. in press). If one considers thickness ratios of the mound facies to the bedded off-mound facies as a rough estimate for equivalent accumulation rates, then mound accumulation rates reach an average of 0.2-0.4 m/1000 a (Aferdou el Mrakib) and 0.4-0.8 m/1000 a (Jebel el Otfal mounds). That means that the smaller, 30-50 m high mud-mounds probably have grown in 40.000-125.000 years, whereas the large Aferdou el Mrakib reef-mound needed about 0.6-1.25 Ma to grow.

Initiation of mound growth

Another problem of the Mader carbonate mounds is: Why are the mounds where they are and what has triggered their growth? Middle Devonian outcrops in the Mader region cover an area of 500-1000 square kilometres. Less than 1% of this area is covered by carbonate mounds, which have been established in different bathymetric positions. Thus, water depth is obviously not the controlling factor for mound growth but for the benthic faunal associations which colonize the mounds. Because the Mader Basin carbonate mounds have grown on a carbonate ramp sloping into a deeper basin, the question is, if upwelling effects can trigger mound growth. The depocentre of the Mader Basin is, however, only a small intrashelf basin without any connection to oceanic realms where nutrient-rich upwelling currents usually come from.

Other explanations for spot-like mound occurrences are 'cold seeps' or 'hot vents' on the seafloor. Cold seeps as sites of mound growth are known from the Cretaceous of the Canadian Arctic (BEAUCHAMP & SAVARD 1992) and from carbonate knolls in the Porcupine Basin off western Ireland and the Vulcan Sub-basin off northwest Australia (HOVLAND & *al*. 1994). These mounds, however, are characterized by an extreme ^{13}C depletion, indicating seeped methane as a major carbon source. Because the carbonates of the Mader Basin mounds have normal marine $\delta^{13}C$ values (Text-fig. 33), they cannot be related to cold methane seeps.

Bryozoan/microbial mounds, which are related to hydrothermal vents, are known from the Lower Carboniferous in southwestern Newfoundland (von BITTER & *al*. 1992). Like modern hydrothermal vents, these are characterized by worm tubes, a high-abundance, low-diversity fauna and abundant sulphide and sulphate mineralizations. None of these features can be recognized in the Mader carbonate mounds, but mineralizations (pyrite, barite, apatite and dolomite) occur in the Middle Devonian mud-mounds of the Ahnet Basin in Algeria (BELKA 1994). The latter strongly resemble the Mader mounds and are suggested to have formed at sites of hydrothermal venting (BELKA 1994). Some Ahnet Basin mounds are aligned along Precambrian lineaments, which may have acted as conduits for upward migration of hydrothermal fluids. Because of their scattered occurrence, a connection to tectonic lineaments cannot be recognized in the Mader mounds. The Aferdou el Mrakib and Guelb el Maharch mounds are connected to NE-SW-trending dolomitized joints,

which are attributed to the Variscan fault system, but could also be reactivated synsedimentary faults. Neptunian dykes, common in the Guelb el Maharch mound, are synsedimentary and may have acted as conduits for hydrothermal fluids. Though the Mader carbonate mounds have not revealed any indications of hydrothermal activity so far, it cannot be excluded that thermal seeps with slightly elevated temperatures (not detectable by stable isotope analyses) and without mineralizations, have stimulated the benthic fauna which form the pioneer stages of mound development.

Modern analogues of ancient mud-mounds

One of the most problematic aspects in the study of ancient mud-mounds is the lack of modern analogues. The Florida Bay mud banks cannot be regarded as recent counterparts, though they are the only 'true' modern mud accumulations in the sense that they consist essentially of fine-grained carbonate. They lack a significant relief (usually < 3 m) and accumulated in extremely shallow water (WANLESS & TAGETT 1989). Moreover, they are regarded either as purely hydrodynamic accumulations of skeletal debris (STOCKMAN & *al*. 1967), or their sediment is suggested to have been formed from the breakdown of codiacean algae and *Thalassia* blade epibionts (BOSENCE & *al*. 1985).

The aphotic, deep-water coral bioherms north of Little Bahama Bank (MULLINS & *al*. 1981) and on the Norwegian shelf (HENRICH & *al*. 1995) cannot be regarded as analogues, because they are true ecological reefs, composed mainly of the deep-water coral *Lophelia*.

The recently discovered carbonate knolls in the Porcupine Basin off western Ireland and in the Vulcan Sub-basin off north-west Australia (HOVLAND & *al*. 1994) display some conspicuous similarities to the carbonate mounds of the Mader area, like water depth (100-1000 m), dimensions (100-1800 m in diameter, 20-200 m in height) and shapes (12-33° slopes). These mounds, however, are also not mud-dominated, but composed by deep-water corals (*Lophelia*) or codiacean algae (*Halimeda*). Additionally, their growth has been initiated by fault-associated hydrocarbon-seepage, evidenced by extremely negative $\delta^{13}C$ values (-34‰ PDB) (HOVLAND & *al*. 1994).

The perhaps best modern analogues are deep-water (600-700 m) lithoherms in the Straits of Florida (NEUMANN & *al*. 1977). They resemble the carbonate mounds of the Mader area concerning dimensions, shapes (20-30° slopes), benthic fauna (crinoids, corals and sponges) and their stromatactoid lithology. They are interpreted as biohermal constructions, formed *in situ* by subsea lithification of successive layers of trapped sediment and deposited skeletal debris (NEUMANN & *al*. 1977). Little is known to date about the recently discovered biogenic mounds on the shelf and upper slope of the southern continental margin of Australia (FEARY & JAMES 1995), which might be other analogues.

SUMMARY

In Devonian times, the eastern Anti-Atlas was part of a huge shelf on the NE-SW-trending passive continental margin of northwestern Gondwana (Sahara Craton), which has been a mid-latitudinal (30-40°S), temperate-water carbonate province. Early Variscan tensional movements caused a disintegration of the formerly stable shelf into a platform and basin topography. In the Mader region, a tectonically-controlled, gently sloping carbonate ramp was established between the rising Mader Platform and the rapidly subsiding depocentre of the Mader Basin. The Middle Devonian deposits of this ramp consists of 200-400 m thick argillaceous, fossiliferous limestones in which three of the described mound occurrences (Aferdou el Mrakib, Guelb el Maharch, Jebel el Otfal) are intercalated. They are located in mid- to outer ramp settings on the northward-sloping ramp, whose bathymetric gradient is reflected by a varied Middle Devonian facies pattern from shallow to deeper water environments and by different faunal associations of individual mounds.

The Aferdou el Mrakib reef-mound (*hemiansatus* to Lower *varcus* Zone) is the largest reefal buildup of the eastern Anti-Atlas. It has an almost circular, truncated cone-shape with a diameter of about 900 m and an elevation of 100-130 m. Abundant frame-builders (stromatoporoids, corals) indicate a formation in relatively shallow water, but the absence of calcareous algae and micritic envelopes suggests a bathymetric position below the euphotic zone. The smaller carbonate buildups of the Mader Basin (Guelb el Maharch, Lower *varcus* Zone; Jebel el

Otfal, *costatus* and *kockelianus* zones) are steep-sided, cone-shaped mud-mounds with base-diameters of 50-180 m and elevations of 10-45 m. They are sometimes elongated in outline and asymmetrical in shape. Steep mound flanks suggest firm substrates, which were lithified by early, synsedimentary cementation and additionally stabilized by microbial mats. The cause of the elongate and asymmetrical shapes is unclear, because no connection to bottom currents could be proved. Compared with the Aferdou mound, the fauna of the smaller mounds is impoverished and dominated by crinoids and tabulate corals which indicate deeper bathymetric positions on the carbonate ramp. Other less spectacular mud-mounds (SE' Jebel Zireg, Lower *varcus* Zone; Jebel Ou Driss, *partitus* Zone) are situated apart from that ramp at localities in the southern and the southwestern Mader area respectively.

The lithology of the Mader carbonate mounds is a massive boundstone (purely descriptive: wackestone to floatstone) with varying amounts of skeletal debris and common stromatactis fabrics. Microspar, originating from recrystallization of a Mg-calcitic precursor carbonate, forms the bulk of the mound volume. The primary fine-grained carbonate is believed to originate from carbonate precipitation by non-skeletal microbial (cyanobacterial/bacterial) communities. Even if their occurrence could only poorly be documented in the Mader carbonate mounds, circumstantial evidences suggest their presence and a close relationship between stromatactis formation and carbonate production. These evidences are: 1) Calcified cyanobacteria in the immediate neighbourhood of stromatactis fabrics, 2) Dark crusts surrounding stromatactis, 3) Homogeneous Mg-calcite mineralogy of fine-grained mound carbonates and 4) Alignment of stromatactis fabris parallel to the accretionary mound surfaces. Microbial communities probably flourished on the mound surfaces precipitating the fine-grained carbonates and consolidating mound flanks by their mucilages. Once embedded, communities decayed and were successively replaced by calcite cements, finally resulting in stromatactis fabrics.

Mound growth was possibly initiated by hydrothermal seepage at the seafloor but evidences for this assumption, like mineralizations or depleted $\delta^{13}C$ values, are lacking. Slightly elevated temperatures may have stimulated the benthic fauna, especially crinoids, forming flat *in situ* lenses, which then served as substrates for microbial colonization.

Accumulation rates of mounds are 10-20 times higher compared to the off-mound facies and are in the order of 0.2-0.8 m/1000 a. Equivalent growth times are 40.000-125.000 years for the smaller mud-mounds (Guelb el Maharch, Jebel el Otfal, Jebel Ou Driss, SE' Jebel Zireg) and 0.6-1.25 Ma for the large Aferdou el Mrakib reef-mound. These growth intervals can be precisely dated by high-resolution conodont biostratigraphy.

Termination of mound growth in the Mader Basin is connected with the drowning of the carbonate ramp by basinal subsidence. All mounds of the Mader Basin are overlain by laminated, poorly-fossiliferous mudstones with an abrupt lithological change to the underlying fossiliferous wackestones. This change is probably caused by a southward-directed onlapping of basinal facies on the carbonate ramp, resulting in poorly oxygenated seafloor conditions.

Diagenetic studies focused on the three mound occurrences Aferdou el Mrakib, Guelb el Maharch and Jebel el Otfal and can be summarized as follows:

1) Marine cementation by radiaxial calcites (RC) formed isopachous layers on the walls of stromatactis cavities. Microdolomite inclusions and low Sr/Mg ratios indicate a high Mg-calcite precursor (HMC) of RC. As RC has not been found in intraskeletal pores, its precipitation obviously depends on high amounts of passing seawater. Despite the early diagenetic alteration of HMC to LMC, RC is believed to have preserved the pristine marine stable isotopic signature of the Mader Basin seawater. This is proved by low variability of oxygen and carbon isotopic compositions and by correspondence with values of unaltered brachiopod shells. Mean values are $\delta^{18}O = -2.6$ (±0.2)‰ PDB and $\delta^{13}C = +2.7$ (±0.5)‰ PDB, obtained from Aferdou el Mrakib and Guelb el Maharch (both lower Givetian). The exceptional high $\delta^{18}O$ values, compared to Middle Devonian data of North America, are interpreted to result from the higher-latitude, colder-water setting of the Mader Basin carbonate mounds. To integrate these values into the Upper Silurian to Middle Devonian $\delta^{18}O$ curve of LAVOIE (1993, 1994), they have to be corrected for the palaeoenvironmental effect by –1‰.

2) Marine cementation passed into shallow burial cementation without any unconformity in

the cement succession. A sequence of non-luminescent scalenohedral cement/bright- or banded-luminescent cement/dull-luminescent blocky spar syntaxially overgrows predating RC and exhibits a typical non-bright-dull CL sequence. Scalenohedral cements (dog-tooth cements) consist of LMC and show a marked change in crystal habit. A lower nucleation density compared with the predating RC indicates stagnant water conditions with lower $CaCO_3$ saturation and lower fluid flow. Bright-luminescent and banded-luminescent cements mimic the scalenohedral cements and indicate the transition to reducing redox conditions in porewaters. The banded-luminescence pattern is interpreted to result from varying Mn/Fe ratio, related to Mn and Fe distribution coefficients in a semi-closed or closed system rather than from fluctuating redox conditions. Dull- to moderate-luminescent blocky spar indicates the transition to deeper burial conditions by slightly depleted $\delta^{18}O$ values (-0.9‰).

3) Deeper burial cementation by ferroan calcite cements occluded the 'rest porosity' of stromatactis cavities and intraskeletal pores. Strongly reducing conditions are indicated by Fe concentrations of up to 3596 ppm (0.64 mole% $FeCO_3$). Stable isotopic values of these cements show a strong depletion in ^{18}O (–4.2 to –6.7‰) and a slight depletion in ^{13}C (-0.8 to –1.2‰) with respect to the assumed marine composition. Simplicistically, oxygen isotopic values of the latest ferroan calcite cements are related to increasing temperatures during burial, indicating precipitation at about 36 to 48.5°C and burial depths of about 420 to 670 m. The slight negative $\delta^{13}C$ shift is interpreted to result from thermocatalytic decarboxylation of organic matter during deeper burial. Progressively stronger ^{18}O and ^{13}C depletion towards the centre of the Mader Basin correlates with higher CAI indices and is related to stronger subsidence and higher heat flow.

4) Also stylolitization took place under deeper burial conditions, but prior to the final cementation of stromatactis cavities and intraskeletal pores; $CaCO_3$, dissolved along stylolites, was a possible source of the late ferroan calcites, which occluded the remaining porosity.

5) Neomorphism of fine-grained mound carbonates produced microspar, which forms the bulk of the mound rocks. High Mg and low Sr concentrations suggest a Mg-calcitic precursor carbonate. Recrystallization under deeper burial conditions, approximately coeval with precipitation of late ferroan calcites, is indicated by dull, mottled CL, relatively high Fe concentrations (up to 1700 ppm) and low $\delta^{18}O$ values (–5.1 to –8.4‰ PDB).

The diagenetic history of the Mader Basin carbonate mounds until the occlusion of primary porosity is characterized by progressive marine burial conditions. Meteoric influences can be excluded because no petrographical, geochemical or sedimentological evidences have been found for subaerial exposure. Moreover, the Mader Basin carbonate mounds subsided rapidly, as is reflected by the bathymetric evolution of the Middle to Upper Devonian succession. All diagenetic events, especially cement zones, are probably diachronous and therefore cannot be correlated within the Mader Basin and not even within individual mounds.

6) Fault-related dolomitization, characterized mainly by replacement matrix dolomites, took place after Variscan compression. Unusual high $\delta^{18}O$ values possibly suggest precipitation of dolomites at low temperatures near the surface after erosion of overlying Upper Devonian and Lower Carboniferous deposits.

Acknowledgements

Jobst WENDT (Tübingen) initiated this study and has acted as supervisor throughout the project. He has contributed immensely by the guidance of wonderful field seasons in Morocco, aiding me with his 15 years of experience in the eastern Anti-Atlas. Funding for the project was given by the Deutsche Forschungsgemeinschaft (DFG), which also provided four-wheel drive cars for field works in 1993-1996. I am indebted to Mohamed Bensaïd and Mohamed Dahmani (Ministère d'Energie et des Mines, Rabat) for issuing a working permit and allowing the export of samples. Jörg HAYER (Tübingen) kindly assisted during the field work in 1994. Technical assistance in Tübingen was provided by Wolfgang GERBER (photograph work), Ralf KRAUßER (thin sections) and Horst HÜTTEMANN (scanning electron microscopy). Gitta WAHL is gratefully acknowledged for dissolving and preparing more than 100 kg of conodont samples, and Christian KLUG contributed some brilliant drawings. I am also very indebted to Zdzislaw BELKA (Tübingen), who determined the conodonts, provided many advices and helpful discussions and introduced me to SHAW's method of graphic correlation. Stable isotope analyses were made by B. MEYER-SCHACK and Monika SEGL (Bremen), other geochemical

analyses by Dieter BUHL (Bochum), Beatrice ADEL and Kurt MENGEL (Clausthal-Zellerfeld). Dierk BLOMEIER and Petra LAESKE (Kiel) are acknowledged for arranging and performing microprobe analyses. Tabulate corals were determined by Francis TOURNEUR (Louvain, Belgium), rugose corals by Marie COEN-AUBERT (Brussels, Belgium), brachiopods by Grzegorz RACKI (Sosnowiec, Poland), trilobites by Raimund FEIST (Montpellier, France), shark teeth by Michal GINTER (Warszawa, Poland) and goniatites by Dieter KORN (Tübingen). Sara J. METCALF improved the English of the manuscript. Finally, I thank again Jobst WENDT, Zdzislaw BELKA and in addition Marion KAZMIERCZAK, Gitta WAHL and Dieter KORN (all Tübingen), who thoroughly reviewed the manuscript and provided many corrections and improvements.

REFERENCES

ALBERTI, G.K.B. 1980. Neue Daten zur Grenze Unter/Mittel-Devon, vornehmlich aufgrund der Tentaculiten und Trilobiten im Tafilalt (SE-Marokko). *N. Jb. Geol. Paläont. Mh.*, **1980**, 581-594. Stuttgart.

— 1981a. Scutelluidae (Trilobita) aus dem Unter-Devon des Hamar Laghdad (Tafilalt, SE-Maider) und das Alter der "mud-mounds" (Ober-Zlichovium bis tiefstes Dalejum). *Senck. Leth.*, **62**, 193-204. Frankfurt/Main.

— 1981b. Daten zur stratigraphischen Verbreitung der Nowakiidae (Dacryoconarida) im Devon von NW-Afrika (Marokko, Algerien). *Senck. Leth.*, **62**, 205-216. Frankfurt/Main.

— 1982. Zur Frage einer Emersion der nördlichen NW-Sahara am Ende des Lochkoviums (Unter-Devon). *Newsl. Stratigr.*, **11**, 8-16. Stuttgart.

ALLAN, J.R. & MATTHEWS, R.K. 1982. Isotope signatures associated with early meteoric diagenesis. *Sedimentology*, **29**, 797-817. Oxford.

BARNABY, R.J. & RIMSTIDT, J.D. 1989. Redox conditions of calcite cementation interpreted from Mn and Fe contents of authigenic calcites. *Geol. Soc. Am. Bull.*, **101**, 795-804. Boulder.

BATES, N.R. & BRAND, U. 1991. Environmental and physiological influences on isotopic and elemental compositions of brachiopod shell calcite, implications for the isotopic evolution of Paleozoic oceans. *Chem. Geol.*, **94**, 67-78. Amsterdam.

BATHURST, R.G.C. 1959. The cavernous structure of some Mississippian Stromatactis reefs in Lancashire, England. *J. Geol.*, **67**, 506-521. Chicago.

— 1982. Genesis of Stromatactis cavities between submarine crusts in Palaeozoic carbonate mud buildups. *J. Geol. Soc. London*, **139**, 165-181. London.

BEAUCHAMP, B. & SAVARD, M. 1992. Cretaceous chemosynthetic carbonate mounds in the Canadian Arctic. *Palaios*, **7**, 434-450. Tulsa.

BECKER, R.T. & HOUSE, M.R. 1994. International Devonian goniatite zonation, Emsian to Givetian with new records from Morocco. *Cour. Forsch.-Inst. Senckenberg*, **169**, 79-135. Frankfurt/Main.

BELKA, Z. 1991. Conodont colour alteration patterns in Devonian rocks of the eastern Anti-Atlas, Morocco. *J. African Earth Sci.*, **12**, 417-428. Oxford.

— Dewońskie budowle weglanowe (*Carbonate buildups*) Sahary Środkowej i ich związek z podmorskimi źródłami termalnymi (Carbonate mud buildups in the Devonian of the Central Sahara: evidences for submarine hydrothermal venting). *Przegl. Geol.*, **5**, 341-346. Warszawa.

BELKA, Z., KAUFMANN, B. & BULTYNCK, P. (in press). A conodont-based quantitative biostratigraphy for the Eifelian of the eastern Anti-Atlas, Morocco. *Geol. Soc. Am. Bull.* Boulder.

BENSAÏD, M., BULTYNCK, P., SARTENAER, P., WALLISER, O.H., ZIEGLER, W. 1985. The Givetian-Frasnian boundary in pre-Sahara Morocco. *Cour. Forsch. Inst. Senckenberg*, **75**, 287-300. Frankfurt/Main.

BONHOMME, M. & HASSENFORDER, B. 1985. Le métamorphisme hercynien dans les formations tardi- et post-panafricaines de l'Anti-Atlas occidental (Maroc). Données isotopiques Rb/Sr et K-Ar des fractions fines. *Sci. Géol. Bull.*, **38**, 175-183. Strasburg.

BOSENCE, D.W., ROWLANDS, R.J. & QUINER, M.L. 1985. Sedimentology and budget of a Recent carbonate mound, Florida Keys. *Sedimentology*, **32**, 317-343. Oxford.

BOSENCE, D.W.J. & BRIDGES, P.H. 1995. A review of the origin and evolution of carbonate mud-mounds. *In*: C.L.V. MONTY, D.W.J. BOSENCE, P.H. BRIDGES & B.R. PRATT (*Eds*), Carbonate Mud-Mounds: Their Origin and Evolution. *Spec. Publs. Int. Assoc. Sediment.*, **23**, 3-9. Oxford.

BOULVAIN, F. 1993. Sédimentologie et Diagenèse des Monticules micritiques "F2J" du Frasnien de l'Ardenne. Serv. *Géol. Belg., Prof. Pap.*, **260**, pp. 1-436. Brussels.

BOURQUE, P.-A. & BOULVAIN, F. 1993. A model for the origin and petrogenesis of the Red Stromatactis Limestone of Paleozoic carbonate mounds. *J. Sed. Petrol.*, **63**, 607-619. Tulsa.

BOURQUE, P.-A. & GIGNAC, H. 1983. Sponge-constructed stromatactis mud mounds, Silurian of Gaspe, Quebec. *J. Sed. Petrol.*, **53**, 521-532. Tulsa.

BRACHERT, T.C., BUGGISCH, W., FLÜGEL, E., HÜSSNER, H., JOACHIMSKI, M.M., TOURNEUR, F. & WALLISER, O.H. 1992. Controls of mud mound formation: the Early Devonian Kess-Kess carbonates of the Hamar Laghdad, Antiatlas, Morocco. *Geol. Rdsch.*, **81**, 15-44. Berlin.

BRAITHWAITE, C.J.R. 1993. Cement Sequence Stratigraphy in Carbonates. *J. Sed. Petrol.*, **63**, 295-303. Tulsa.

BRAND, U. 1989. Global climatic changes during the Devonian-Mississippian: stable isotope biogeochemistry of brachiopods. *Palaeogeogr., Palaeoclimat., Palaeoecol.*, **75**, 311-329. Amsterdam.

BRIDGES, P.H. & CHAPMAN, A.J. 1988. The anatomy of a deep water mud-mound complex to the southwest of the Dinantian platform in Derbyshire, U.K. *Sedimentology*, **35**, 226-233. Oxford.

BULTYNCK, P. 1985. Lower Devonian (Emsian) – Middle Devonian (Eifelian and lowermost Givetian) conodont successions from the Ma'der and the Tafilalt, southern Morocco. *Cour. Forsch.-Inst. Senckenberg*, **75**, 261-285. Frankfurt/Main.

— 1987. Pelagic and neritic conodont successions from the Givetian of pre-Sahara Morocco and the Ardennes. *Bull. Inst. Roy. Sci. Natur. Belg., Sci. Terre*, **57**, 149-181. Brussels.

— 1989. Conodonts from a potential Eifelian/Givetian Global Boundary Stratotype at Jbel ou Driss, southern Ma'der, Morocco. *Bull. Inst. Roy. Sci. Natur. Belg., Sci. Terre*, **59**, 95-103. Brussels.

— 1991. Section Jbel Ou Driss. *In*: O.H. WALLISER (*Ed.*), Morocco Field Meeting of the Subcommision on Devonian Stratigraphy, Guide Book, 17-23.

BULTYNCK, P. & HOLLARD, H. 1980. Distribution comparée de Conodontes et Goniatites dévoniens des plaines du Dra, du Ma'der et du Tafilalt (Maroc). *Aardk. Meded.*, **1**, 1-73. Brussels.

BULTYNCK, P. & JACOBS, L. 1981. Conodontes et sédimentologie des couches de passage du Givetien au Frasnien dans le Tafilalt et dans le Ma'der (Maroc présaharien). *Bull. Inst. Roy. Sci. Natur. Belg., Sci. Terre*, **53**, 1-34. Brussels.

BURCHETTE, T.P. 1981. European Devonian Reefs: A review of current concepts and models. *In*: D.F. TOOMEY (*Ed.*), European Fossil Reef Models. SEPM *Spec. Publ.*, **30**, 85-142. Tulsa.

BUXTON, T.M. & SIBLEY, D.F. 1981. Pressure solution features in shallow buried limestone. *J. Sed. Petrol.*, **51**, 19-26. Tulsa.

CAMOIN, G. & MAURIN, A.F. 1988. Rôles des microorganismes (bactéries, cyanobactéries) dans la genèse des "Mud Mounds". Exemples du Turonien des Jebels Biréno et Mrhila (Tunisie). *C.R. Acad. Sci. Paris*, **307** (Série II.) 401-407. Paris.

CARPENTER, S.J. & LOHMANN, K.C 1989. $\delta^{18}O$ and $\delta^{13}C$ variations in Late Devonian marine cements from the Golden Spike and Nevis Reefs, Alberta, Canada. *J. Sed. Petrol.*, **59**, 792-814. Tulsa.

CARPENTER, S.J., LOHMANN, K.C, HOLDEN, P., WALTER, L.M., HUSTON, T.J. & HALLIDAY, A.N. 1991. $\delta^{18}O$ values, $^{87}Sr/^{86}Sr$ and Sr/Mg ratios of Late Devonian abiotic marine calcite; implications for the composition of ancient seawater. *Geochim. Cosmochim. Acta*, **55**, 1991-2010. London.

CHAFETZ, H.S. & BUCZYNSKI, C. 1992. Bacterially induced lithification of microbial mats. *Palaios*, **7**, 277-293. Tulsa.

CHLUPAC, I. & KUKAL, Z. 1986. Reflection of possible global Devonian events in the Barrandian area, C.S.S.R. *In*: O.H. WALLISER (*Ed.*), Global Bioevents, a critical approach. *Lect. Notes Earth Sci.*, **8**, 169-179. Berlin.

COPPER, P. 1988. Ecological succession in Phanerozoic reef communities: is it real? *Palaios*, **3**, 136-151. Tulsa.

COSTERTON, J.W., IRWIN, R.T. & CHENG, K.J. 1981. The bacterial glycocalyx in nature and disease. *Ann. Rev. Microbiol.*, **35**, 299-324.

CRAIG, H. 1957. Isotopic standards for carbon and oxygen correction factors for mass spectrometric analysis of carbon dioxide. *Geochim. Cosmochim. Acta*, **12**, 133-149. London.

DELÉPINE, G. 1941. Les goniatites du Carbonifère du Maroc et des confins Algéro-Marocains du sud (Dinantien-Westphalien). *Notes Mém. Serv. Géol. Maroc*, **56**, 1-108. Rabat.

DESTOMBES, J., HOLLARD, H. & WILLEFERT, S. 1985. Lower Palaeozoic rocks of Morocco. *In*: D.H. HOLLAND (*Ed.*), Lower Palaeozoic rocks of northwestern and west central Africa, 91-336. *John Wiley & Sons Ltd.*; Chichester.

DEYNOUX, M. 1985. Terrestrial or waterlain glacial diamictites? Three case studies from the Late Precambrian and Late Ordovician glacial drifts in West Africa. *Palaeogeogr., Palaeoclimat., Palaeoecol.*, **57**, 97-141. Amsterdam.

DICKSON, J.A.D. 1966. Carbonate identification and genesis as revealed by staining. *J. Sed. Petrol.*, **36**, 491-505. Tulsa.

DICKSON, J.A.D. & COLEMAN, M.L. 1980. Changes in carbon and oxygen isotope composition during limestone diagenesis. *Sedimentology*, **27**, 107-118. Oxford.

DREVER, J.I. 1982. The geochemistry of natural waters. 288 S., (Englewood Cliffs). New Jersey.

DROMGOOLE, E.L. & WALTER, L.M. 1990. Iron and

manganese incorporation into calcite: effects of growth kinetics, temperature, and solution chemistry. *Chem. Geol.*, **81**, 311-336. Amsterdam.

DUMESTRE, A. & ILLING, L.V. 1967. Middle Devonian reefs in Spanish Sahara. *In*: D.H. OSWALD (*Ed.*), International Symposium on the Devonian System, Calgary, vol. 2. *Alberta Soc. Petrol. Geol.*, 333-350. Calgary.

DUNNINGTON, H.V. 1967. Aspects of diagenesis and shape change in stylolitic limestone reservoirs. *Proc. 7th World Petroleum Congr. Mexico*, **2**, 339-352. Mexico.

DUPONT, E. 1881. Sur l'origine des calcaires Dévoniens en Belgique. *Bull. Acad. Roy. Sci. Belg.,* (3) **2**, 264-280. Brussels.

ELLOY, R. 1972. Réflexions sur quelques environments récifaux du Paléozoique. *Bull. Centr. Rech. Pau, Soc. Nat. Pétrol. Aquitaine*, **6**, 1-105. Pau.

EMERY, D. & DICKSON, J.A.D. 1989. A syndepositional meteoric phreatic lens in the Middle Jurassic Lincolnshire Limestone, England, U.K. *Sed. Geol.*, **65**, 273-284. Amsterdam.

FEARY, D.A. & JAMES, N.P. 1995. Cenozoic biogenic mounds and buried Miocene(?) barrier reef on a predominantly cool-water carbonate continental margin – Eucla Basin, western Great Australian Bight. *Geology*, **23**, 427-430. Boulder.

FLAJS, G. & HÜSSNER, H. 1993. A Microbial Model for the Lower Devonian Stromatactis Mud Mounds of the Montagne Noire (France). *Facies*, **29**, 179-194. Erlangen.

FOLK, R.L. 1965. Some aspects of recristallization in ancient limestones. *SEPM Spec. Publ.*, **13**, 14-48. Tulsa.

FRANK, J.R., CARPENTER, A.B. & OGLESBY, W. 1982. Cathodoluminescence and composition of calcite cement in the Taum Sauk Limestone (Upper Cambrian), southeast Missouri. *J. Sed. Petrol.*, **52**, 631-638. Tulsa.

FRIEDMAN, I. & O'NEIL, J.R. 1977. Compilation of stable isotope fractionation factors of geochemical interest. *U.S. Geol. Surv. Prof. Pap.*, **440-K**, 1-12. Washington.

GAO, G. 1993. The temperatures and oxygen isotope composition of early Devonian oceans. *Nature*, **361**, 712-714. London.

GIBSON, M.A., CLEMENT, C.R. & BROADHEAD, T.W. 1988. Bryozoan-dominated carbonate mudmounds in a cratonic setting from the basal Devonian of the southeastern United States. *In*: N.J. MCMILLIAN, A.F. EMBRY & D.J. GLASS (*Eds*), Devonian of the world, vol. II. *Can. Soc. Petrol. Geol.*, 541-552. Calgary.

GINSBURG, R.N. & LOWENSTAM, H.A. 1958. The influence of marine bottom communities on the depositional environment of sediments. *J. Geol.*, **66**, 310-318. Chicago.

GIVEN, R.K. & LOHMANN, K.C. 1985. Derivation of the original isotopic composition of Permian marine cements. *J. Sed. Petrol.*, **55**, 430-439. Tulsa.

GIVEN, R.K. & WILKINSON, B.H. 1985. Kinetic control of morphology, composition, and mineralogy of abiotic sedimentary carbonates. *J. Sed. Petrol.*, **55**, 109-119. Tulsa.

GNOLI, M., JAANUSSON, V., LEONE, F. & SERPAGLI, E. 1981. A Lower Devonian stromatactis-bearing carbonate mound from southern Sardinia. *N. Jb. Geol. Paläont. Mh.*, **1981**, 339-345. Stuttgart.

GODEFROID, F. & RACKI, G. 1990. Frasnian gypidulid brachiopods from the Holy Cross Mountains (Poland). Comparitive stratigraphic analysis with the Dinant Synclinorium (Belgium). *Bull. Inst. Roy. Sci. Natur. Belg., Sci. Terre*, **60**, 43-74. Brussels.

GROVER, G. & READ, J.F. 1983. Paleoaquifer and deep burial related cements defined by regional cathodoluminescence patterns, middle Ordovician carbonates, Virginia. *AAPG Bull.*, **67**, 1275-1303. Tulsa.

HECKEL, P.H. 1972. Possible inorganic origin for stromatactis in calcilutite mounds in the Tully limestone, Devonian of New York. *J. Sed. Petrol.*, **42**, 7-18. Tulsa.

— 1973. Nature, origin, and significance of the Tully Limestone. *Geol. Soc. Am. Spec. Pap.*, **138**, 1-244. Boulder.

— 1974. Carbonate buildups in the geologic record: a review. *In*: L.F. LAPORTE (*Ed.*), Reefs in Time and Space. *SEPM Spec. Publ.*, **18**, 90-154. Tulsa.

HENN, A.H. 1985. Biostratigraphie und Fazies des hohen Unter-Devons bis tiefen Ober-Devons der Provinz Palencia, Kantabrisches Gebirge, N. Spanien. *Gött. Arb. Geol. Paläont.*, **26**, 1-100. Göttingen.

HENRICH, R., FREIWALD, A., BETZLER, C., BADER, B., SCHÄFER, P., SAMTLEBEN, C., BRACHERT, T.C., WEHRMANN, A., ZANKL, H., KÜHLMANN, D.H.H. 1995. Controls on Modern Carbonate Sedimentation on Warm-temperate to Arctic Coasts, Shelves and Seamounts in the Northern Hemisphere: Implications for Fossil Counterparts. *Facies*, **32**, 71-108. Erlangen.

HOLLARD, H. 1967. Le Dévonien du Maroc et du Sahara nord-occidental. *In*: D.H. OSWALD (*Ed.*), International Symposium on the Devonian System, Calgary, vol. 1. *Alberta Soc. Petrol. Geol.*, 203-244. Calgary.

— 1970. Silurien-Dévonien-Carbonifère. *In*: G. CHOUBERT & A. FAURE-MURET (*Eds*), Coll. Int. Corr. Precambrien, Livret-Guide de l'Excursion Anti-Atlas Occidental et Central. *Notes Mém. Serv. Géol. Maroc*, **229**, 171-188. Rabat.

— 1974. Recherches sur la stratigraphie des formations du Dévonien moyen, de l'Emsien supérieur au Frasnien, dans le Sud du Tafilalt et dans le Ma'der (Anti-Atlas oriental). *Notes Mém. Serv. Géol. Maroc*, **264**, 7-68. Rabat.

— 1981. Tableaux de corrélations du Silurien et du Dévonien de l'Anti-Atlas. *Notes Mém. Serv. Géol. Maroc*, **308**, 23. Rabat.

HORBURY, A.D. & ADAMS, A.E. 1989. Meteoric-phreatic diagenesis in cyclic late Dinantian carbonates, northwest England. *Sed. Geol.*, **65**, 319-344. Amsterdam.

HOUSE, M.R. 1985. Correlation of mid-Palaeozoic ammonoid evolutionary events with global sedimentary perturbations. *Nature*, **313**, 17-22. London.

— 1995. Devonian precessional and other signatures for establishing a Givetian timescale. *Geol. Soc. London Spec. Publ.*, **85**, 37-49. London.

HOVLAND, M., CROKER, P.F. & MARTIN, M. 1994. Fault-associated seabed mounds (carbonate knolls?) off western Ireland and north-west Australia. *Mar. Petrol. Geol.*, **11**, 232-246. Oxford.

HURLEY, N.F. & LOHMANN, K.C. 1989. Diagenesis of Devonian reefal carbonates in the Oscar Range, Canning Basin, Western Australia. *J. Sed. Petrol.*, **59**, 127-146. Tulsa.

IRWIN, H., CURTIS, C. & COLEMAN, M. 1977. Isotopic evidence for source of diagenetic carbonates formed during burial of organic-rich sediments. *Nature*, **269**, 209-213. London.

JAEGER, H. & MASSA, D. 1965. Quelques données stratigraphiques sur le Silurien des confins algéro-marocains (Ben Zireg, Djebel Grouz et régions voisines). *Bull. Soc. Géol. France*, **7**, 426-436. Paris.

JAMES, N.P. 1984. Reefs. *In*: R.G. WALKER (*Ed.*), Facies Models. *Geosci. Can. Reprint Ser.*, **1**, 229-244. Toronto.

JAMES, N.P. & BOURQUE, P.-A. 1992. Reefs and mounds. *In*: R.G. WALKER & N.P. JAMES (*Eds*), Facies Models: Response to Sea Level Change. *Geol. Assoc. Can. Reprint Ser.*, 323-345. Toronto.

JEANNETTE, D. & TISSERANT, D. 1977. Les épisodes tectoniques et intrusifs du Précambrien supérieur de l'Anti-Atlas occidental. *Estudios geologicos*, **33**, 315-326. Madrid.

JOHNSON, J.G., KLAPPER, G. & SANDBERG, C.A. 1985. Devonian eustatic fluctuations in Euramerica. *Geol. Soc. Am. Bull.*, **96**, 567-587. Boulder.

JOHNSON, J.G., KLAPPER, G. & ELRICK, M. 1996. Devonian Transgressive-Regressive Cycles and Biostratigraphy, Northern Antelope Range, Nevada: Establishment of Reference Horizons for Global Cycles. *Palaios*, **11**, 3-14. Tulsa.

KAUFMAN, J., CANDER, H.S., DANIELS, L.D. & MEYERS, W.J. 1988. Calcite cement stratigraphy and cementation history of the Burlington-Keokuk Formation (Mississipian), Illinois and Missouri. *J. Sed. Petrol.*, **58**, 312-326. Tulsa.

KAUFMAN, J., HANSON, G.N. & MEYERS, W.J. 1991. Dolomitization of the Devonian Swan Hills Formation, Rosevear Field, Alberta, Canada. *Sedimentology*, **38**, 41-66. Oxford.

KAUFMANN, B. 1995. Middle Devonian mud mounds of the Ma'der Basin in the eastern Anti-Atlas, Morocco. *In*: G. FLAJS, M. VIGENER, H. KEUPP, D. MEISCHNER, F. NEUWEILER, J. PAUL, J. REITNER, K. WARNKE, H. WELLER, P. DINGLE, C. HENSEN, P. SCHÄFER, P. GAUTRET, R.R. LEINFELDER, H. HÜSSNER & B. KAUFMANN: Mud Mounds: A Polygenetic Spectrum of Fine-grained Carbonate Buildups. *Facies*, **32**, 49-57. Erlangen.

KENDALL, A.C. 1985. Radiaxial fibrous calcite: a Reappraisal. *In*: N. SCHNEIDERMANN & P.M. HARRIS (*Eds*), Carbonate Cements. *SEPM Spec. Publ.*, **36**, 59-77. Tulsa.

KENDALL, A.C. & TUCKER, M.E. 1973. Radiaxial-fibrous calcite: a replacement after acicular carbonate. *Sedimentology*, **20**, 365-389. Oxford.

KERANS, C., HURLEY, N.F. & PLAYFORD, P.E. 1986. Marine diagenesis in Devonian reef complexes of the Canning Basin, Western Australia. *In*: J.H. SCHROEDER & B.H. PURSER (*Eds*), Reef Diagenesis, 357-380. *Springer*; Berlin.

KREBS, W. 1974. Devonian carbonate complexes of central Europe. *In*: L.F. LAPORTE (*Ed.*), Reefs in time and space. *SEPM Spec. Publ.*, **18**, 155-208. Tulsa.

LAND, L.S. 1967. Diagenesis of skeletal carbonates. *J. Sed. Petrol.*, **37**, 914-930. Tulsa.

LAND, L.S. & MOORE, C.H. 1980. Lithification, micritization and syndepositional diagenesis of biolithites on the Jamaican island slope. *J. Sed. Petrol.*, **50**, 357-370. Tulsa.

LASEMI, Z. & SANDBERG, P.A. 1984. Transformation of aragonite-dominated lime muds to microcrystalline limestones. *Geology*, **12**, 420-423. Boulder.

LAVOIE, D. 1993. Early Devonian marine isotopic signatures: brachiopods from the upper Gaspé limestones, Gaspé Peninsula, Québec, Canada. *J. Sed. Petrol.*, **63**, 620-627. Tulsa.

— 1994. Early Devonian marine isotopic signatures: brachiopods from the upper Gaspé limestones, Gaspé Peninsula, Québec, Canada – Reply. *J. Sed. Research*, **A64**, 408-411. Tulsa.

LAVOIE, D. & BOURQUE, P.-A. 1993. Marine, meteoric and burial diagenesis of an Early Silurian carbonate platform, Québec Appalachians, Canada. *J. Sed. Petrol.*, **63**, 233-247. Tulsa.

LECOMPTE, M. 1937. Contribution à la connaissance des récifs dévoniens de L'Ardenne. Sur la présence de structures conservées dans des efflorescences cristallines du type stromatactis. *Bull. Musée r. Hist. Natur. Belg.*, **13/15**, 1-14. Brussels.

LEES, A. 1964. The structure and origin of the Waulsortian reefs of west-central Eire. *Phil. Trans. Roy. Soc. London, Series B*, **247**, 483-531. London.

LEES, A. & MILLER, J. 1985. Facies variation in Waulsortian buildups, Part 2; Mid-Dinantian buildups from Europe and North America. *Geol. J.*, **20**, 159-180. Chichester.

LE MAÎTRE, D. 1944. Contribution à l'étude du Dévonien du Tafilalt: 1: La faune coblencienne de Haci-Remlia (SW de Taouz). *Notes Mém. Serv. Géol. Maroc*, **61**, 1-94. Rabat.

— 1947. Le récif coralligène de Ouihalane. *Notes Mém. Serv. Géol. Maroc*, **67**, 1-113. Rabat.

LINDBERG, R.D. & RUNNELS, D.D. 1984. Ground water redox reactions: an analysis of equilibrium state applied to Eh measurements and geochemical modeling. *Science*, **225**, 925-927. Washington.

LOHMANN, K.C 1988. Geochemical patterns of meteoric diagenetic systems and their application to study of paleokarst. *In*: N.P. JAMES & P.W. CHOQUETTE (*Eds*), Paleokarst, 58-80. *Springer*; New York.

LOHMANN, K.C & MEYERS, W.J. 1977. Microdolomite inclusions in cloudy prismatic calcites: A proposed criterion for former high-magnesium calcites. *J. Sed. Petrol.*, **47**, 1078-1088. Tulsa.

LONGMAN, M.W. 1981. A process approach to recognizing facies of reef complexes. *In*: D.F. TOOMEY (*Ed.*), European Fossil Reef Models. *SEPM Spec. Publ.*, **30**, 9-40. Tulsa.

LOTTMANN, J. 1990. Die *pumilio*-Events (Mittel-Devon). *Gött. Arb. Geol. Paläont.*, **44**, 1-98. Göttingen.

MACHEL, H.G. 1990a. Faziesinterpretation des Briloner Riffs mit Hilfe eines Faziesmodells für devonische Riffkarbonate. *Geol. Jb. Reihe D*, **95**, 43-83. Hannover.

— 1990b. Submarine Frühdiagenese, Spaltenbildungen und prätektonische Spätdiagenese des Briloner Riffs. *Geol. Jb. Reihe D*, **95**, 85-137. Hannover.

MACHEL, H.G. & ANDERSON, J.H. 1989. Pervasive subsurface dolomitization of the Nisku Formation in central Alberta. *J. Sed. Petrol.*, **59**, 891-911. Tulsa.

MACHEL, H.G. & BURTON, E.A. 1991. Factors governing cathodoluminescence in calcite and dolomite, and their implications for studies of carbonate diagenesis. *In*: C.E. BARKER & O.C. KOPP (*Eds*), Luminescence Microscopy and Spectroscopy: Qualitative and Quantitative Applications. *SEPM Short Course*, **25**, 37-57. Tulsa.

MASSA, D. (avec la collaboration de A. COMBAZ & G. MANDERSCHEID) 1965. Observations sur les séries Siluro-Dévoniennes des confins Algéro-Marocains du Sud. *Notes Mém. Comp. Franc. Pétrol.*, **8**, 1-187. Paris.

MATTES, D.H. & MOUNTJOY, E.W. 1980. Burial dolomitization of the Upper Devonian Miette buildup, Jasper National Park, Alberta. *In*: D.H. ZENGER, J.B. DUNHAM & R.L. ETHINGTON (*Eds*), Concepts and Models of Dolomitization. *SEPM Spec. Publ.*, **28**, 259-297. Tulsa.

MATYSZKIEWICZ, J. 1993. Genesis of Stromatactis in an Upper Jurassic carbonate buildup (Mlynka, Cracow region, Southern Poland): internal reworking and erosion of organic growth cavities. *Facies*, **28**, 87-96. Erlangen.

MAURIN, A.V. & NOŤL , D. 1977. A Possible Bacterial Origin for Famennian Micrites. *In*: E. FLÜGEL (*Ed.*), Fossil Algae, 136-142. *Springer*; Berlin.

MAURIN, A.F., PHILIP, J. & BRUNEL, P. 1981. Possible microbial accretions in Cenomanian mounds, SE France. *In*: C. MONTY (*Ed.*), Phanerozoic Stromatolites, Case Histories, 121-133. *Springer*; Berlin.

MCHARQUE, T.R. & PRICE, R.C. 1982. Dolomite from clay in argillaceous or shale associated marine carbonates. *J. Sed. Petrol.*, **52**, 873-886. Tulsa.

MEYERS, W.J. 1978. Carbonate cements: their regional distribution and interpretation in Mississippian limestones of south western New Mexico. *Sedimentology*, **25**, 371-400. Oxford.

— 1991. Calcite cement stratigraphy: An overview. *In*: C.E. BARKER & O.C. KOPP (*Eds*), Luminescence microscopy and spectroscopy: Qualitative and Quantitative Applications. *SEPM Short Course*, **25**, 133-147. Tulsa.

MEYERS, W.J. & HILL, B.E. 1983. Quantitative studies of compaction in Mississippian skeletal limestones, New Mexico. *J. Sed. Petrol.*, **53**, 231-242. Tulsa.

MICHARD, A. 1976. Elements de Geologie Marocaine. *Notes Mém. Serv. Géol. Maroc*, **252**, 1-408. Rabat.

MONTY, C.L.V. 1982. Cavity or fissure dwelling stromatolites (endostromatolites) from Belgian Devonian mud mounds. *Ann. Soc. Géol. Belg.*, **105**, 343-344. Liège.

— 1995. The rise and nature of carbonate mud--mounds: an introductory actualistic approach. *In*: C.L.V. MONTY, D.W.J. BOSENCE, P.H. BRIDGES & B.R. PRATT (*Eds*), Carbonate Mud-Mounds: Their Origin and Evolution. *Spec. Publs. Int. Assoc. Sediment.*, **23**, 11-48. Oxford.

MONTY, C.L.V., BERNET-ROLLANDE, M.C. & MAURIN, A.F. 1982. Re-interpretation of the Frasnian classical 'reefs' of the southern Ardennes, Belgium. *Ann. Soc. Géol. Belg.*, **105**, 339-341. Liège.

MONTY, C.L.V., BOSENCE, D.W.J., BRIDGES, P.H. & PRATT, B.R. (*Eds*) 1995. Carbonate Mud Mounds – Their Origin and Evolution. *Spec. Publs. Int. Assoc. Sediment.*, **23**, 1-537. *Blackwell Science*; Oxford.

MOORE, P.F. 1988. Devonian reefs in Canada and some adjacent areas. *In*: H.H. GELDSETZER, N.P. JAMES & G.E. TEBBUTT (*Eds*), Reefs. Canada and adjacent areas. *Can. Soc. Petrol. Geol. Mem.*, **13**, 367-390. Calgary.

MOUNTJOY, E.W. & HALIM-DIHARDJA, M.K. 1991. Multiple phase fracture and fault-controlled burial dolomitization, Upper Devonian Wabamun Group, Alberta. *J. Sed. Petrol.*, **61**, 590-612. Tulsa.

MOUSSINE-POUCHKINE, A. 1971. Les constructions récifales du Dévonien moyen du Pays Bas de l'Ahnet (Sahara Central, Algérie). *Bull. Soc. Hist. Natur. Afrique du Nord*, **62**, 79-88. Algiers.

MULLINS, H.T., NEWTON, C.R., HEATH, K. & VANBUREN, H.M. 1981. Modern deep-water coral mounds north of Little Bahama Bank: criteria for recognition of deep-water coral bioherms in the rock record. *J. Sed. Petrol.*, **51**, 999-1013. Tulsa.

NEUMANN, A.C., KOFOED, J.W. & KELLER, G.H. 1977. Lithoherms in the Straits of Florida. *Geology*, **5**, 4-10. Boulder.

PAREYN, C. 1961. Les massifs Carbonifères du Sahara sud-oranais. *Publ. Centr. Rech. Saharienne, Sér. Géol.*, 2 vols., 1-325 and 1-244. Paris.

PINGITORE, N.E. 1978. The behaviour of Zn^{2+} and Mn^{2+} during carbonate diagenesis: theory and applications. *J. Sed. Petrol.*, **48**, 799-814. Tulsa.

PIQUE, A. & MICHARD, A. 1989. Moroccan Hercynides: a synopsis. The Paleozoic sedimentary and tectonic evolution at the northern margin of West Africa. *Am. J. Sci.*, **289**, 286-330. New Haven.

PLAYFORD, P.E. 1980. Devonian 'Great Barrier Reef' of Canning Basin, western Australia. *AAPG Bull.*, **64**, 814-840. Tulsa.

POPP, B.N., ANDERSON, T.F. & SANDBERG, P.A. 1986. Textural, elemental, and isotopic variations among constituents in Middle Devonian limestones, North America. *J. Sed. Petrol.*, **56**, 715-727. Tulsa.

PRATT, B.R. 1982. Stromatolitic framework of carbonate mudmounds. *J. Sed. Petrol.*, **52**, 1203-1227. Tulsa.

— 1995. The origin, biota and evolution of deep-water mud-mounds. *In*: C.L.V. MONTY, D.W.J. BOSENCE, P.H. BRIDGES & B.R. PRATT (*Eds*), Carbonate Mud-Mounds: Their Origin and Evolution. *Spec. Publs. Int. Assoc. Sediment.*, **23**, 49-123. Oxford.

PRAY, L.C. 1958. Fenestrate bryozoan core facies, Mississippian bioherms, southwestern United States. *J. Sed. Petrol.*, **28**, 261-273. Tulsa.

REEDER, R.J., FAGIOLI, R.O. & MEYERS, W.J. 1990. Oscillatory zoning of Mn in solution-grown calcite crystals. *Earth Sci. Rev.*, **29**, 39-46. Amsterdam.

REITNER, J. 1993. Modern Cryptic Microbialite/Metazoan Facies from Lizard Island (Great Barrier Reef, Australia) – Formation and Concepts. *Facies*, **29**, 3-40. Erlangen.

REQUADT, H. & WEDDIGE, K. 1978. Lithostratigraphie und Conodontenfaunen der Wissenbacher Fazies und ihrer Äquivalente in der südwestlichen Lahnmulde (Rheinisches Schiefergebirge). *Mainzer Geowiss. Mitt.*, **7**, 183-237. Mainz.

RICKEN, W. 1991. Variation of Sedimentation Rates in Rhythmically Bedded Sediments. Distinction Between Depositional Types. *In*: G. EINSELE, W. RICKEN & A. SEILACHER (*Eds*), Cycles and Events in Stratigraphy, 167-187. *Springer*; Berlin.

RIDING, R. 1991. Calcified Cyanobacteria. *In*: R. RIDING (*Ed.*), Calcareous algae and stromatolites, 55-87. *Springer*; Berlin.

ROBBINS, L.L. & BLACKWELDER, P.L. 1992. Biochemical and ultrastructural evidence for the origin of whitings: A biologically induced calcium carbonate precipitation mechanism. *Geology*, **20**, 464-468. Boulder.

SALLER, A.H. 1986. Radiaxial calcite in Lower Miocene strata subsurface Enewetak Atoll. *J. Sed. Petrol.*, **56**, 743-762. Tulsa.

SANDBERG, P.A. 1985. Aragonite cements and their occurrence in ancient limestones. *In*: N. SCHNEIDERMANN & P.M. HARRIS (*Eds*), Carbonate Cements. *SEPM Spec. Publ.*, **36**, 33-57. Tulsa.

SCHWARZACHER, W. 1961. Petrology and structure of some Lower Carboniferous reefs in northwestern Ireland. *AAPG Bull.*, **45**, 1481-1503. Tulsa.

SCOTESE, C.R. & MCKERROW, W.S. 1990. Revised World maps and introduction. *In*: W.S. MCKERROW & C.R. SCOTESE (*Eds*), Palaeozoic

Palaeogeography and Biogeography. *Geol. Soc. London Mem.*, **12**, 1-21. London.

SCHNEIDER, W. 1977. Diagenese devonischer Karbonatkomplexe Mitteleuropas. *Geol. Jb. Reihe D*, **21**, 1-107. Hannover.

STEINEN, R.P. 1982. SEM observations on the replacement of Bahamian aragonitic mud by calcite. *Geology*, **10**, 471-475. Boulder.

STERNBACH, C.A. & FRIEDMAN, G.M. 1986. Dolomites formed under conditions of deep burial: Hunton Group carbonate rocks (Upper Ordovician to Lower Devonian) in the deep Anadarko Basin of Oklahoma and Texas. *Carbonates and Evaporites*, **1**, 69-73. Troy.

STOCKMAN, K.W., GINSBURG, R.N. & SHINN, E.A. 1967. The production of lime mud by algae in South Florida. *J. Sed. Petrol.*, **37**, 633-648. Tulsa.

STOW, D.A.V. & MILLER, J. 1984. Mineralogy, petrology and diagenesis of sediments at Site 530, southeast Angola Basin. *Initial Reports Deep Sea Drilling Project*, **75**, 857-873. Washington.

TALENT, J.A. & YOLKIN, E.A. 1987. Transgression-regression patterns for the Devonian of Australia and southern West Siberia. *Cour. Forsch.-Inst. Senckenberg*, **92**, 235-249. Frankfurt/Main.

TALENT, J.A., MAWSON, R., ANDREW, A.S., HAMILTON, P.J. & WHITFORD, D.J. 1993. Middle Palaeozoic extinction events: faunal and isotope data. *Palaeogeogr., Palaeoclimat., Palaeoecol.*, **104**, 139-152. Amsterdam.

THOMPSON, J.B. & FERRIS, F.G. 1990. Cyanobacterial precipitation of gypsum, calcite, and magnesite from natural alkaline lake water. *Geology*, **18**, 995-998. Boulder.

TOWE, K.M. & HEMLEBEN, K.M. 1976. Diagenesis of magnesian calcite: evidence from miliolacean foraminifera. *Geology*, **4**, 337-339. Boulder.

TRUYOLS-MASSONI, M., MONTESINOS, J.R., GARCIA-ALCALDE, J.L. & LEYVA, F. 1990. The Kacak-Otomari Event and its characterization in the Palentine Domain (Cantabrian One, NW Spain). *In*: KAUFFMAN & O.H. WALLISER (*Eds*), Extinction Events in Earth History. *Lect. Notes Earth Sci.*, **30**, 133-143. Berlin.

TSIEN, H.H. 1977. Morphology and development of Devonian reefs and reef complexes in Belgium. *Proc. Int. Coral Reef Symp. Miami*, **2**, 191-200. Miami.

— 1985a. Algal-Bacterial Origin of Micrites in Mud Mounds. *In*: D.F. TOOMEY & M.H. NITECKI (*Eds*), Paleoalgology, 290-296. *Springer*; Berlin.

— 1985b. Origin of stromatactis – a replacement of colonial microbial accretion. *In*: D.F. TOOMEY & M.H. NITECKI (*Eds*), Paleoalgology, 274-289. *Springer*; Berlin.

— 1988. Devonian paleogeography and reef development of Northwestern and Central Europe. *In*: N.J. MCMILLIAN, A.F. EMBRY & D.J. GLASS (*Eds*), Devonian of the World, vol. II. *Can. Soc. Petrol. Geol.*, 341-358. Calgary.

VEIZER, J., FRITZ, P. & JONES, B. 1986. Geochemistry of brachiopods: oxygen and carbon isotopic records of paleozoic oceans. *Geochim. Cosmochim. Acta*, **50**, 1679-1696. London.

VON BITTER, P., SCOTT, S.D. & SCHENK, P.E. 1992. Chemosynthesis: An alternate hypothesis for Carboniferous biotas in bryozoan/microbial mounds, Newfoundland, Canada. *Palaios*, **7**, 466-484. Tulsa.

WADLEIGH, M.A. & VEIZER, J. 1992. $^{18}O/^{16}O$ and $^{13}C/^{12}C$ in lower Paleozoic articulate brachiopods: implications for the isotopic composition of seawater. *Geochim. Cosmochim. Acta*, **56**, 431-443. London.

WALKER, K.R. & ALBERSTADT, L.P. 1975. Ecological succession as an aspect of structure in fossil communities. *Paleobiology*, **1**, 238-257. Washington.

WALLACE, M.W. 1987. The role of internal erosion and sedimentation in the formation of stromatactis mudstones associated lithologies. *J. Sed. Petrol.*, **57**, 695-700. Tulsa.

WALLISER, O.H. 1985. Natural boundaries and Commission boundaries in the Devonian. *Cour. Forsch.-Inst. Senckenberg*, **75**, 401-408. Frankfurt/Main.

WALLISER, O.H. (*Ed.*) 1991. Morocco Field Meeting of the Subcommision on Devonian Stratigraphy, International Union of Geological Sciences, Guide Book, 1-79.

WALLISER, O.H., BULTYNCK, P., WEDDIGE, K., BECKER, R.T. & HOUSE, M.R. 1995. Definition of the Eifelian-Givetian Stage boundary. *Episodes*, **18**, 107-115. Nottingham.

WALLS, R.A., MOUNTJOY, E.W. & FRITZ, P. 1979. Isotopic composition and diagenetic history of carbonate cements in Devonian Golden Spike reef, Alberta, Canada. *Geol. Soc. Am. Bull.*, **90**, 963-982. Boulder.

WANLESS, H.R. 1979. Limestone response to stress – pressure solution and dolomitization. *J. Sed. Petrol.*, **49**, 437-462. Tulsa.

WANLESS, H.R. & TAGETT, M.G. 1989. Origin, growth and evolution of carbonate mudbanks in Florida Bay. *Bull. Mar. Sci.*, **44**, 454-488. Tulsa.

WARNKE, K. & MEISCHNER, D. 1995. Origin and depositional environment of Lower Carboniferous mud

mounds of Northwestern Ireland. *In*: G. FLAJS, M. VIGENER, H. KEUPP, D. MEISCHNER, F. NEUWEILER, J. PAUL, J. REITNER, K. WARNKE, H. WELLER, P. DINGLE, C. HENSEN, P. SCHÄFER, P. GAUTRET, R.R. LEINFELDER, H. HÜSSNER & B. KAUFMANN: Mud Mounds: A Polygenetic Spectrum of Fine-grained Carbonate Buildups. *Facies*, **32**, 36-42. Erlangen.

WELLER, H. 1989. Der Rübeländer Mud Mound im Riffkomplex von Elbingerode (Harz) und seine sedimentologischen Eigenschaften. *Hercynia*, **26**, 321-337. Halle.

WENDT, J. 1985. Disintegration of the continental margin of northwestern Gondwana, Late Devonian of the eastern Anti-Atlas (Morocco). *Geology*, **13**, 815-818. Boulder.

— 1988. Facies pattern and palaeogeography of the Middle and Late Devonian in the eastern Anti-Atlas (Morocco). *In*: N.J. MCMILLIAN, A.F. EMBRY & D.J. GLASS (*Eds*), Devonian of the World, vol. I. *Can. Soc. Petrol. Geol.*, 467-480. Calgary.

— 1991. Depositional and Structural Evolution of the Middle and Late Devonian on the Northwestern Margin of the Sahara Craton (Morocco, Algeria, Libya). *In*: M.J. SALEM, A.M. SBETA & M.R. BAKBAK (*Eds*), The Geology of Libya, vol. 6, 2195-2210. *Elsevier*; Amsterdam.

— 1993. Steep-sided carbonate mud mounds in the Middle Devonian of the eastern Anti-Atlas, Morocco. *Geol. Mag.*, **130**, 69-83. Cambridge.

— 1995. Shell directions as a tool in palaeocurrent analysis. *Sed. Geol.*, **95**, 161-186. Amsterdam.

WENDT, J. & BELKA, Z. 1991. Age and depositional environment of Upper Devonian (early Frasnian to early Famennian) black shales and limestones (Kellwasser facies) in the eastern Anti-Atlas, Morocco. *Facies*, **25**, 51-90. Erlangen.

WENDT, J., BELKA, Z. & MOUSSINE-POUCHKINE, A. 1993. New architectures of deep-water carbonate buildups: Evolution of mud mounds into mud ridges (Middle Devonian, Algerian Sahara). *Geology*, **21**, 723-726. Boulder.

WILSON, J.L. 1975. Carbonate Facies in Geologic History, 1-471. *Springer*; Berlin.

ZANKL, H. 1969. Structural and textural evidence of early lithification in limestones. *Sedimentology*, **12**, 241-256. Oxford.

ZEEH, S., BECHSTÄDT, T., MCKENZIE, J. & RICHTER, D.K. 1995. Diagenetic evolution of the Carnian Wetterstein platforms of the Eastern Alps. *Sedimentology*, **42**, 199-222. Oxford.

PLATE 1

Aferdou el Mrakib reef-mound

1 – Reef-mound, seen from W; height above underlying strata is 100-130 m; underlying upper Eifelian limestones (*arrowed*) are preserved only at the base of the mound, where the resistant mound structure has protected them from erosion

2 a-2b – Close-up view of the left third of Fig. 1, seen from SW; interfingering of massive reef-mound facies with bedded mound debris facies (indicated by thick line)

1

2a

2b

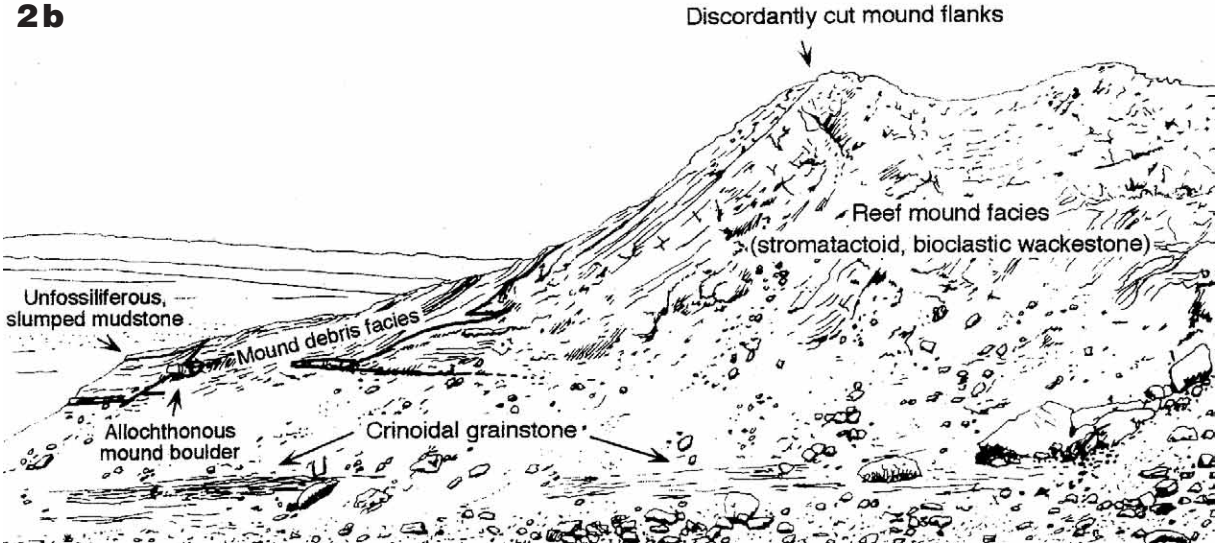
Discordantly cut mound flanks
Reef mound facies
(stromatactoid, bioclastic wackestone)
Unfossiliferous,
slumped mudstone
Mound debris facies
Allochthonous
mound boulder
Crinoidal grainstone

PLATE 2

Aferdou el Mrakib reef-mound

1 – Reef-mound, seen from ENE; width of the buildup is 900 m; the underlying upper Eifelian limestones (*arrowed*) are preserved only in the immediate surrounding of the mound, where the resistant mound structure has protected them from erosion

2 – Huge, mound-derived boulder in mound debris facies; author (1.85 m) for scale

3 – Stromatactis in reef-mound facies, aligned parallel to the accretionary surface of the mound; coin diameter is 24 mm

4 – Overturned "*Phillipsastrea*" in mound debris facies

5 – Domical stromatoporoid in reef-mound facies; thick-shelled pentamerids (*Devonogypa* sp., arrowed); coin diameter is 24 mm

6 – Solitary, rugose corals (mainly *Cystiphylloides* sp.) in reef-mound facies; coin diameter is 24 mm

7 – Reef-mound facies with phaceloid rugose corals, belonging to the bizarre group of *Fletcheria* MILNE-EDWARDS & HAIME; coin diameter is 24 mm

8 – Pervasively dolomitized reef-mound facies with mouldic porosity; coin diameter is 24 mm

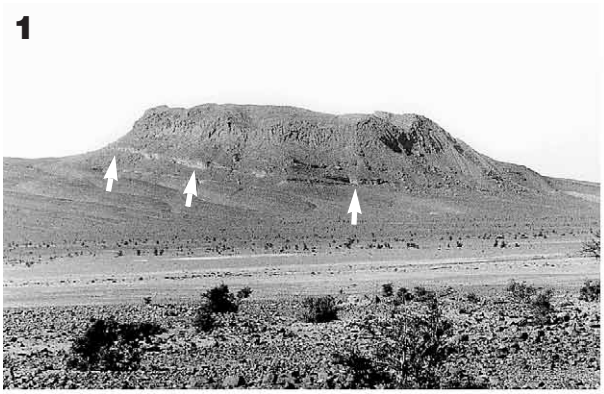
1

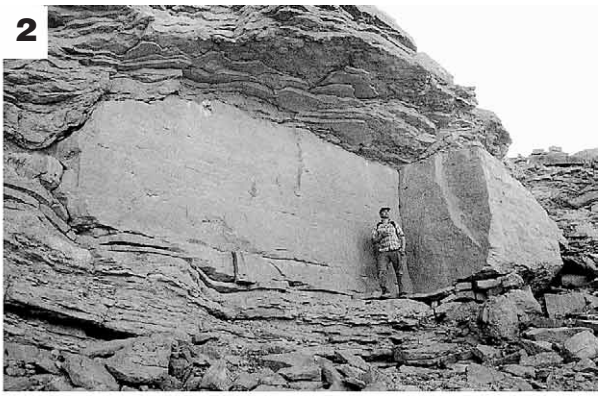
2

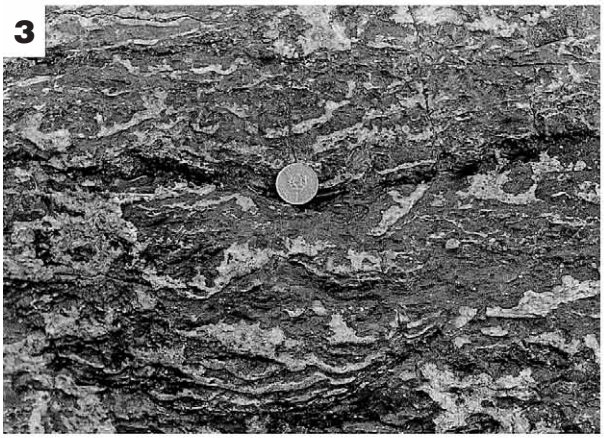
3

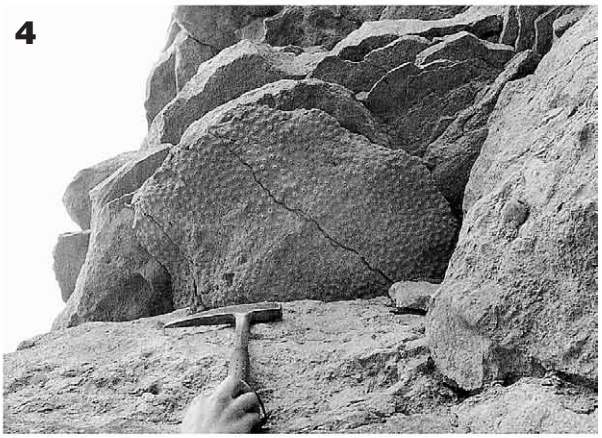
4

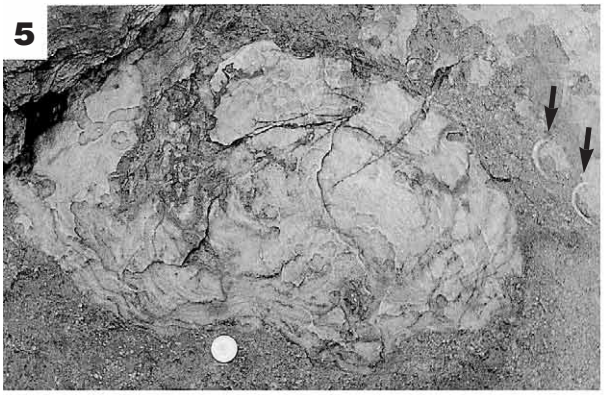
5


6

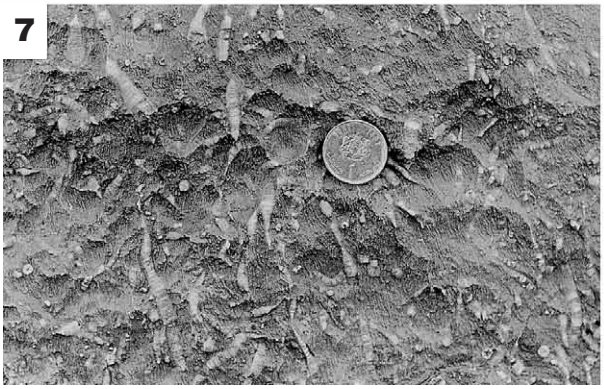
7


8

PLATE 3

Aferdou el Mrakib reef-mound, microfacies

1 – Reef-mound facies (stromatactoid boundstone) with irregular open-space structures; cloudy, radiaxial calcite cement forms 1 mm-thick, isopachous layers on the cavity walls; platy tabulate coral (alveolitid) on cavity roof (a), solitary, rugose corals (b: disphyllid or acantophyllid, c: *Macgea minima* BRICE, 1979) and stylolite (d); sample P 150

2 – Reef-mound facies with stromatactis, filled with radiaxial calcite cement, and aligned parallel to the accretionary surface of the mound; sample M 106

3 – Reef-mound facies (bioclastic boundstone); abundant alveolitids [a: *Platyaxum* (*Platyaxum*) *escharoides* (STEININGER, 1849]; sample M 33

4 – Coral-stromatoporoid boundstone, underlying Aferdou el Mrakib reef-mound; solitary, rugose corals (a: *Cystiphylloides* sp.), tabulate corals [b: *Thamnopora nicholsoni* (FRECH, 1885), c: alveolitids (*Alveolites tenuissimus* LECOMPTE, 1933]; sample M 30

5 – Spar-filled, stromatactoid open-space structures in reef-mound facies, aligned parallel to the accretionary surface of the mound; trilobite carapace (a) on cavity roof and thin, dark crusts (*arrowed*) surrounding cavities, probably of cyanobacterial origin (R. RIDING, *pers. comm.*); sample P 153

6 – Reef-mound facies (stromatactoid boundstone); brachiopod (left) and stromatactis (right) with infillings. Thin section P 150

7 – Tabulate coral (cf. *Pachystriatopora*) in reef-mound facies; thin section P 151

8 – Microproblematicum [*Rothpletzella devonica* (MASLOV, 1956), probably a cyanobacterium] in the immediate neighbourhood of a stromatactis cavity; thin section P 150

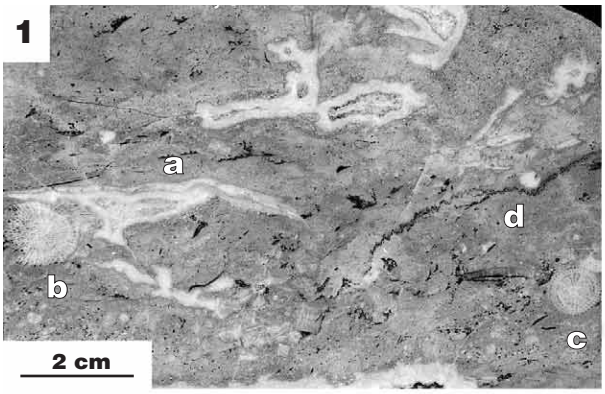
1
a
b
c
d
2 cm

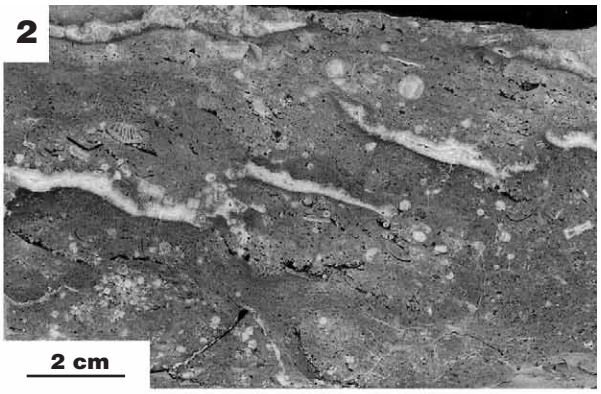
2
2 cm

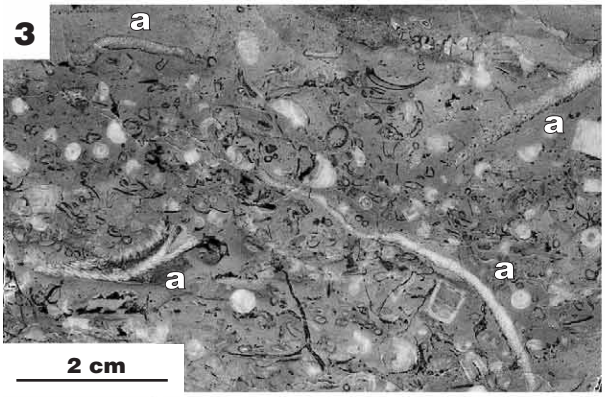
3
a
a
a
a
2 cm

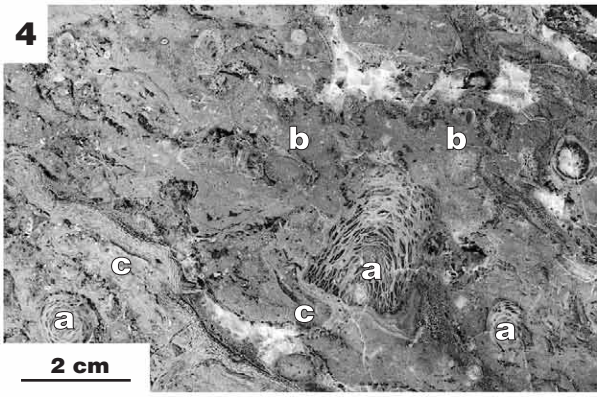
4
b
b
c
a
c
a
a
2 cm

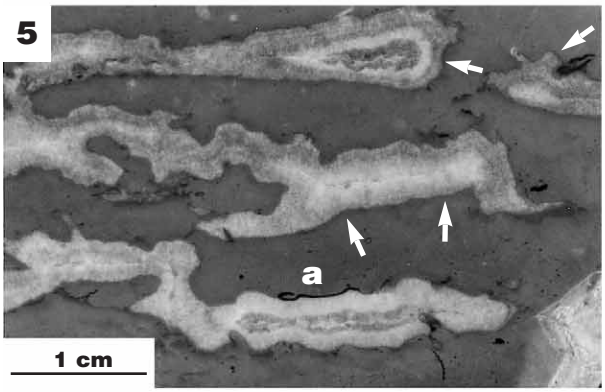
5
a
1 cm

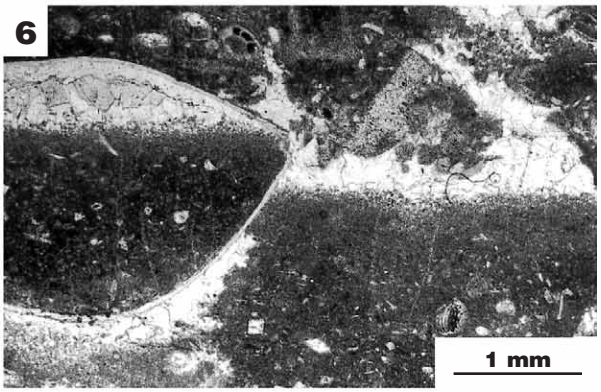
6
1 mm

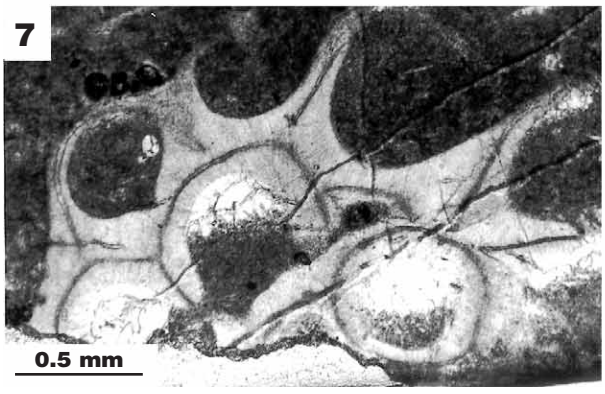
7
0.5 mm

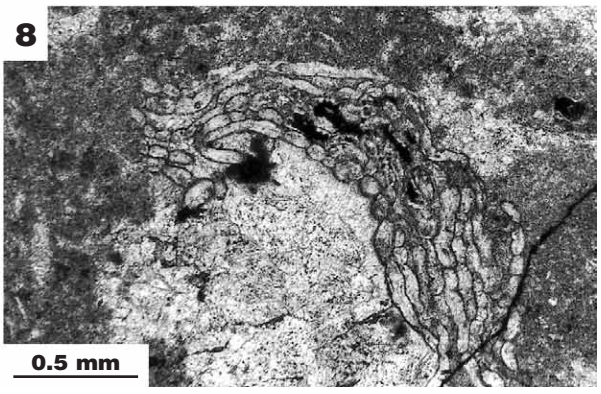
8
0.5 mm

PLATE 4

Guelb el Maharch mud-mound

1 – Mud-mound, seen from SSW; weight of the mound is about 45 m; the base is covered by Quaternary deposits; a – neptunian dyke (arrow a) cuts the mound vertically; infilling of dyke is shown on Pl. 5, Fig. 2; person (arrow b) for scale

2 – Neptunian dyke in mud-mound facies; dyke is filled by dark mound sediments; coin diameter is 24 mm

3 – Irregular cavity in mud-mound facies; cavity is filled with dolomitized internal sediment (*see* also Pl. 16, Fig. 4); isopachous calcite cement layer (arrowed), lining the cavity wall; coin diameter is 24 mm

1

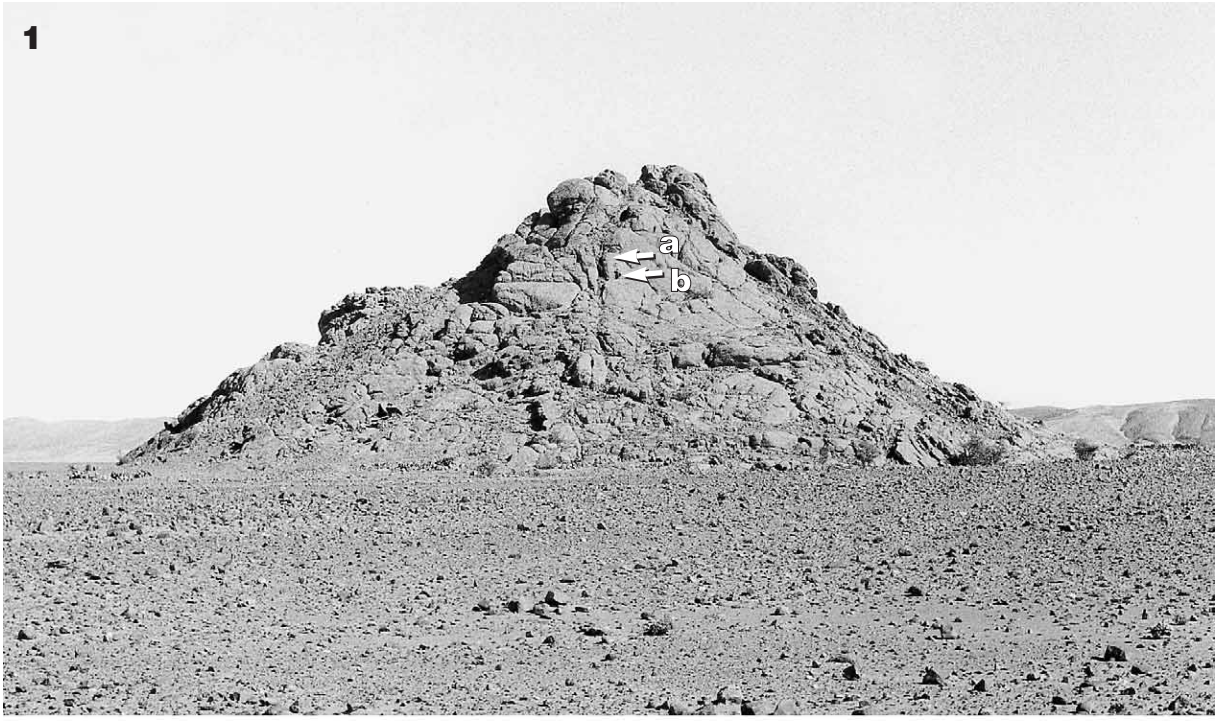

2

3

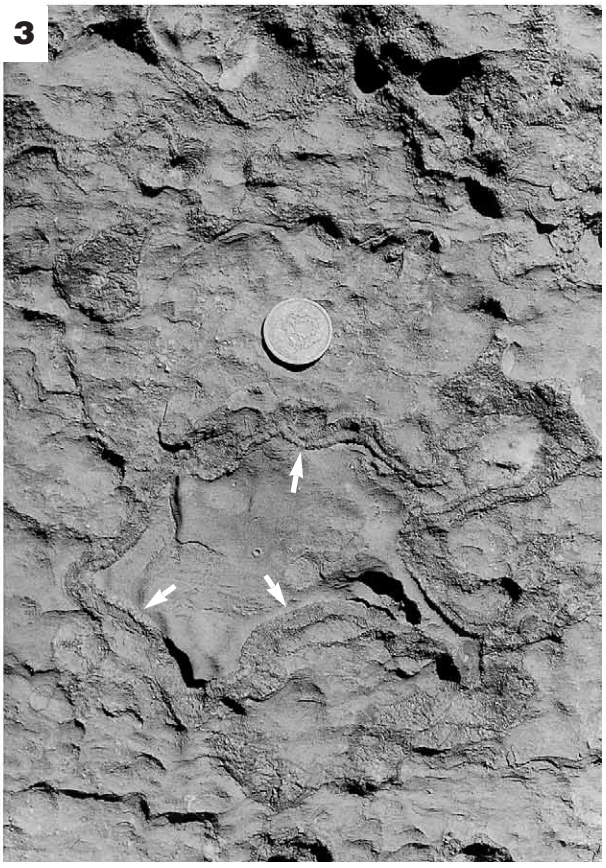

PLATE 5

Guelb el Maharch mud-mound, microfacies

1 – Irregular cavity in mud-mound facies; cavity wall is lined with cloudy, layered, isopachous, fibrous calcite cement; dark, laminated internal sediment; sample M 96

2 – Infilling of neptunian dyke (*see* Pl. 4, Fig. 1), consisting of dark crinoidal-brachiopod rudstone; sample M 98

3 – Mud-mound facies (stromatactoid boundstone) with spar-filled, irregular open-space structures; stromatactis (a) and abundant auloporids (mainly *Bainbridgia* sp.) and internal sediments (*arrowed*); infilling of cavity in the lower right is dolomitized, but nevertheless preserves ghost-lamination; sample P 156

4 – Mud-mound facies (stromatactoid boundstone) with spar-filled, irregular open-space structures; layered, fibrous calcite cements (a) line the cavity walls; central infillings (b) are dolomitized internal sediments (*see* also Pl. 16, Fig. 4); sample M 99

5 – Rugose coral (cf. *Fletcheria*) in mud-mound facies; thin section P 156

6 – Fenestrate bryozoans (cut by calcite-filled joint) in mud-mound facies; thin section P 160

7 – Tabulate coral (cf. *Crenulipora*) in mud-mound facies; thin section P 163

8 – Tabulate corals (*Bainbridgia* sp.) in mud-mound facies; thin section P 161


1
2 cm

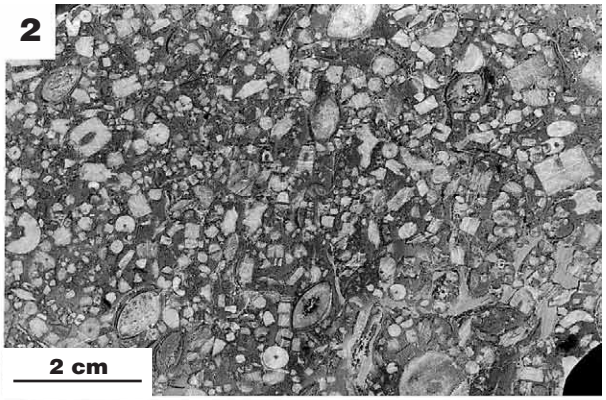
2
2 cm

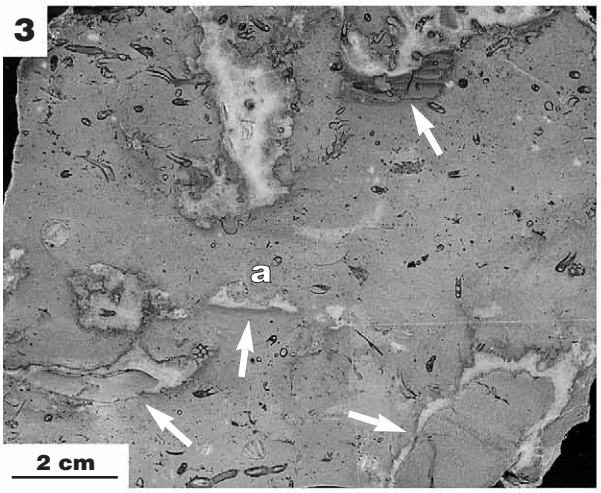
3
a
2 cm

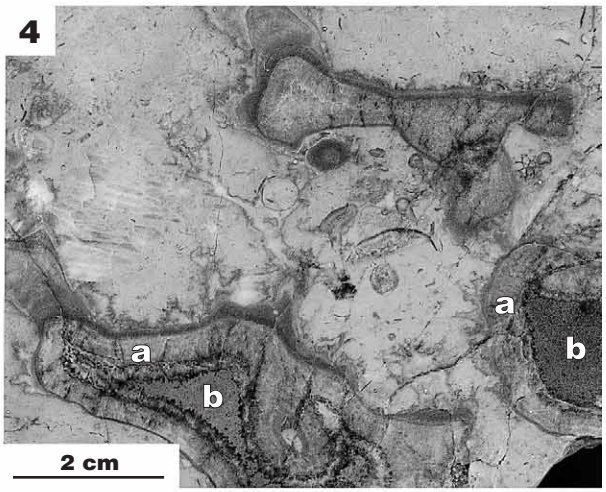
4
a
b
a
b
2 cm

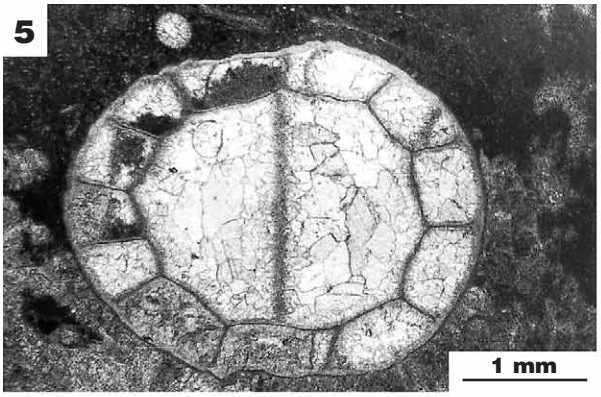
5
1 mm

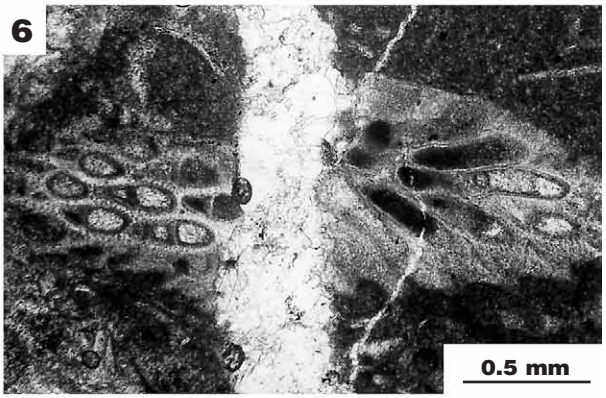
6
0.5 mm

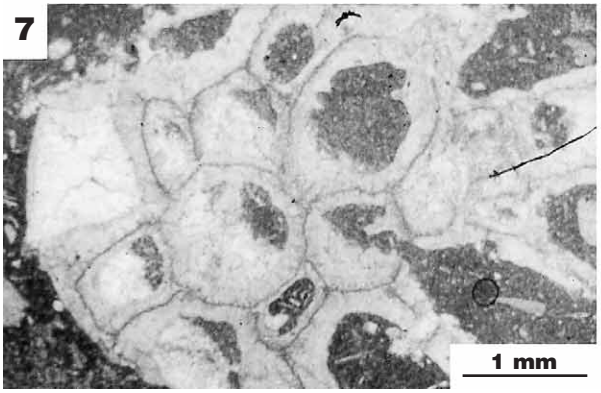
7
1 mm

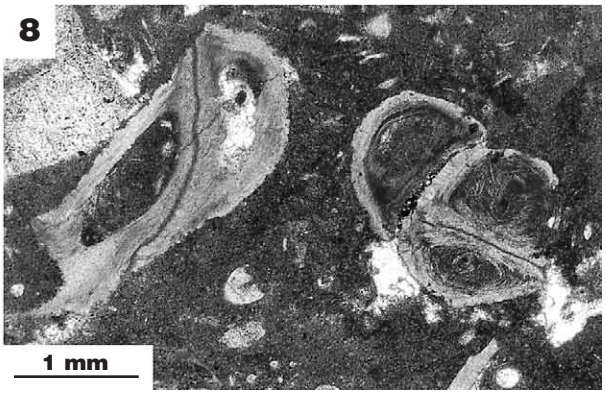
8
1 mm

PLATE 6

Jebel el Otfal, mud-mound no. 2

1 – Mud-mound no. 2, seen from S (mound no. 3); the largest mound of Jebel el Otfal rises 40 m above slightly tilted lower Eifelian wackestones; the mound wedges out into a 2 m-thick crinoidal grainstone bed (arrow a) and is underlain by a crinoidal limestone lense (arrow b). *Pinacites-Subanarcestes* bed (arrow c) and overlying, dark mudstones (d)

2a-2b – mud-mound no. 2, seen from SE; note mound-underlying crinoidal limestone lense and that mound wedges out towards the left into the inter-mound crinoidal limestone bed; note also the strong asymmetry of the mound (steeper southwestern (left) than northeastern flank (right)), which still remains significant after correction for rotation of the underlying strata to the horizontal

1


b
a
d
c

2a

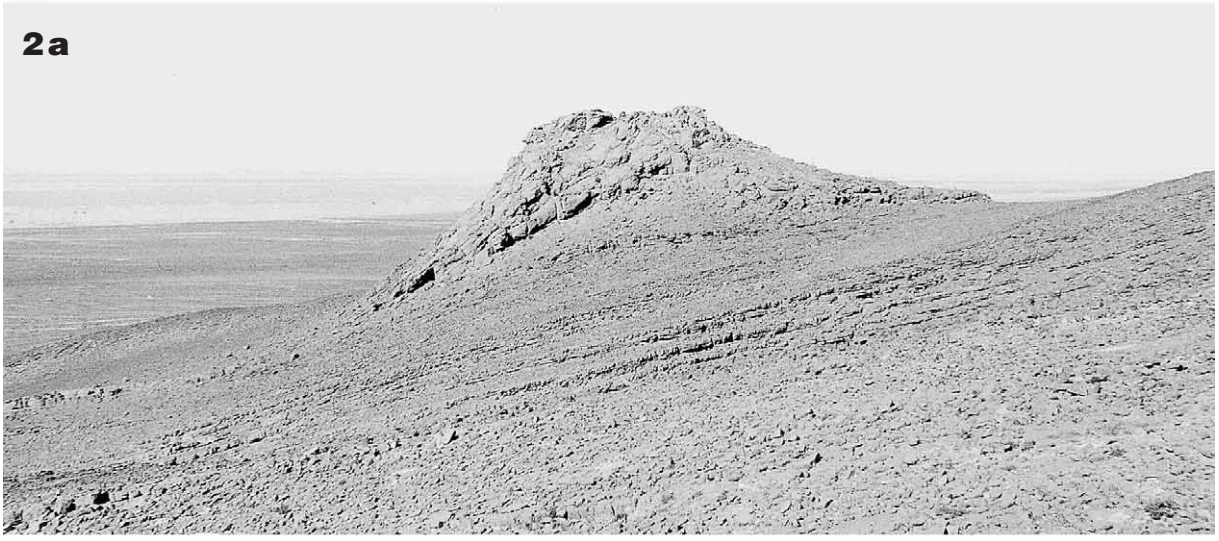

2b

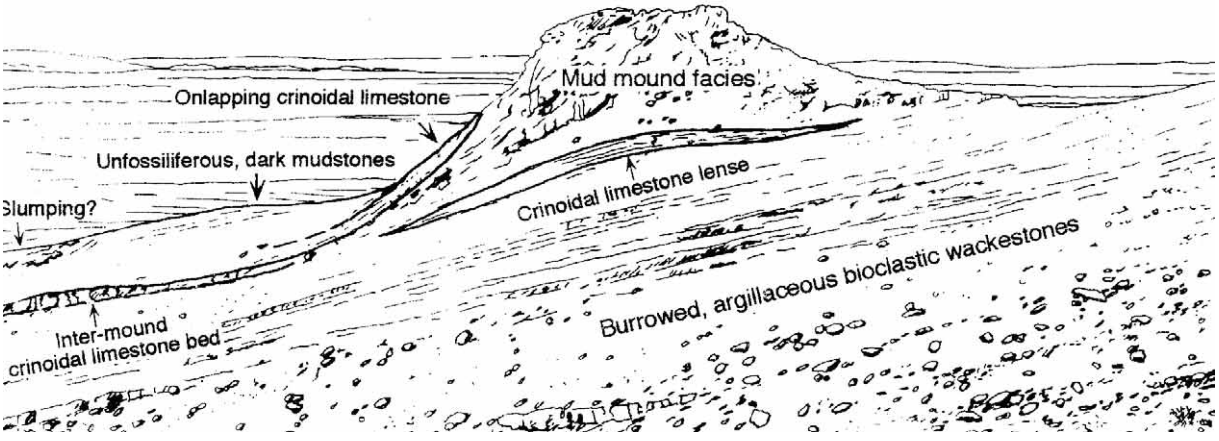
Mud mound facies
Onlapping crinoidal limestone
Unfossiliferous, dark mudstones
Slumping?
Crinoidal limestone lense
Inter-mound crinoidal limestone bed
Burrowed, argillaceous bioclastic wackestones

PLATE 7

Jebel el Otfal mud-mounds

1 – Mud-mound no. 1, seen from SW; the mound rises 20 m above the gravel plain, the base and approximately the lower 10 m are not exhumed; person (arrowed) for scale; mud-mound no. 2 in the background

2 – Mud-mound no. 3, seen from NE; the mound rises 10 m above the gravel plain, the base and approximately the lower 40 m are covered

3 – Mud-mound no. 4, seen from W; the mound rises 15 m above the gravel plain; underlying lower Eifelian wackestones (a) and overlying dark mudstones (b); person (arrowed) for scale

1

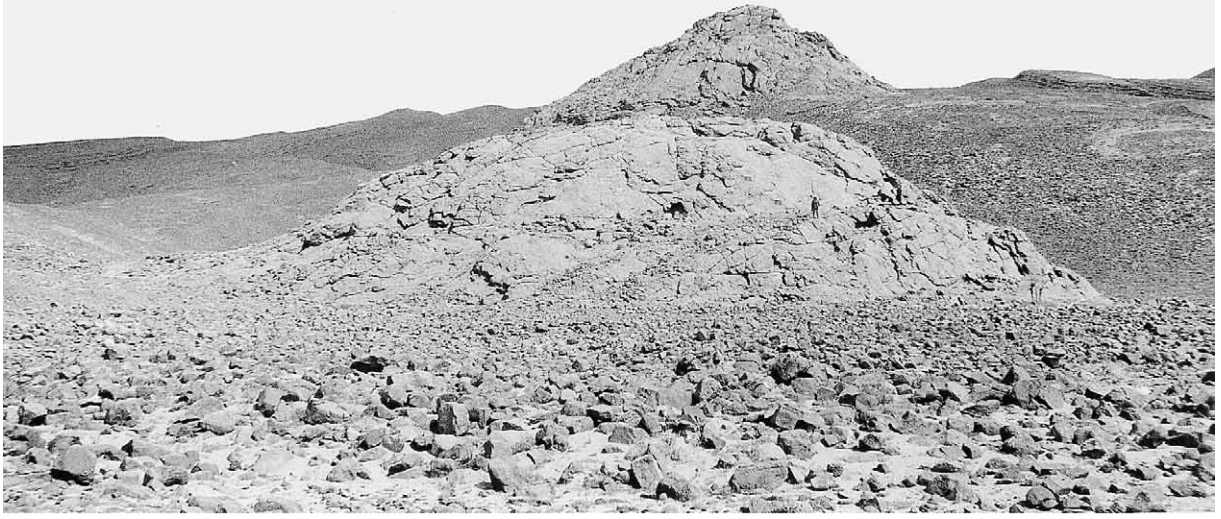

2

3

PLATE 8

Jebel el Otfal mud-mounds

1 – Stromatactis in mud-mound facies (mound no. 4), aligned parallel to the accretionary surface of the mound; coin diameter is 24 mm

2 – Irregular cavity in mud-mound facies (mound no. 3); cavity is filled with dolomitized internal sediment with preserved ghost-lamination in the lower part (arrow); isopachous calcite cement layer, lining the cavity wall; coin diameter is 24 mm

3 – Coiled end of crinoid stem (*Acanthocrinus* sp.) in mud-mound facies (mound no. 3)

4 – *In situ* disintegration of crinoid in crinoidal limestone lense underlying mound no. 2; coin diameter is 24 mm

5 – Tabulate coral (cf. *Pachystriatopora*) and abundant crinoid ossicles in mud-mound facies (mound no. 3); coin diameter is 24 mm

6 – Burrows (*Planolites*) in argillaceous, bioclastic wackestones, underlying mud-mound facies at Jebel el Otfal; coin diameter is 24 mm

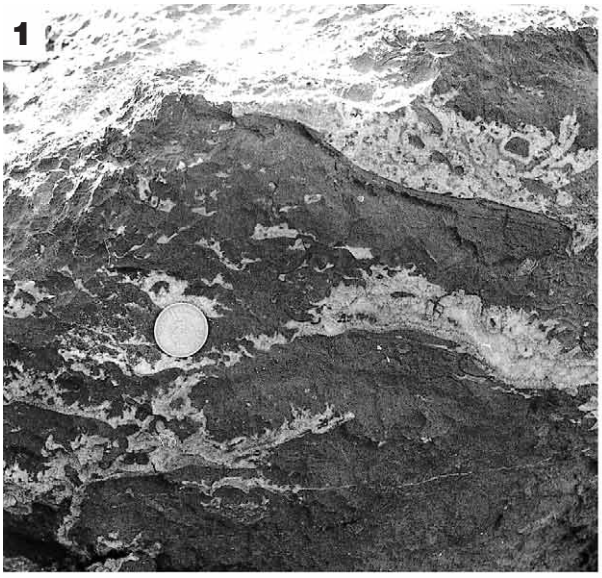
1

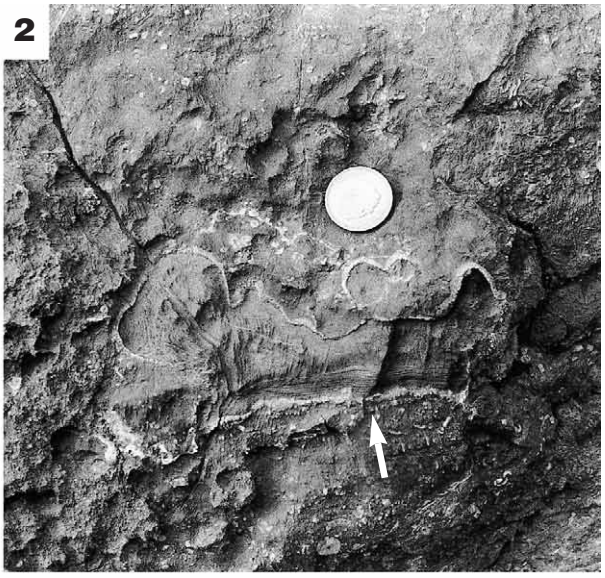
2

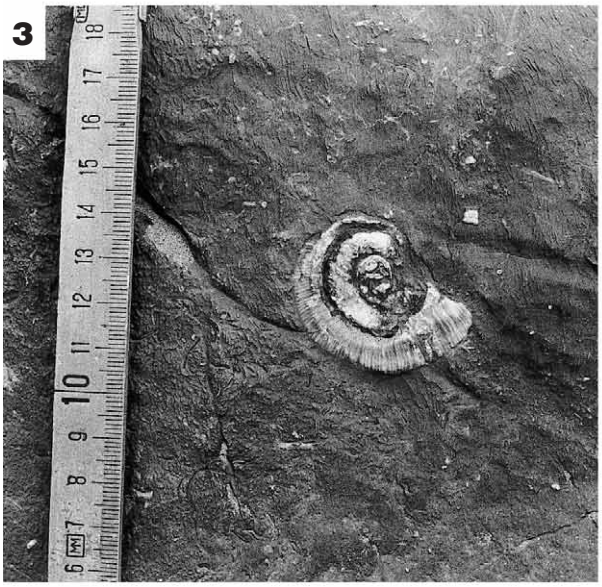
3

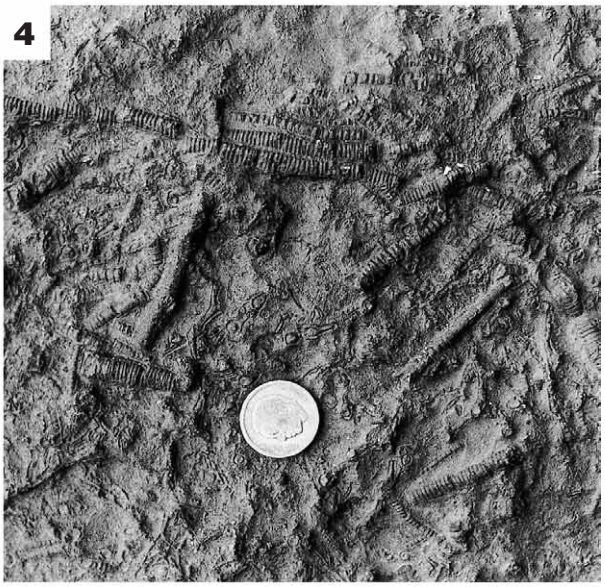
4


5

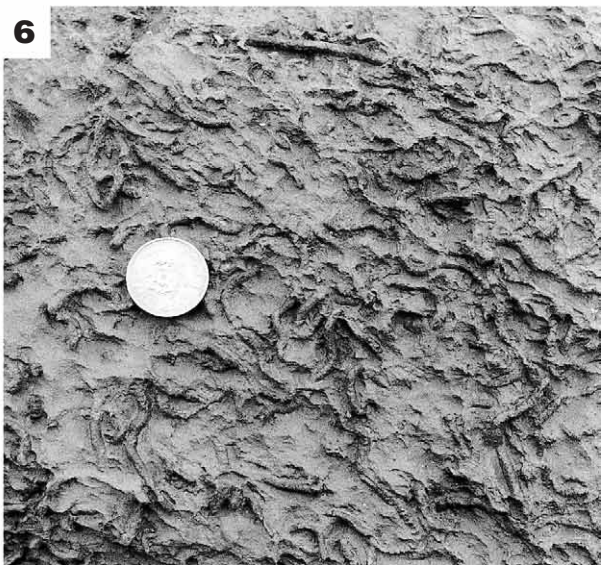
6

PLATE 9

Jebel el Otfal mud-mounds, microfacies

1 – Stromatactis in mud-mound facies (mound no. 2), aligned parallel to the accretionary surface of the mound; sample M 85

2 – Auloporid floatstone lense underlying mound no. 2 with abundant *Bainbridgia* sp; sample P 110

3 – Accumulated trilobite carapaces in mud-mound facies (mound no. 4); note spar-filled shelter pores; sample 618/5

4 – Phaceloid rugose corals (cf. *Fletcheria*) in mud-mound facies (mound no. 1); sample M 75

5 – Siliceous sponge spicules of hexactinellids in mud-mound facies (mound no. 1); thin section P 136

6 – Fistuliporid bryozoans in mud-mound facies (mound no. 2); thin section P 123

7 – Tabulate coral (*Dualipora preciosa* TERMIER & TERMIER 1980) in mud-mound facies (mound no. 4); thin section 618/3

8 – Microproblematicum (*Rothpletzella* sp., arrowed) encrusting tabulate coral (*Bainbridgia* sp.) in mud-mound facies (mound no. 2); thin section P 126

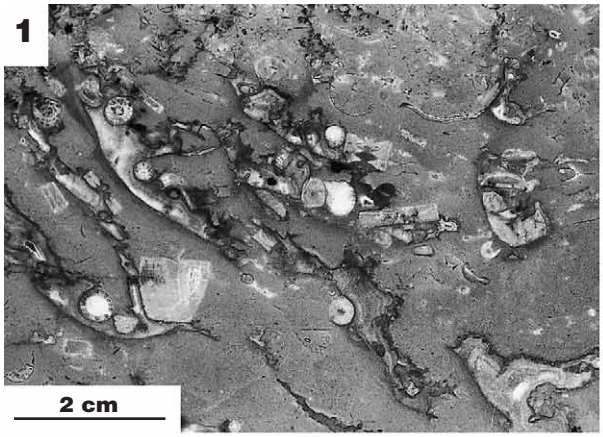
1
2 cm

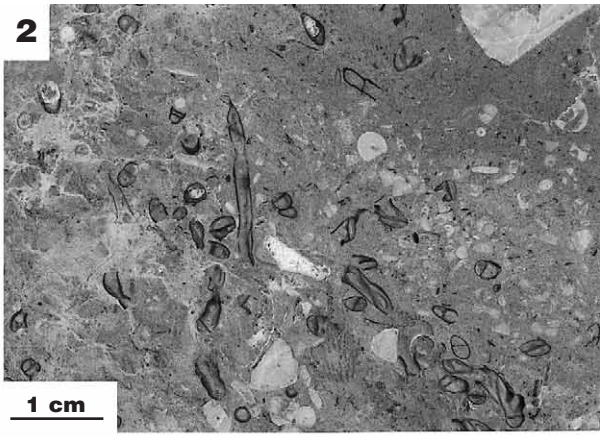
2
1 cm

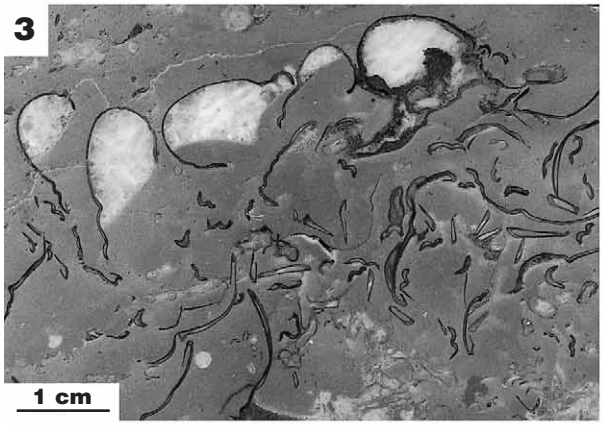
3
1 cm


4
1 cm


5
1 mm

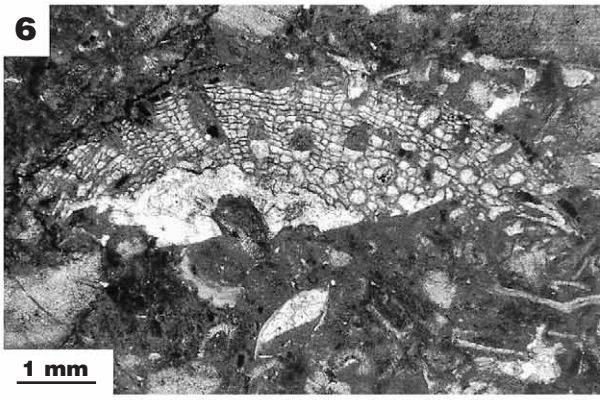
6
1 mm

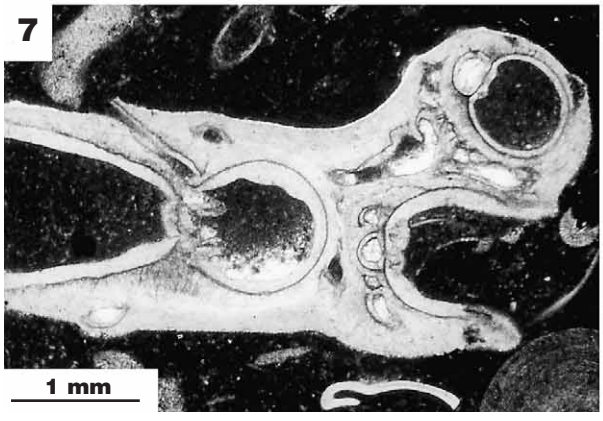
7
1 mm

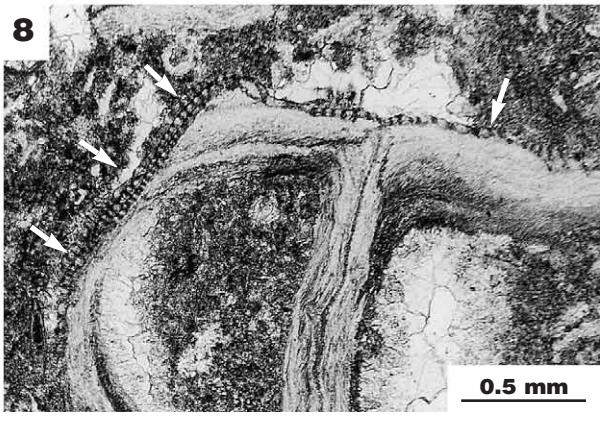
8
0.5 mm

PLATE 10

Mounds of Jebel Ou Driss and SE of Jebel Zireg

1 – Mud-mound of Jebel Ou Driss, seen from SE; it rises 4 m above the surrounding bedded off-mound facies, under which the bulk mound volume is covered; person (*arrowed*) for scale

2 – The most easternward one of three mounds SE of Jebel Zireg, seen from S; mound-shape is due to higher erosion resistance of S-dipping dolomite lense than the argillaceous off-mound strata; person (*arrowed*) for scale

3 – Tabulate corals (cf. *Zemmourella*) in mud-mound facies of Jebel Ou Driss; coin diameter is 24 mm

4 – Stromatactis in mud-mound facies of Jebel Ou Driss; abundant tabulate corals (*Zemmourella* cf. *taouzia*), partly cement-enveloped (*arrowed*) and dark seams surrounding cavities, probably of cyanobacterial origin (R. RIDING, *pers. comm.*); sample P 1

5 – Solitary, rugose corals (*Neomphyma* sp. or *Sociophyllum* sp.) in mud-mound facies of Jebel Ou Driss; sample P 3

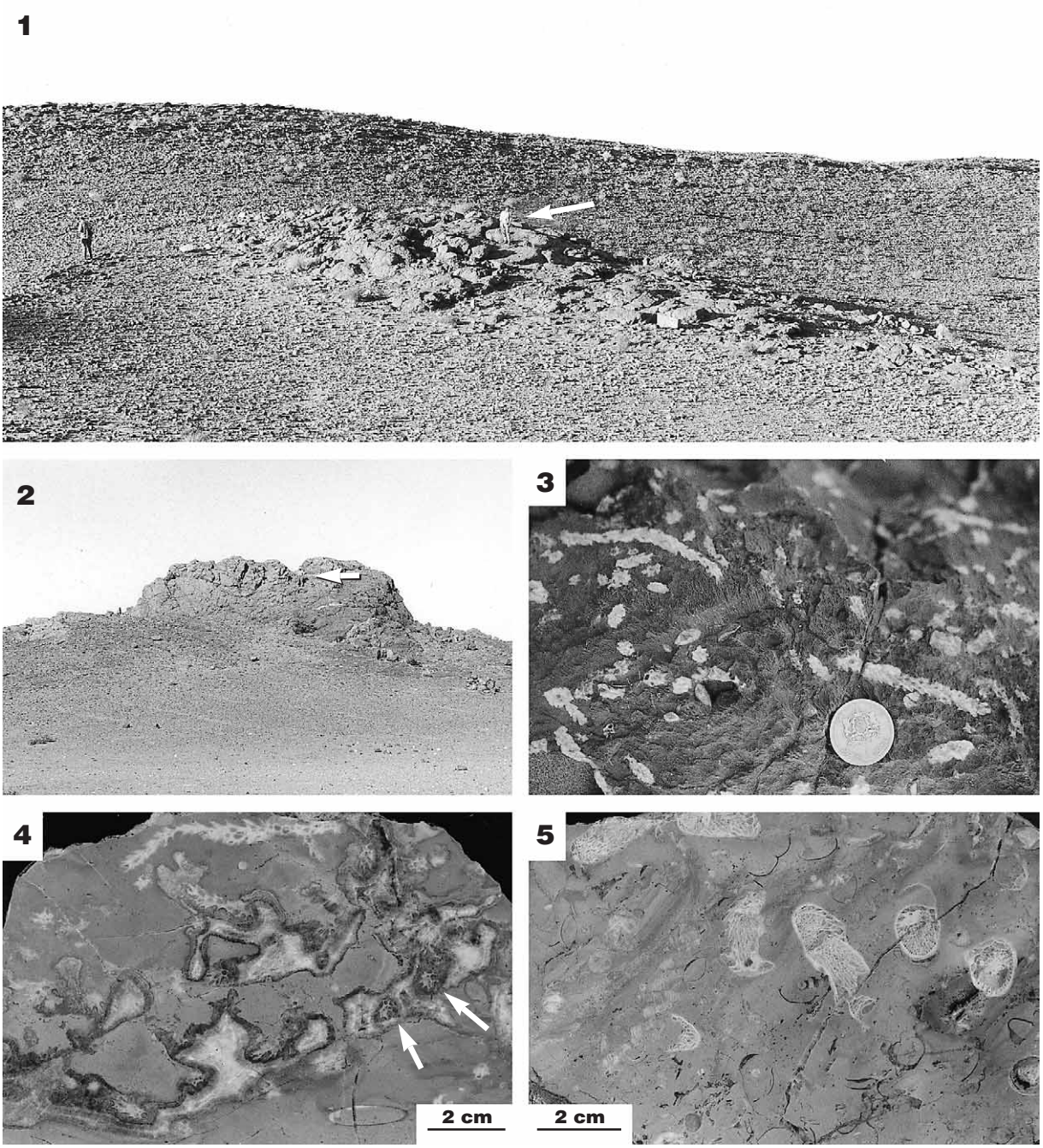
1
2
3
4
2 cm
5
2 cm

PLATE 11

Conodonts of the Mader carbonate mounds

1 – *Belodella* sp. Guelb el Maharch, mud-mound facies, sample M 101, ×37

2 – *Belodella* sp. Guelb el Maharch, mud-mound facies, sample M 101, × 46

3 – *Belodella* sp. Aferdou el Mrakib, reef-mound facies, sample P 148, 155, × 46

4 – *Belodella* sp. Aferdou el Mrakib, reef-mound facies, sample P 148, 155, × 46

5 – *Belodella* sp. Aferdou el Mrakib, reef-mound facies, sample P 148, 155, × 46

6 – *Icriodus corniger* WITTEKINDT, 1966; Jebel ou Driss, mud-mound facies, sample P 2, × 46

7 – *Icriodus struvei* WEDDIGE, 1977; Guelb el Maharch, mud-mound facies, sample P 159, 164, M 96, M 101, × 60

8 – *Icriodus regularicrescens* BULTYNCK, 1970; Aferdou el Mrakib, reef-mound facies, sample M 35, × 37

9 – *Icriodus platyobliquimarginatus* BULTYNCK, 1987; Aferdou el Mrakib, underlying strata, sample M 46, × 65

10 – *Icriodus subterminus* YOUNGQUIST, 1947; Aferdou el Mrakib, top of mound-underlying crinoidal limestones, sample M 48, × 60

11 – *Icriodus obliquimarginatus* BISCHOFF & ZIEGLER, 1957; Aferdou el Mrakib, underlying strata, sample M 46, × 60

12 – *Icriodus arkonensis* STAUFFER, 1938; Aferdou el Mrakib, top of mound-underlying crinoidal limestones, sample 348/6, × 60

13 – *Icriodus brevis* STAUFFER, 1940; Guelb el Maharch, mud-mound facies, sample P 156, × 60

14 – *Icriodus* sp. A sensu WEDDIGE, 1977; Aferdou el Mrakib, top of mound debris facies, sample M 45, × 46

15 – *Icriodus difficilis* ZIEGLER & KLAPPER, 1976; Aferdou el Mrakib, top of mound debris facies, sample 432/3, × 46

16 – *Polygnathus linguiformis bultyncki* WEDDIGE, 1977; Jebel Ou Driss, mound-underlying strata, sample P 5, × 46

17 – *Polygnathus costatus patulus* KLAPPER, 1971; Guelb el Maharch, mud-mound facies, sample P 159, 164, × 37

18 – *Polygnathus costatus patulus* → *P. costatus costatus* transitional form BULTYNCK, 1985; Jebel el Otfal, mud-mound no. 2, sample Md. 2, × 46

19 – *Polygnathus costatus partitus* KLAPPER, ZIEGLER & MASHKOVA, 1978; Jebel el Otfal, mound-overlying *Pinacites-Subanarcestes* Bed, sample M 79, × 46

20 – *Polygnathus costatus costatus* KLAPPER, 1971; Jebel el Otfal, mound-overlying *Pinacites-Subanarcestes* Bed, sample M 79, × 46

21 – *Polygnathus linguiformis pinguis* WEDDIGE, 1977; Jebel el Otfal, mound-overlying *Pinacites-Subanarcestes* Bed, sample M 79, × 28

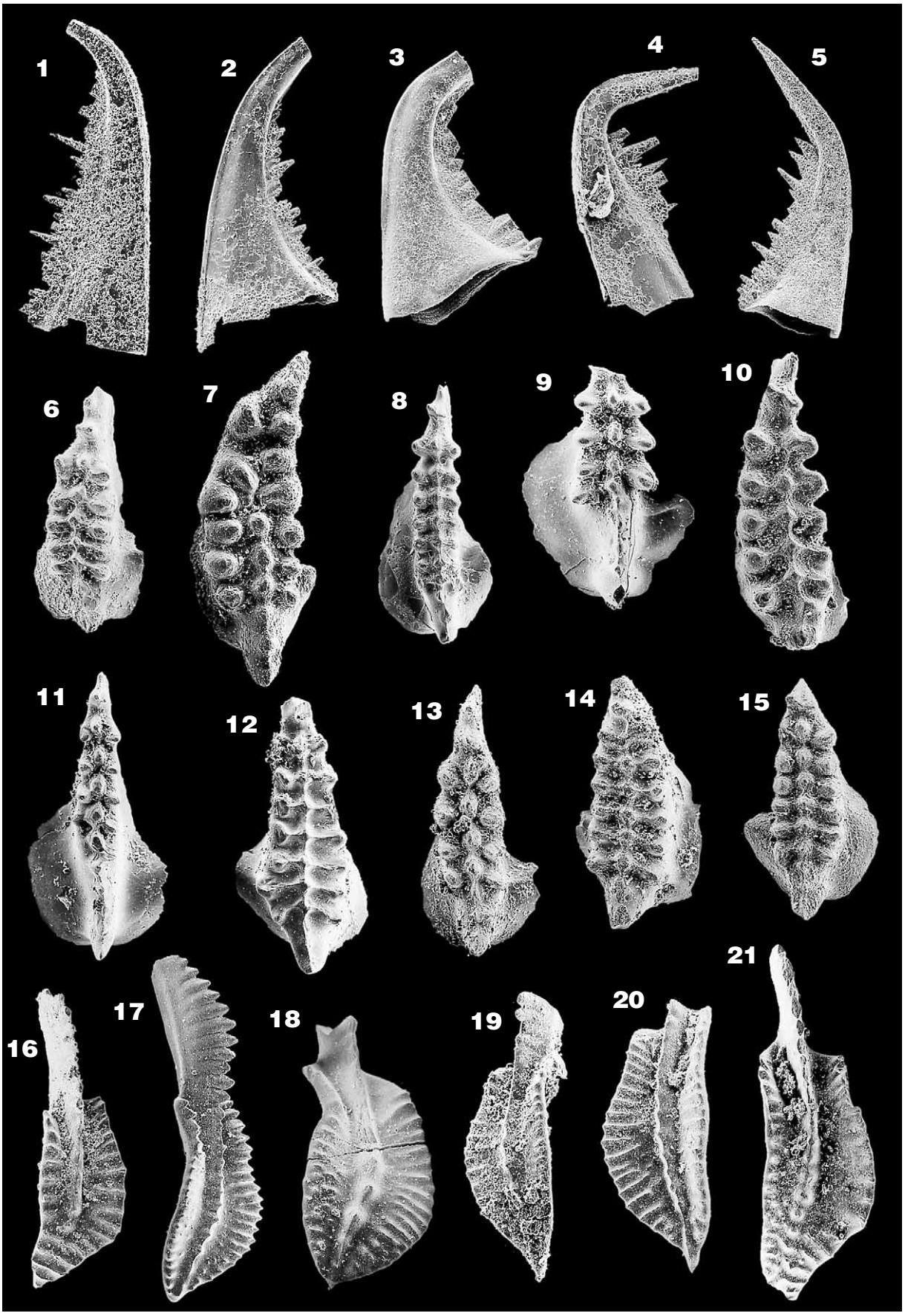
1
2
3
4
5
6
7
8
9
10
11
12
13
14
15
16
17
18
19
20
21

PLATE 12

Conodonts of the Mader carbonate mounds

1 – *Polygnathus angusticostatus* WITTEKINDT, 1966; Jebel Maharch, mound-underlying cephalopod bed, exposed 800 m SE of Guelb el Maharch mud-mound, sample M 95, × 60

2 – *Polygnathus linguiformis alveolus* WEDDIGE, 1977; Aferdou el Mrakib, top of mound-underlying crinoidal limestones, sample M 31, × 46

3-4 – *Polygnathus angustipennatus* BISCHOFF & ZIEGLER, 1957; Jebel Maharch, mound-underlying cephalopod bed, exposed 800 m SE of Guelb el Maharch mud-mound, sample M 95, × 46

5 – *Polygnathus robusticostatus* BISCHOFF & ZIEGLER, 1957; Jebel Maharch, mound-underlying cephalopod bed, exposed 800 m SE of Guelb el Maharch mud-mound, sample M 95, × 37

6 – *Polygnathus linguiformis linguiformis* BULTYNCK, 1970; Aferdou el Mrakib, reef-mound facies, sample M 103, × 28

7-8 – *Tortodus intermedius* (BULTYNCK, 1966); Jebel el Otfal, mud-mound no. 4, sample P 140, 141, × 60

9 – *Tortodus kockelianus kockelianus* (BISCHOFF & ZIEGLER, 1957); Jebel Maharch, mound-underlying cephalopod bed, exposed 800 m SE of Guelb el Maharch mud-mound, sample M 95, × 60

10 – *Polygnathus eiflius* BISCHOFF & ZIEGLER, 1957; Aferdou el Mrakib, reef-mound facies, sample M 35, × 46

11 – *Polygnathus linguiformis klapperi* CLAUSEN, LEUTERITZ & ZIEGLER, 1979; Aferdou el Mrakib, top of mound debris facies, sample M 45, × 37

12 – *Polygnathus ensensis* ZIEGLER & KLAPPER, 1976; Aferdou el Mrakib, reef-mound facies, sample M 38, × 46

13 – *Polygnathus hemiansatus* BULTYNCK, 1987; Aferdou el Mrakib, reef-mound facies, sample P 146, × 46

14 – *Polygnathus timorensis* KLAPPER, PHILIP & JACKSON, 1970; Aferdou el Mrakib, top of mound debris facies, sample M 45, × 37

15 – *Polygnathus timorensis* → *P. ansatus* transitional form Z. BELKA, *pers. comm*; Aferdou el Mrakib, top of mound debris facies, sample M 45, × 51

16 – *Polygnathus xylus* STAUFFER, 1940; Aferdou el Mrakib, reef-mound facies, sample M 35, × 65

17 – *Polygnathus linguiformis* ssp. B *sensu* WEDDIGE, 1977; Aferdou el Mrakib, underlying strata, sample M 46, × 42

18 – *Polygnathus* aff. P. *kennetensis* SAVAGE, 1976; Guelb el Maharch, mud-mound facies, sample P 159, 164, × 46

19 – *Polygnathus rhenanus* KLAPPER, PHILIP & JACKSON, 1970; Aferdou el Mrakib, reef-mound facies, sample 432/6, × 28

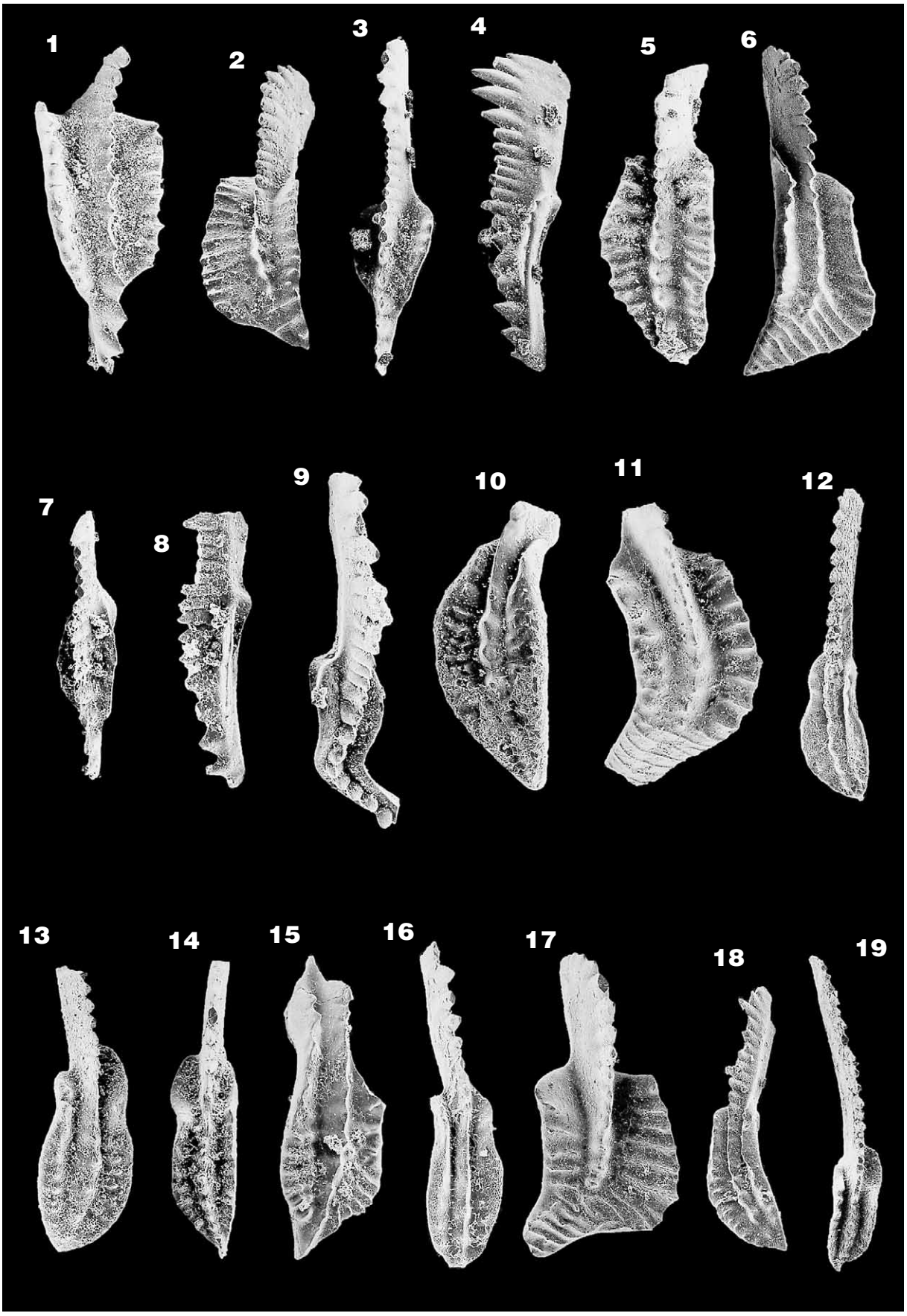
1
2
3
4
5
6
7
8
9
10
11
12
13
14
15
16
17
18
19

PLATE 13

Microfossils of the Mader carbonate mounds

1 – Shark tooth (*Phoebodus fastigatus* GINTER & IVANOV, 1992); labial view, right cusp broken; Aferdou el Mrakib, top of mound debris facies, sample M 45, × 37

2 – Shark tooth (*Phoebodus fastigatus* GINTER & IVANOV, 1992); labial view, dirty or partially dissolved specimen; Aferdou el Mrakib, top of mound debris facies, sample M 45, × 28

3 – Shark tooth (*Phoebodus fastigatus* GINTER & IVANOV, 1992); fragment of a main cusp (right) and of an intermediate cusp (left); Aferdou el Mrakib, top of mound debris facies, sample M 45, × 37

4 – Shark tooth (*Phoebodus fastigatus* GINTER & IVANOV, 1992); fragment of a main cusp; Aferdou el Mrakib, top of mound debris facies, sample M 45, × 37

5-6 – Agglutinated foraminifer (*Sorosphaera* sp.); Jebel el Otfal, mud-mound no. 3, sample M 73, × 37

7 – Agglutinated foraminifer (*Sorosphaera* sp.); Jebel el Otfal, mud-mound no. 4, sample M 62, 65, × 46

8 – Agglutinated foraminifer (*Sorosphaera* sp.); Jebel el Otfal, mud-mound no. 4, sample M 62, 65, × 60

9 – Siliceous sponge spicule (smooth hexact) of hexactinellid; Aferdou el Mrakib, reef-mound facies, sample P 146, × 28

10 – Siliceous sponge spicule (smooth hexact) of hexactinellid; Aferdou el Mrakib, reef-mound facies, sample M 104, × 65

11 – Pentamerid (*Ivdelinia* sp.); Aferdou el Mrakib; reef-mound facies, × 0.74

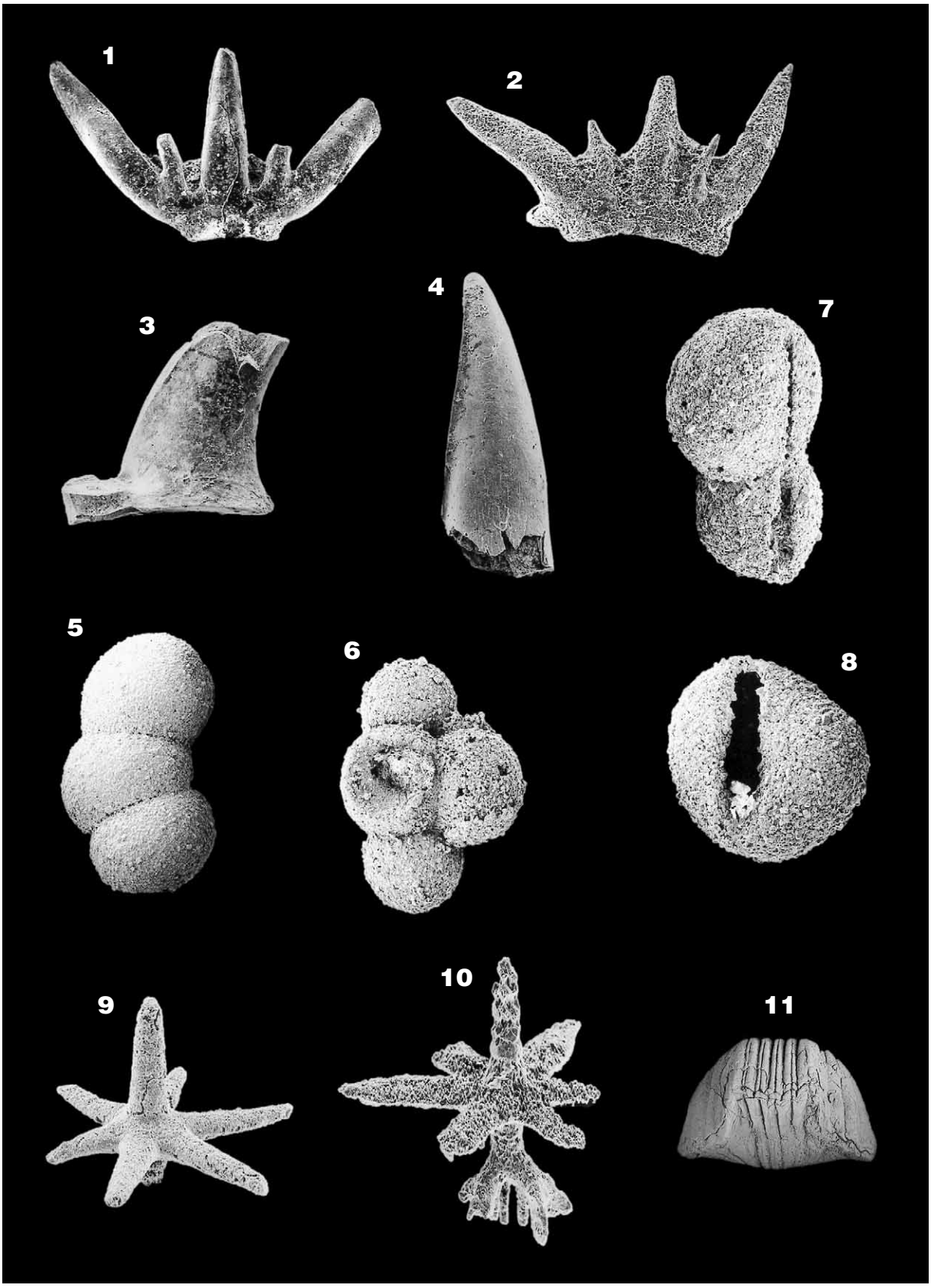
1
2
3
4
7
5
6
8
9
10
11

PLATE 14

Calcite cements of the Mader Basin carbonate mounds

1a – Transmitted-light view of cloudy (= inclusion-rich) radiaxial calcite (RC), forming an isopachous layer on the wall (dark field at bottom) of a stromatactis cavity; radiaxial calcite displays well developed curved twins and is followed by clear, equant blocky spar (BS); Aferdou el Mrakib reef-mound (thin section P 151)

1b – Crossed-nicols view of 1a, showing undulose extinction of RC crystal at left margin (*arrowed*)

1c – CL view of 1a, displaying dull-luminescent microspar matrix (a), non-luminescent RC (b), with dull, mottled CL at the bottom and moderate, mottled CL at the transition to the non-luminescent scalenohedral cement (c); bright-luminescent cement (*arrowed*) forms the outer margin of scalenohedral cement; moderate-luminescent, non-ferroan blocky spar I (d) and dull-luminescent, strong-ferroan blocky spar II (e) occlude the remainder of the pore space

2 – CL view of spar-filled fossil shelter cavity with moderate-luminescent trilobite carapace (a) as cavity roof and dull- to moderate-luminescent microspar matrix (b) at bottom and top; well developed scalenohedral cements (c) with thin, bright- and banded-luminescent outer margins are followed by dull- to moderate-luminescent (d) and moderate- to bright-luminescent (e) blocky spar; note that scalenohedral cements (c) show substrate-specific growth, preferring the LMC matrix rather than the LMC trilobite carapace; Jebel el Otfal, mound no. 4 (thin section P 141)

3 – CL view of spar-filled intraskeletal pore space within moderate-luminescent tabulate coral skeleton (*Bainbridgia* sp.) (a), surrounded by dull, mottled luminescent microspar matrix (b); scalenohedral cements (c) are followed by moderate-luminescent, non-ferroan blocky spar I (d), dull-luminescent, strong-ferroan blocky spar II (e), dull- to moderate-luminescent, ferroan blocky spar III (f) and bright-luminescent, ferroan blocky spar IV (g); note the trigonal crystal habit of scalenohedral cements (*arrowed*) and the absence of a bright-luminescent zone on their margins, probably resulting from the restricted diagenetic environment within the isolated coral fragment; Guelb el Maharch (thin section P 163)

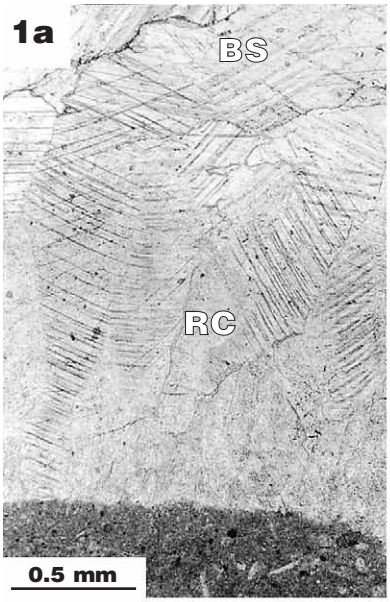
1a
BS
RC
0.5 mm

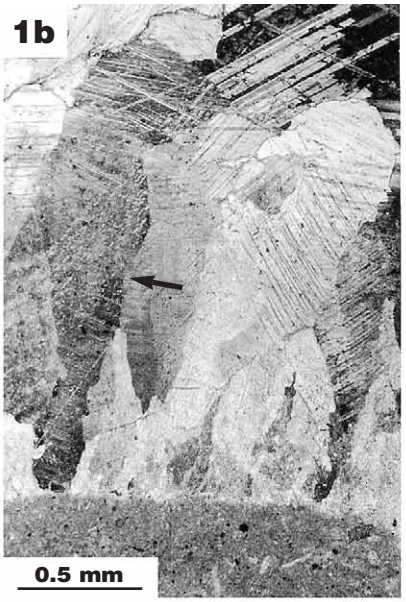
1b
0.5 mm

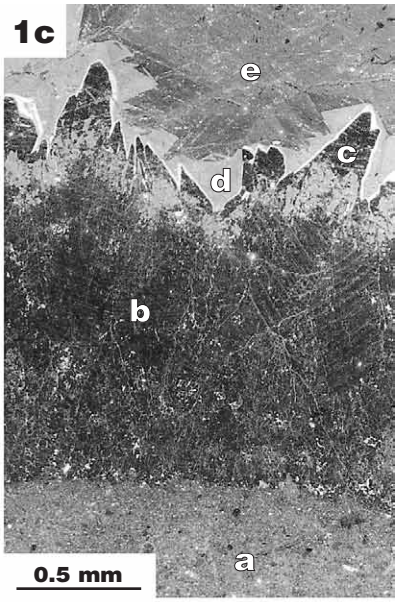
1c
e
c
d
b
a
0.5 mm


2
b
a
d
e
c
b
0.5 mm

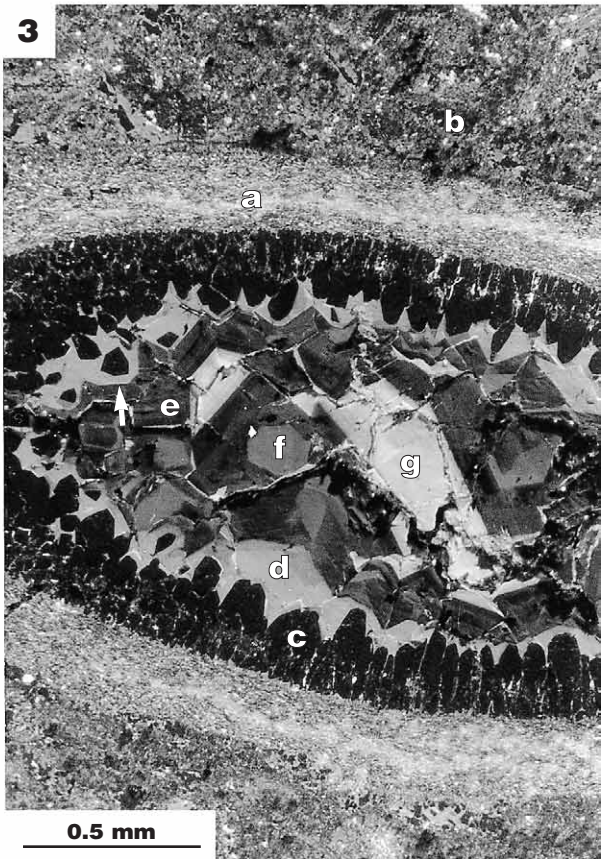
3
b
a
e
f
g
d
c
0.5 mm

PLATE 15

Calcite cements of the Mader Basin carbonate mounds

1a – Transmitted-light view shows the crystal terminations of inclusion-rich radiaxial calcites (RC), followed by clear blocky spars (BS) with a strong-ferroan (potasium ferricyanide stain) zone (a) within a stromatactis cavity; Aferdou el Mrakib reef-mound (thin section P 150)

1b – CL view of 1a, displaying a varied cement sequence of radiaxial calcite (RC) with mottled, moderate-luminescent crystal terminations, followed by non-luminescent scalenohedral cements (SC), banded-luminescent cements (BLC), moderate-luminescent, non-ferroan blocky spar I (BS I), dull-luminescent, strong-ferroan blocky spar II (BS II) and dull- to moderate luminescent blocky spar III (BS III); note 'oscillatory zoning' within moderate-luminescent growth band (*arrowed*) of banded-luminescent cement

2a – Transmitted-light view shows inclusion-rich radiaxial calcites (RC), forming isopachous layer on the wall (dark field at the bottom) of a stromatactis cavity, overgrown by clear scalenohedral cement (SC), which in turn is followed by strong-ferroan (potassium ferricyanide stain) blocky spar (BS); Jebel el Otfal, mound no. 1 (thin section P 135)

2b – CL view of 2a, showing dull-luminescent microspar matrix (a), mottled, bright-luminescent crystal inceptions of radiaxial calcites (b), dull-luminescent crystal boundaries of radiaxial calcites, banded-luminescent outer margins (*arrowed*) of scalenohedral cements and dull-luminescent, strong-ferroan blocky spar II (BS II); note the absence of moderate-luminescent, non-ferroan blocky spar I

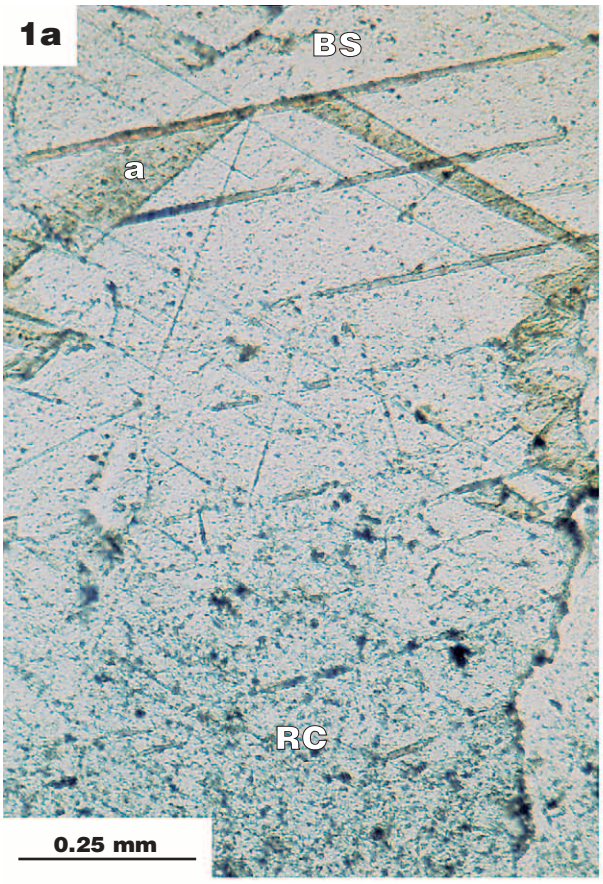
1a
BS
a
RC
0.25 mm

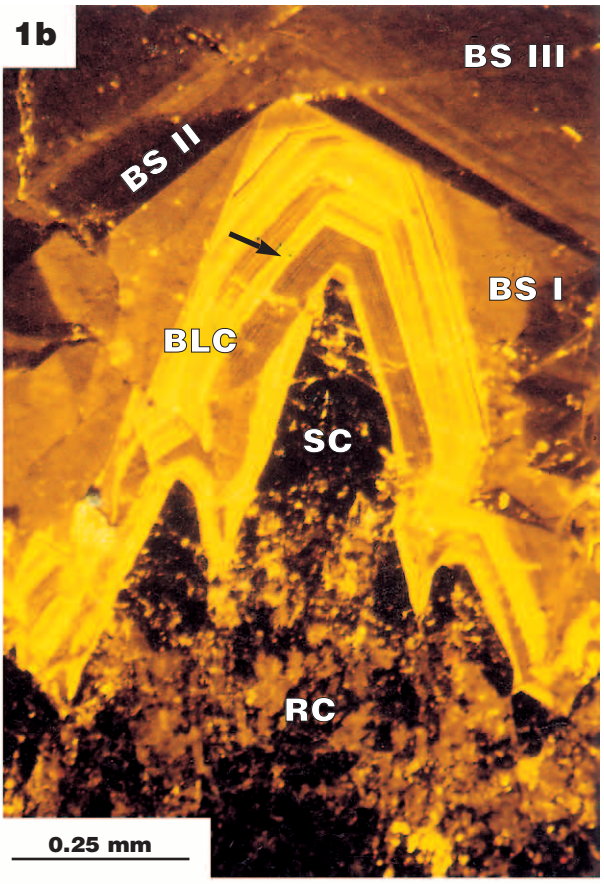
1b
BS III
BS II
BS I
BLC
SC
RC
0.25 mm

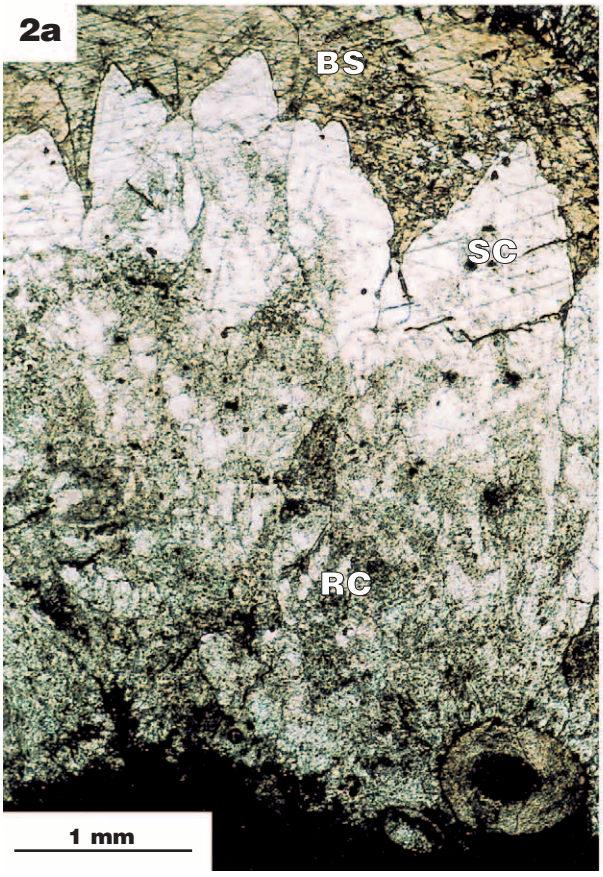
2a
BS
SC
RC
1 mm

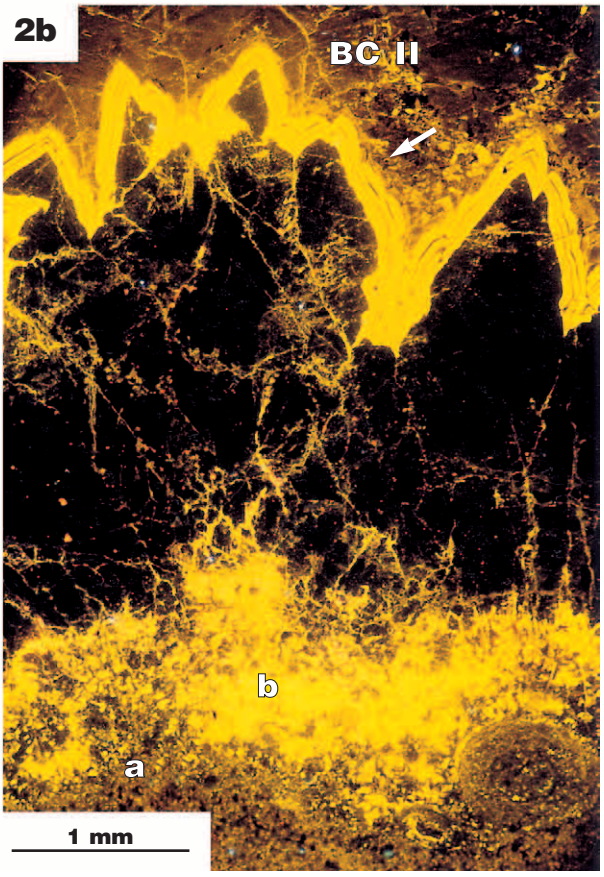
2b
BC II
b
a
1 mm

PLATE 16

Diagenesis of the Mader Basin carbonate mounds

1 – Non-luminescent, inclusion-free, syntaxial LMC cement (a) on crinoid ossicle (b); banded-luminescent cement (c) forms the outer margin of syntaxial cement; note moderate-luminescent microdolomite inclusions (*arrowed*) within crinoid ossicle; Aferdou el Mrakib reef-mound (thin section P 150)

2 – Stylolites with vertically arranged teeth, indicating pressure from sediment overburden; sprouting dolomite rhombs (*arrowed*); Aferdou el Mrakib reef-mound (thin section P 150)

3 – CL view of replacement matrix dolomite; zoned dolomite rhombs; Aferdou el Mrakib reef-mound (thin section P 149)

4 – CL view of non-luminescent (= strong-ferroan), idiotopic mosaic dolomite, which is a replacement of a sedimentary cavity infilling (*see* Pl. 4, Fig. 3; Pl. 5, Figs 3-4; Pl. 8, Fig. 2); note moderate-luminescent outer margins of dolomite rhombs, possibly caused by meteoric weathering after exhumation; Jebel el Otfal, mound no. 2 (thin section P 123)

5 – SEM photomicrograph of microdolomite inclusions (verified by EDAX) in radiaxial calcite; samples were polished and etched (0.3% HCl, 30 s); pits have possibly been left from former fluid inclusions; Aferdou el Mrakib reef-mound (SEM sample P 151)

6 – SEM photomicrograph of microspar matrix; samples were highly polished (1 μm) and slightly etched (0.15% formic acid, 15-20 s); clay minerals (verified by EDAX) between the intercrystalline boundaries were obviously pushed aside during growth of microspar crystals; small flakes within the microspar crystals are possibly relics of the precursor micritic carbonate; Guelb el Maharch mud-mound (SEM sample P 156)

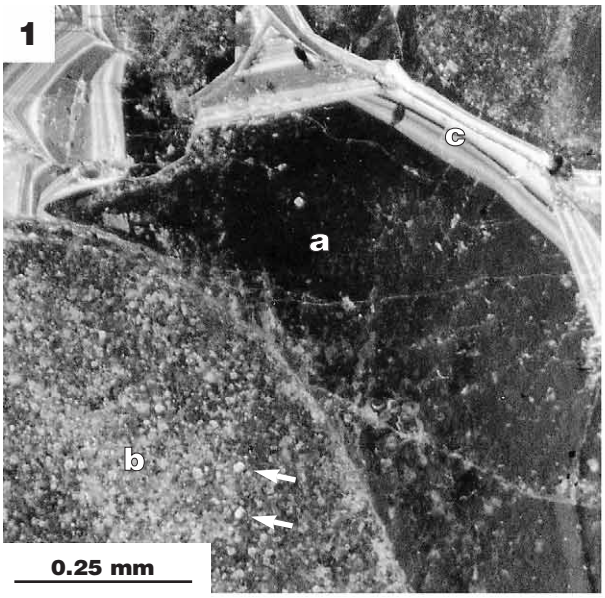
1
a
b
c
0.25 mm

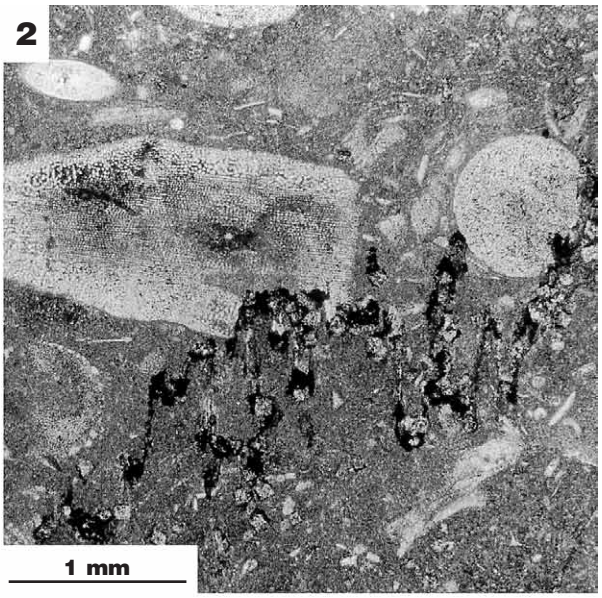
2
1 mm

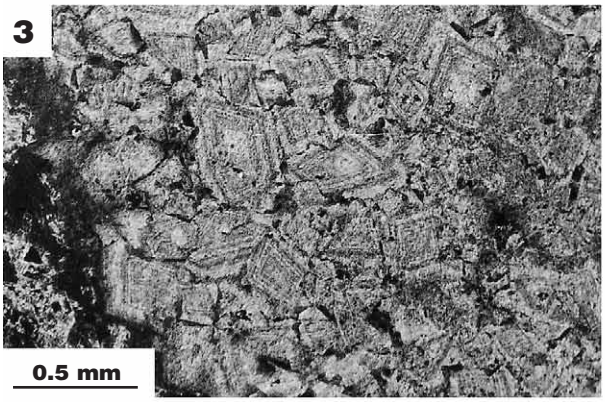
3
0.5 mm

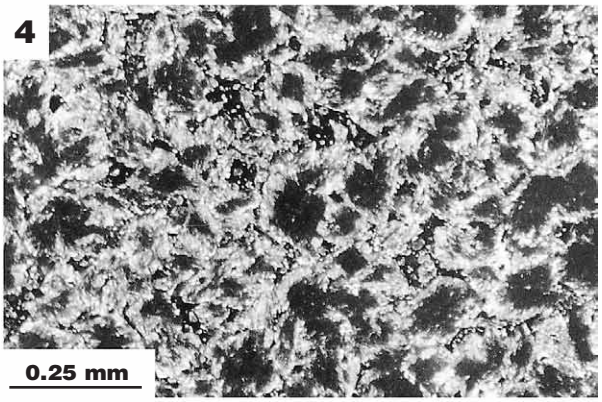
4
0.25 mm

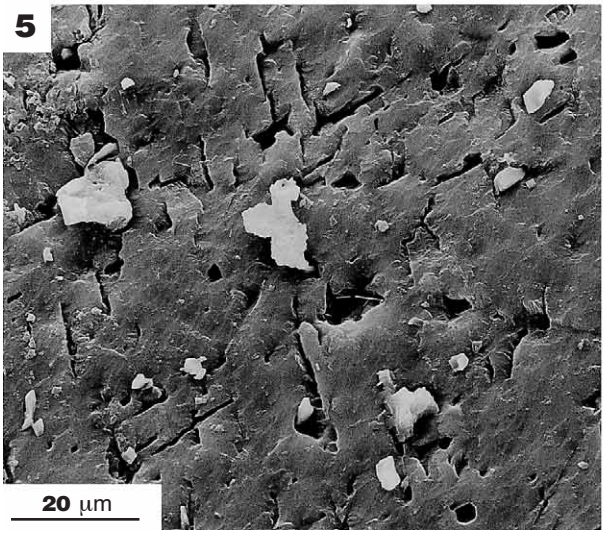
5
20 μm

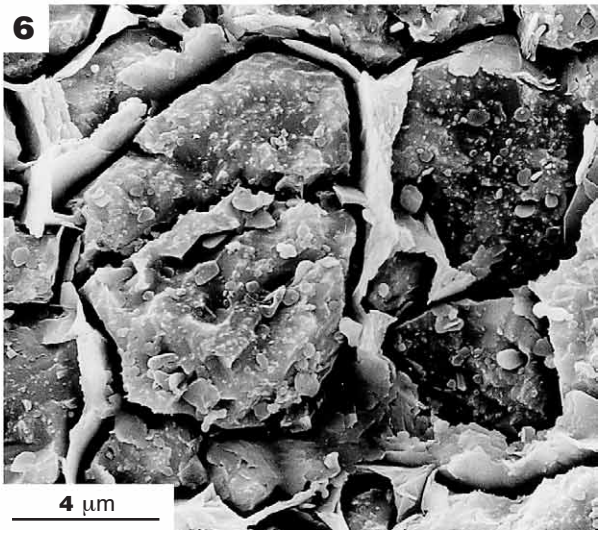
6
4 μm